Theses and Dissertations--Civil Engineering

Civil Engineering

2013

PRESSURE MEASUREMENT AT THE BALLAST-TIE INTERFACE OF RAILROAD TRACK USING MATRIX BASED TACTILE SURFACE SENSORS

Michael T. McHenry
University of Kentucky, mchenland@aol.com

PRESSURE MEASUREMENT AT THE BALLAST-TIE INTERFACE OF
RAILROAD TRACK USING MATRIX BASED TACILE SURFACE SENSORS

THESIS

A thesis submitted in partial fulfillment of the
requirements for the degree Master of Science in Civil Engineering
in the College of Engineering at the University of Kentucky

By

Michael McHenry
Lexington, Kentucky
Co-Advisors: Dr. Jerry G. Rose, Professor
and   Dr. Reginald Souleyrette, Professor
Department of Civil Engineering
Lexington, Kentucky
2013

ABSTRACT OF THESIS

PRESSURE MEASUREMENT AT THE BALLAST-TIE INTERFACE OF
RAILROAD TRACK USING MATRIX BASED TACILE SURFACE SENSORS

The pressure distribution at the ballast-tie interface of railroad track plays a key role in overall track support. Failure of the ballast or tie can result from excessive loads that were not designed for, requiring increased maintenance and reducing railroad operating efficiency. Understanding the forces acting on the ballast and tie are required to design higher performance and longer lasting track. To further this understanding, the use of Matrix Based Tactile Surface Sensors (MBTSS) is employed to measure the actual pressure distribution at the ballast-tie interface, characterized by individual ballast particle contact points and non-uniform pressures. The research explores this application of MBTSS including the development of sensor protection and calibration procedures. Results from laboratory ballast box testing conducted at the Transportation Technology Center, Inc. (TTCI) are presented. Conservative estimates of peak pressure under a typical wheel load on new ballast averaged 1450 psi and on fouled ballast averaged 680 psi. Contact areas varied across the range of ballast gradations and are shown to increase under increased applied load. A parameter to describe the "roughness" of the ballast-tie pressure distribution is offered. Results from in-track testing performed at TTCI, including pressure distributions along ten test ties, are also presented.

KEYWORDS: Matrix Based Tactile Surface Sensors, Railroad Ballast, Railroad Ties, Ballast-Tie Interface, Pressure

Michael McHenry

PRESSURE MEASUREMENT AT THE BALLAST-TIE INTERFACE OF

RAILROAD TRACK USING MATRIX BASED TACILE SURFACE SENSORS

By

Michael McHenry

<div align="right">

Dr. Jerry Rose
Co-Director of Thesis

Dr. Reginald Souleyrette
Co-Director of Thesis

Dr. Y.T. Wang
Director of Graduate Studies

</div>

ACKNOWLEDGEMENTS

TABLE OF CONTENTS

LIST OF TABLES

LIST OF FIGURES

CHAPTER 1. INTRODUCTION

Railroad Track Overview

Conventional, mainline railroad track is composed of steel rail fastened to cross-ties that rest on a layer of crushed rock, called ballast. According to Gillespie (1853), the term *ballast* originates from the aggregate used as ballast in empty cargo ships returning to England in the 19th century. The use of ballast to support track represents a significant development in the design of railroads. Prior to the implementation of ballast, cross-ties were laid directly on the subgrade soil. The addition of a ballast layer allows for higher quality track that can carry heavier loads, provide higher operating efficiency, and maintain track serviceability. Figure 1.1 shows a typical cross-section of conventional ballasted railroad track.
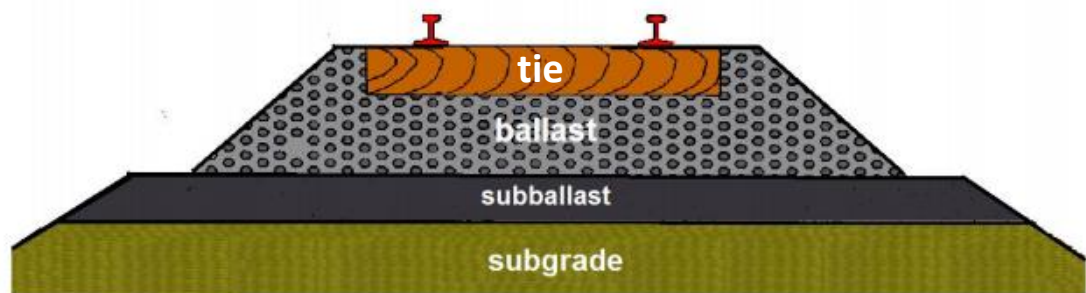
Figure 1.1 Ballasted railroad track cross-section (Rose and Lees, 2008)

Ballast

Ballast serves the following purposes (Hay, 1982, Selig and Waters, 1994 and Kerr, 2003):

1) Transfers and distributes loading from the ties to the underlying subballast or subgrade of the track structure at a tolerable level

2) Provides longitudinal and lateral track support to resist imposed loading from vehicles and thermal rail stress

3) Provides drainage through the support structure and away from the track

4) Allows for adjustment of the ties and rail to achieve proper surface and alignment through tamping, stone blowing, shovel packing, etc.

1

5) Prevents growth of vegetation in the track

6) Reduces the occurrence of track frost heave

To best perform these functions, quality ballast should be tough, hard, angular, and resistant to chemical and environmental weathering (Kerr, 2003). Historically, many materials have been used as ballast including crushed rock, crushed slag, cinders, and gravel (Hay, 1982). Today, mainline ballast on Class I railroads is typically crushed granite, quartzite, or trap rock. Figure 1.2 shows a conventional ballast.

Figure 1.2 Example of new, conventional, mainline, crushed rock ballast

Ballast fouling occurs when the void space in the ballast is filled with finer particles. As this happens, one or more of the above functions can be inhibited. Major mechanisms of ballast fouling include (Selig and Waters, 1994):

1) Internal fouling as a result of degradation of the ballast itself

2) "Pumping" of subgrade soil particles into the ballast layer

3) External fouling as a result of blown soil fines or coal dust

Figure 1.3 shows fouled ballast for comparison with Figure 1.2.

Figure 1.3 An example of fouled ballast

Selig and Waters (1994) presented evidence that fouling material was more likely to be made up of degraded ballast fines (internal fouling) than from the other two external fouling mechanisms.

Fouling is typically measured by quantifying the amount of material (by weight) in the ballast smaller than a specified grain size. For example, Selig and Waters (1994) define *Fouling Index (FI)* as:

$$FI = (\%\ Passing\ the\ No.\ 4\ sieve) + (\%\ Passing\ the\ No.\ 200\ sieve) \quad \text{(Eq. 1.1)}$$

The percent passing the No. 200 sieve is added to the percent passing the No. 4 sieve as clay sized particles are thought to have a greater detrimental effect on ballast performance. It has been well established that ballast fouling contributes to track geometry degradation and an increased need for maintenance (Selig and Waters, 1994). Much like ballast, the cross-tie component of the railroad track serves specific purposes and has distinct failure modes.

Ties

The cross-tie, or tie (also referred to as a sleeper in Europe) serves the following purposes (Hay, 1982):

1) Holds the rails transversely and provide proper gage (through use of a fastening system)
2) Transmits a reduced pressure to the ballast bed below
3) Assists in restriction to lateral, longitudinal and vertical movement of the track

Common materials used for cross-ties include wood (timber), concrete, steel, and plastic, although concrete and wood constitute the vast majority of ties in service.

Ties can fail in a multitude of ways leading to track geometry defects and the need for maintenance. The reader is referred to Zeman (2010) for a more detailed description of tie failure mechanisms, particularly in concrete ties. Of particular interest to this research study are flexural cracking failures. Positive flexural cracking can occur at the rail seat area due to reduced support directly beneath the rail. Figure 1.4 shows a positive flexural crack beneath a concrete tie rail seat. Focus
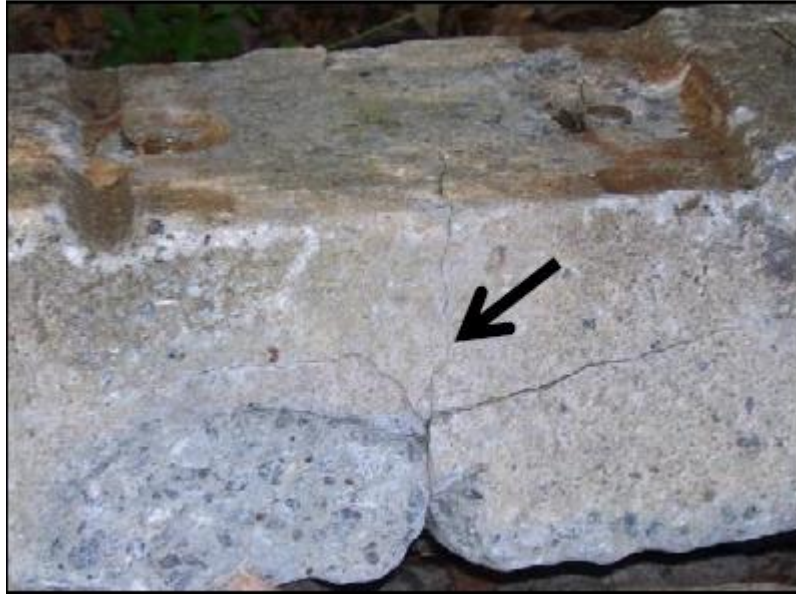
Figure 1.4 Positive flexural crack beneath a concrete tie rail seat (Zeman, 2010)

Ties also fail in a mechanism known as center-binding. Center-binding is the result of excessive negative bending of the tie near the centerline of the track due to reduced support of the tie at its ends, and increased load at its center. Figure 1.5 shows a center-bound condition for a concrete tie.
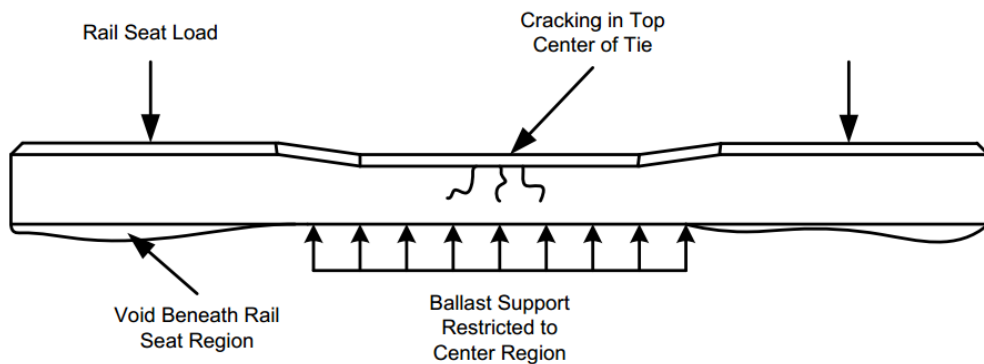
Figure 1.5 Schematic of a center-bound concrete tie (Lutch, 2009)

Both mechanism of flexural cracking can negatively impact the primary purpose of the tie as stated above.

The Ballast-Tie Interface

A vital and particularly influential area in the track structure exists between the ballast and tie. Combining functions of the tie and ballast, the interface serves the purpose of:

1) Beginning the distribution of pressure through the ballast layer

2) Allowing for adjustment of track geometry and

3) Providing frictional resistance for lateral and longitudinal track stability.

The ballast-tie interface is characterized by rough, angular ballast contacting the relatively smooth underside of the cross-tie. The hardness of the surfaces in contact can vary significantly due to the various ballasts and tie materials used. Sufficiently low contact and resulting high pressures on the ballast particles and tie may lead to ballast particle breakage, ballast fouling, differential track settlement, and/or tie failure. Tie failure (e.g. in the case of a center-bound tie) could also result from insufficient support conditions (pressure distribution) at the ballast-tie interface.

Significance of Ballast-Tie Pressure Data

As rail traffic grows, axle loads increase, and railroads become a more economical transport mode, high quality and low maintenance railroad track becomes a greater necessity. Sato (1997) has shown that the frequency distribution of the rate of track deterioration is exponential in nature (i.e. as track quality worsens, its influence on further deterioration is compounded). As with any component, failure results from that component experiencing a load that it cannot support. In order to achieve higher performing and lower maintenance designs, the behavior of the track structure and the interaction between its components must continue to be studied and better understood. A thorough understanding of the forces at the ballast-tie interface and their variability under load is required to better understand issues that negatively impact track quality such as ballast degradation (fouling), tie failure, and loss of track geometry. Figure 1.6 presents a typological continuum, a suggested structure to frame the significance of ballast-tie pressure and contact area data in the grand scheme of increasing railroad operating efficiency.

Independent Variables				Dependent Variables
Ballast-tie Pressure and Load Distribution, Contact Area	Ballast Characteristics - Hardness, Angularity, Gradation, Tie Characteristics –	Tie Structural Design, Ballast Degradation, Trackbed Support Characteristics	Track Geometry Degradation	Maintenance Planning and Strategies
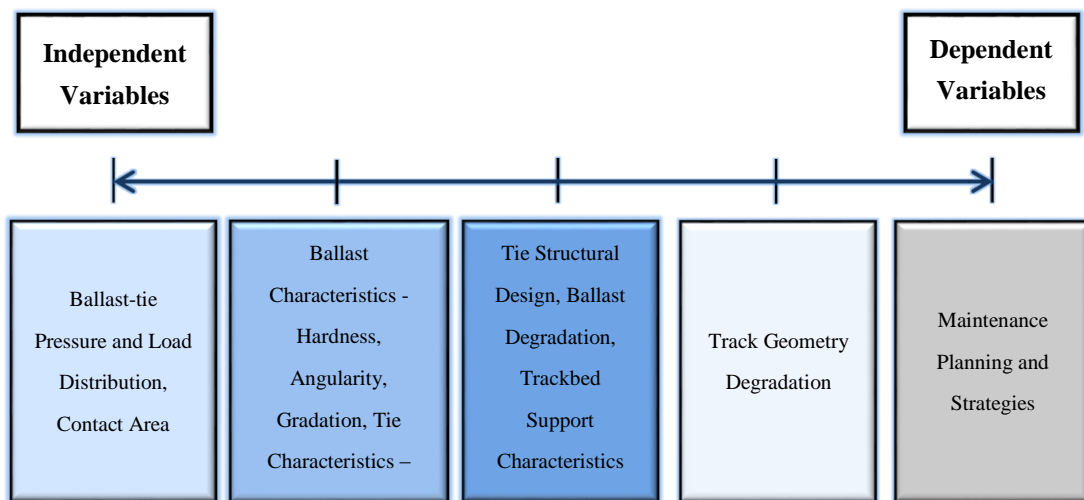
Figure 1.6 Typological continuum, a suggested structure to view ballast-tie data

The continuum consists of a multitude of variables, the most independent of which is ballast-tie contact pressures and pressure distribution data on the far left. A better understanding of these variables could lead to increased comprehension of the role of ballast rock characteristics, such as angularity and gradation, to overall track quality. Further along the continuum, ballast-tie pressure distribution data strengthens tie structural design methods, and ballast degradation modeling. The most dependent variable on the continuum is track maintenance modeling, ultimately leading to enhanced track maintenance strategies and policy making. The contribution of the current research project falls to the left on the continuum, but strongly impacts more dependent variables to the right.

Problem Statement

It is typical for the ballast-tie contact surface to be represented as two-thirds the tie footprint (the outer third on each end of the tie). In U.S. practice, a uniform and average pressure distribution is assumed over this contact surface (AREMA, 2010). In reality, however, the ballast-tie interface is characterized by high pressures due to low effective contact areas between the tie and the individual ballast particles that make up the contact surface. To illustrate the comparison between average pressure distribution and actual pressure distribution, Figure 1.7 depicts a cross-section of the portion of ballast directly beneath the tie. A cross section of the

average pressure distribution, shown in blue is distributed along the entire width of the tie. The dashed red lines represent the actual pressure distribution, a series of high loads corresponding with the contact locations of the individual ballast particles beneath the tie.
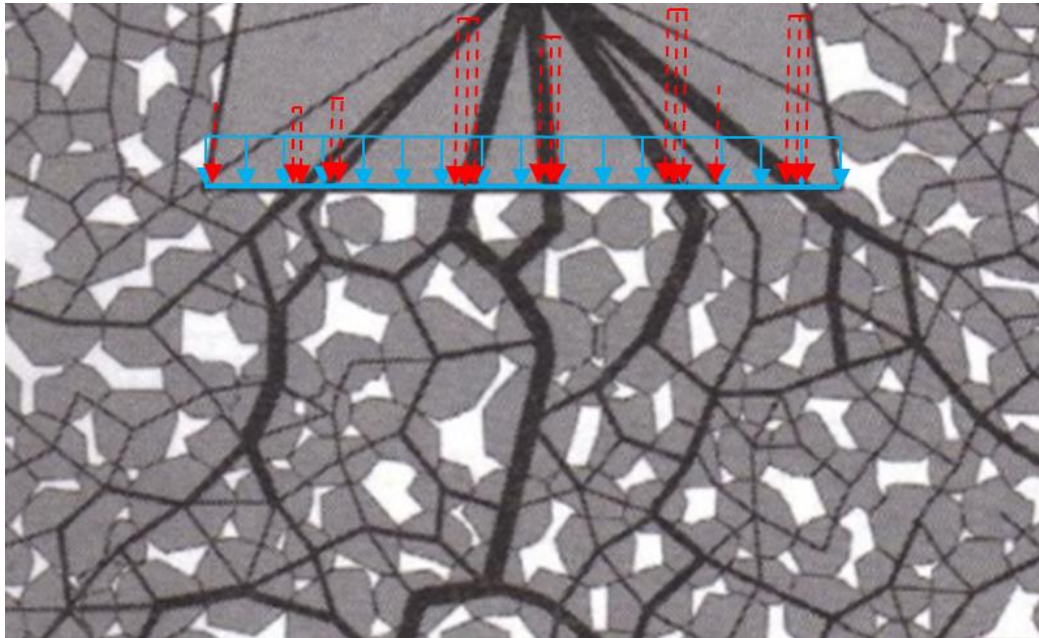
Figure 1.7 A conceptual comparison between average pressure distribution and actual pressure distribution at the ballast-tie interface (background image from Lichtberger, 2011)

In Figure 1.7, the sum of the total force acting through the cross section is the same for each pressure distribution. However, it can be seen that the actual pressure distribution may result in significantly higher loads being carried into individual ballast particles.

The low contact areas and high pressures at the ballast-tie interface are not currently designed for in American Railway Engineering and Maintenance-of-Way Association's (AREMA) Manual for Railway Engineering – the U.S. standard for recommended railroad engineering practice. Furthermore, little research has been conducted to measure the true fine-scale loading environment where the ballast contacts the tie.

Objectives and Methodology

To update the standards-of-practice and to better understand the loading environment of the tie and ballast, it is desirable to realize the true pressure distribution at the ballast-tie interface. The true pressure distribution at the ballast-tie interface accounts for the minimal contact area and the high resulting pressures on the ballast and tie components. It can be considered in three dimensions:

1) The distribution of pressure along the length of the tie

2) The distribution of pressure across the width of the tie

3) The distribution of pressure over time under dynamic loading conditions

Dimensions 1 and 2, combined, account for the areal distribution of pressure at the interface, while dimension 3 accounts for the temporal distribution of pressure on the plane defined by 1 and 2.

Current technology, namely Matrix Based Tactile Surface Sensors (MBTSS), allows all three dimensions of the ballast-tie pressure distribution to be realized. The primary aim of this research study was to develop and implement an MBTSS system to measure pressures at the ballast-tie interface of railroad track.

The following objectives of the research were identified:

1) Develop a method to protect, install and operate a Matrix Based Tactile Surface Sensor (MBTSS) system at the ballast tie interface to measure pressures during in-track testing

2) Investigate the contact area between the ballast and tie for various ballast conditions

3) Quantify the peak pressures at the ballast-tie interface

4) Realize the pressure distribution along the length of the tie and compare results with previous research

5) Develop a quantitative means to assess the roughness of the pressure distribution

6) Provide recommendations and suggestions for future research and applications of the data

Content of Thesis

Chapter 2 provides a review of the literature on the ballast-tie interface. Chapter 3 discusses the MBTSS system used in this research study and the protection of the pressure sensors. Chapter 4 presents results from preliminary calibration and validation testing for the system. Chapter 5 presents the laboratory ballast box testing conducted at the Transportation Technology Center, Inc. (TTCI). Chapter 6 highlights the development of an index to measure the roughness of the pressure distribution observed at the ballast-tie interface and presents analysis using this index from the laboratory testing. Chapter 7 presents the methods and results of the first in-track testing with the MBTSS system at TTCI's Facility for Accelerated Service Testing (FAST). Lastly, Chapter 8 summarizes the conclusions from this study and discusses recommendations for future research.

CHAPTER 2. LITERATURE REVIEW

Significance of Ballast-Tie Interface

A review of the literature confirms the importance of the pressures being carried from the tie into the ballast. Lichtberger (2011) affirms that, "the ballast pressure value under the running wheel is often regarded as a decisive factor for the development of defects in track geometry." Sato (1997) discusses a mathematical relationship between the ballast pressure and the frequency of track maintenance.

Pressure Measurement at the Ballast-Tie Interface

Studies to determine pressures at the ballast-tie interface of the track have been undertaken in the past. Previous research has focused primarily on the pressure distribution along the length of the tie, particularly as an input for tie design, and to incorporate into recommended practices.

Early Ballast-Tie Pressure Research

A.N. Talbot, as chair of American Railway Engineering Association (AREA) and American Society of Civil Engineering (ASCE) Special Committee on Stresses in Railroad Track from 1918 through 1940, is credited with much of the early work on stress measurements in railroad track. Of particular interest to this research project is the Committee's Second Progress Report, published in 1919. In this report, Talbot (1919) discusses the challenges of measuring pressures at the ballast-tie interface. He cites variability in support conditions from one tie to another, disturbance of the track while inserting pressure capsule instrumentation, and the number of pressure capsules needed to cover the length of the tie as deterrents to directly measuring ballast-tie pressures. The reader is referred to First Progress Report of the committee (Talbot, 1919) to learn more about the use of these pressure capsules.

To obtain an estimate of ballast-tie pressures, an indirect method was implemented in testing on the Illinois Central Railroad and the Chicago, Milwaukee,

and St. Paul Railroad (Talbot, 1919). The flexural curve of ties was measured under load and the relationship between flexure, bending moment, and load were used to obtain stress distributions (Talbot, 1919). The sharper the flexural curve, the higher the bending moment, and the higher the stress at the ballast-tie interface. Talbot (1919), in reference to the flexural data collected notes the variability of the support conditions observed at the ballast-tie interface:

> *"It is evident that there must be great differences in the way in which the bearing pressure varies along the length of the tie under the conditions to which ties are subjected. In many ties there is play between the tie and its bed at one point or another or even a considerable portion of its length which not only gives unevenness of track depression but increased the intensity of bearing pressure at some point along the tie and gives added bending stresses in the tie."*

Talbot (1919) also noted the prevalence of center-bound conditions in the ties tested.

Given the variability in tie flexure, Talbot (1919) presents a series of hypothetical distributions of bearing pressure on the ballast. He provides descriptions of the situations that each distribution represents. This figure with a description of each distribution is reproduced as Figure 2.1.
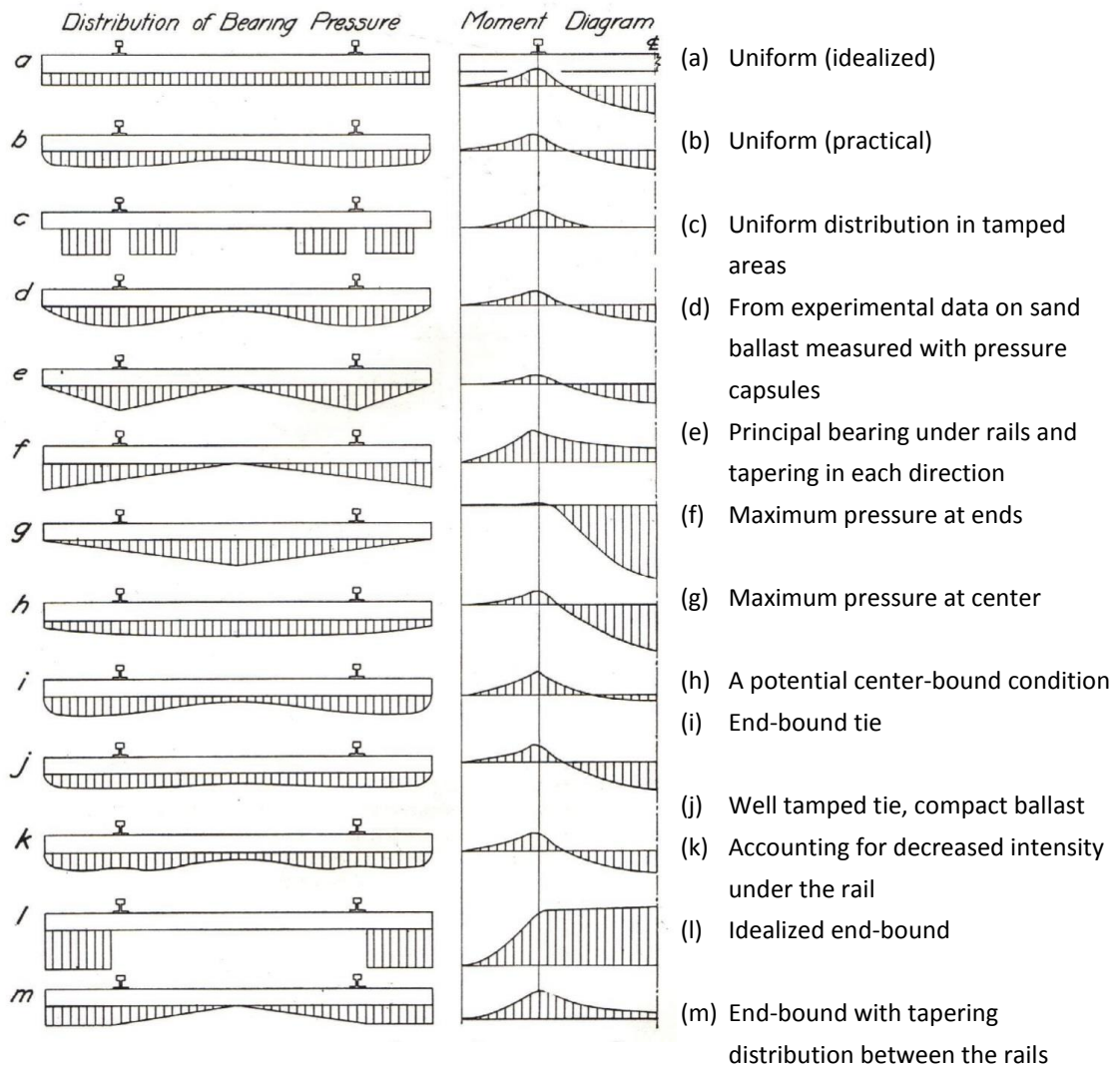
Figure 2.1 Hypothetical distributions of bearing pressure at the ballast-tie interface (from Talbot, 1919)

Measuring the Contact Area at the Ballast-Tie Interface

Recent work conducted as part of the U.S. Department of Transportation's Federal Railroad Administration (FRA) Task Order 225 in 2009, presented in an unpublished paper, titled *Evaluation of Tie Bottom Contact with Ballast and Ballast Degradation*, explores the contact area between the ballast and tie as well as ballast degradation at the ballast-tie interface. This research involved a series of laboratory tests conducted at the Association of American Railroad's Transportation Technology Center, Inc. (TTCI) in Pueblo, Colorado. In this testing, a section of tie roughly 24 inches long was placed on layer of ballast (contained in a ballast box)

and loaded vertically by a dynamic load actuator. Prior to testing, the bottom of the tie was painted black. The tie was loaded at 29 kips at a rate of 1.5 Hz. Observations were made throughout the testing regime at various numbers of cycles. The contact area was determined by photographic analysis of photos of the underside of the ties. The number of white pixels was used to indicate locations where the black paint had chipped away due to ballast contact. The underside of the concrete tie after 430,000 cycles is shown in Figure 2.2.

Figure 2.2 Section of concrete tie showing chipped off black paint in areas of ballast particle contact. (FRA Task Order 225)

Tests were performed for a conventional wood tie, a wood tie with an elastic under-tie pad, and a conventional concrete tie.

For the concrete tie, the ballast was found to be in contact with 10 percent and 15 percent of the available tie area after 215,000 and 430,000 cycles respectively. For wood tie track, the contact area increased to 30 percent and 40 percent of the available tie area after 2,000 cycles and 215,000 cycles respectively. Comparing the two tie types after 215,000 cycles, the wood tie showed 40 percent contact and the concrete tie showed 10 percent contact. It is important to note that these percentages of contact area cannot necessarily be assumed to apply to the

entire length of an in-service tie as the contact areas being measured were directly under the applied load over a short section of tie. A similar study for full length ties may indicate changes in contact area along the length of the tie. It was noted in this study that the timber tie surface deforms (indents) under loading, a common observation for ties taken out of service. Indentations are presumed to increase the effective contact area. The underside of a typical wood tie removed from service is shown in Figure 2.3.

Figure 2.3 Underside of a conventional wood tie removed from service showing indentations from ballast particles. (FRA Task Order 225)

The FRA Task Order 225 study provided some insight into the behavior of the ballast-tie interface. However, because it was conducted with only a section of tie approximately 24 inches long, the interface pressures along the entire length of a tie could not be determined. Also, the "chipped paint" method of measuring contact area could not be interpreted dynamically, thus the changes in pressure and pressure distribution over time (as load increases and decreases) could not be determined. It can only be assumed that the contact areas measured are those when the tie is fully engaged with the ballast bed, and thus at the peak of applied load. Using the observed ballast-tie contact areas, the study concludes that

> *"A reduction of tie/ballast contact area of 60 to 90 percent will raise the ballast pressures by 2.5 to 10 times above the values calculated using an elastic layer track model. Thus, the actual ballast pressures may be 100 to*

15

400 psi, rather than the calculated 40 to 50 psi for mainline track with a good subgrade. Some consideration should be given to reviewing and revising, if needed, the recommended practices for ballast pressures. For example, (the) American Railway Engineering and Maintenance of Way Association recommends a maximum ballast pressure of 80 psi for mainline track."

A 1978 study conducted by the Graz University of Technology in Graz, Austria (Henn, 1978) concluded the contact area at the ballast-tie interface for wood ties was between 4 and 10 percent and for prestressed concrete ties between 1 and 9 percent. New track was also shown to have contact areas between 0.5 and 3 percent.

AREMA Manual's Ballast-Tie Recommendations

The American Railway Engineering and Maintenance-of-Way Association (AREMA) Manual for Railway Engineering in Chapter 30 – Ties, Part 1, Article 1.3.3 presents a figure estimating the percentage of wheel-to-rail load carried by an individual tie for varying degrees of track modulus (μ), tie type, and tie spacing. This figure is reproduced as Figure 2.4.
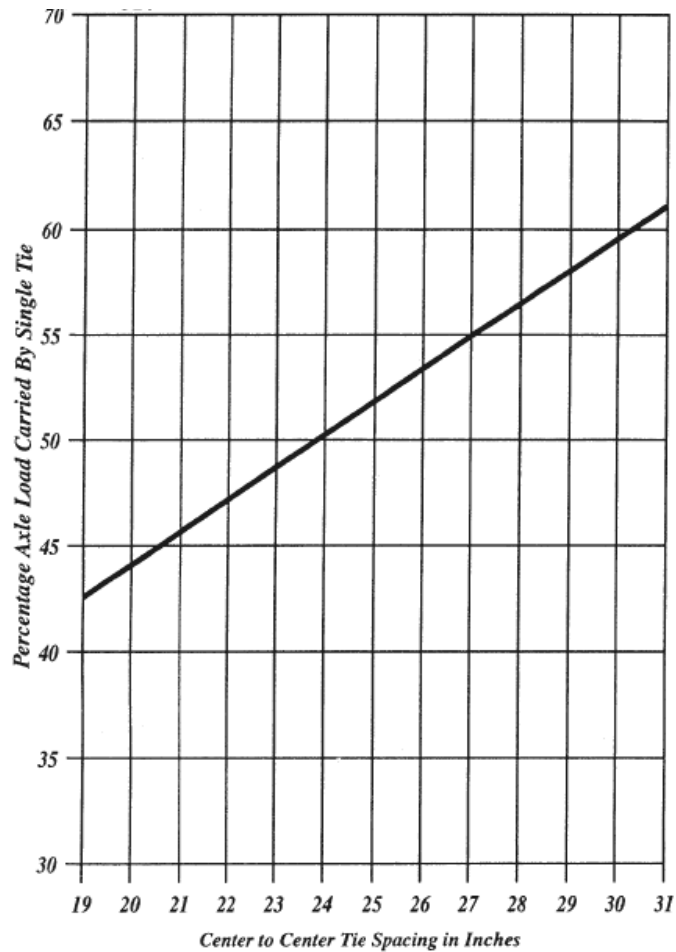
Figure 2.4 Percentage of axle load carried by a single conventional concrete tie for varying tie spacing - the distribution factor (AREMA, 2012)

The AREMA manual in Chapter 30 – Ties, Part 1, Article 1.3.6.1 affirms that tie-to-ballast pressures are not uniformly distributed across or along the bottom of a tie. AREMA recommends the average pressure at the bottom of the tie should be calculated as the axle load multiplied by distribution and impact factors and divided by the bearing area of the tie as shown in Equation 2.1 (AREMA, 2012)

$$P_{avg} = \frac{L_{axle} * \frac{DF}{100} * (1 + \frac{IF}{100})}{A}$$ (Eq. 2.1)

where P$_{avg}$ is the average bearing pressure at the ballast-tie interface, L_{axle} is the applied axle load, *DF* is the distribution factor (estimated by Figure 2.4) and *IF* is the impact factor, equal to a percentage increase over the static vertical load intended to estimate the dynamic forces due to irregularities in the wheel and rail (AREMA, 2010). *A* is the bearing area of the tie.

17

Article 1.3.6.1 notes the two differing methods presented in the Manual for Railway Engineering for determining *A*. In Chapter 30 – Ties, Part 4, Article 4.1.2.5.1.1, the effective bearing area of the tie appears to be defined as the *entire* footprint of the tie. The AREMA Manual for Railway Engineering, Chapter 16 - Economics of Railway Engineering and Operations, Part 10, Article 10.11.1 defines the bearing area of the tie as *two-thirds* of the tie footprint as shown in Figure 2.5. In Figure 2.5, L_{eff} is equal to one-third of the tie length, L.
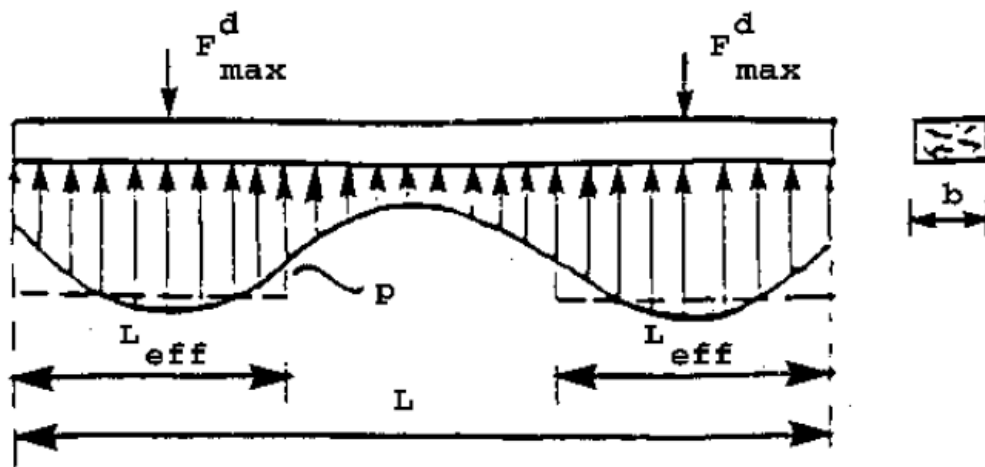
Figure 2.5 Assumed pressure distribution showing L_{eff}, the assumed length of bearing under each rail (from AREMA, 2010 and Kerr, 1989)

The recommended maximum allowable ballast pressure is also not consistent between the two AREMA chapters. Chapter 30 recommends a limit on ballast pressure of 85 psi over the entire footprint of the tie "for high-quality, abrasion resistant ballast" (AREMA, 2010). This recommendation appears to have been proposed by the old American Railway Engineering Association's Committee 10 – Concrete Ties (Zeman, 2010). Chapter 16, however, limits the maximum allowable ballast pressure to 65 psi on a smaller area (two-thirds of the tie footprint) (AREMA, 2010). This effectively makes Chapter 16's recommendations of ballast pressure limits 50 percent lower than Chapter 30's. No explanation appears to be given to justify these limits. Considering their context, it appears that the Chapter 30 recommendations are developed for existing track, while the Chapter 16

recommendations are more suitable for new construction. Hay (1982) notes that 65 psi is the limit on the ballast pressures for wood tie track and that 85 psi, similarly, is the limit for concrete tie track.

Justification of Two-Thirds the Tie Footprint

Two-thirds of the tie footprint is typically justified as the area of the tie that is considered tamped during surfacing maintenance, and thus the area in bearing. Figure 2.6, reproduced from Lichtberger (2011), shows the density of ballast compaction relative to the areas conventionally tamped.
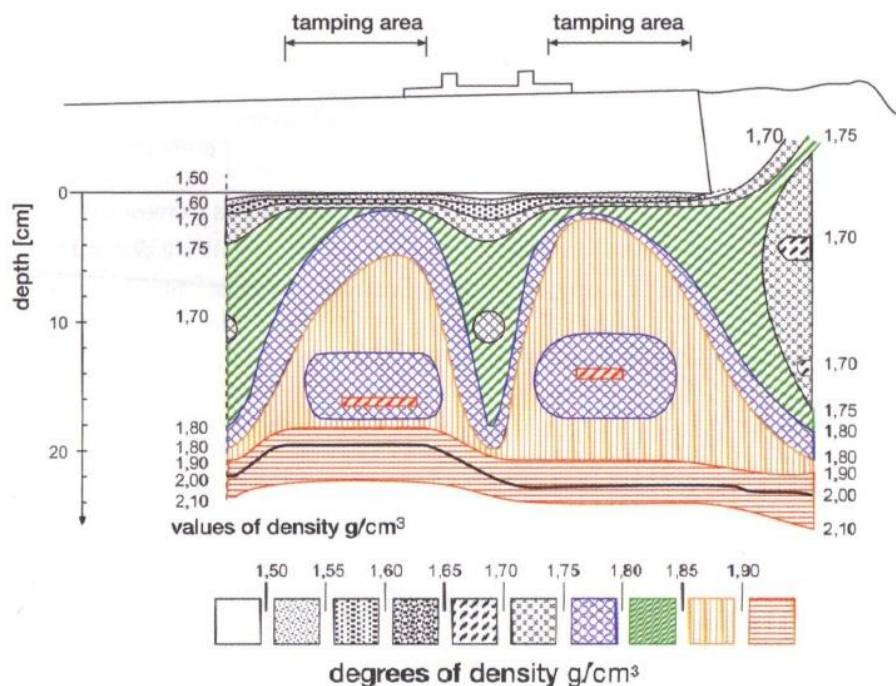
Figure 2.6 Ballast density and the corresponding influence of tamping (Lichtberger, 2011)

It is interesting to note in Figure 2.6, the relatively low compaction of ballast directly below the rail. Figure 2.1 (k), idealized to a greater extent in Figure 2.1 (c), depicts a reduction of bearing pressure directly beneath the rail. The concept of reduced bearing pressure directly beneath the rails, more recently, has been explored by Giannakos (2011), asserting that the stress distribution corresponding to the

19

maximum moments actually measured in track is parabolic in nature, and not uniform.

Techniques to Reduce Ballast-Tie Pressures

To combat the high pressures between individual ballast particles and the tie, various commercially-available elastic under-tie pads have been developed and implemented, primarily on European railways. These pads are simply an additional layer of elastic material placed underneath the tie. They are typically cast into concrete ties before they have cured. Two companies that manufacture such pads, Getzner (headquartered in Bürs, Austria) and CDM (headquartered in Overijse, Belgium), both claim the under-tie pads increase contact area between the ballast and tie (thus reducing pressures on the ballast) and mitigate noise and vibration due to passing trains (Getzner, 2013 and CDM, 2013). Interest in elastic under-tie pads has grown in North America. Akhtar et al. (2006) present North American applications of elastic under-tie pads to reduce stress on concrete deck bridges, for example.

Another technique used to reduce pressures on the ballast involves the use of "frame" ties or "half frame ties as shown in Figure 2.7. These types of ties operate on the principal of increased contact area with the ballast directly under the rail. Akhtar et al. (2012) discuss ongoing testing of half-frame ties at TTCI.

(a)   (b)

Figure 2.7 (a) frame ties (from Lichtberger, 2011) and (b) half-frame ties at TTCI

Lichtberger (2011) recommends the use of smaller aggregate and/or "soled" ties to increase the effective contact surface between the tie and ballast. He states, "The higher the number of contact points, the better the load transmission mechanism and the slower the initial deterioration under the first traffic after maintenance." A figure presented by Lichtberger (2011), showing the contact forces at the ballast-tie interface and between individual ballast particles, is reproduced in Figure 2.8. Line thickness can be considered proportional to the magnitude of force being represented.
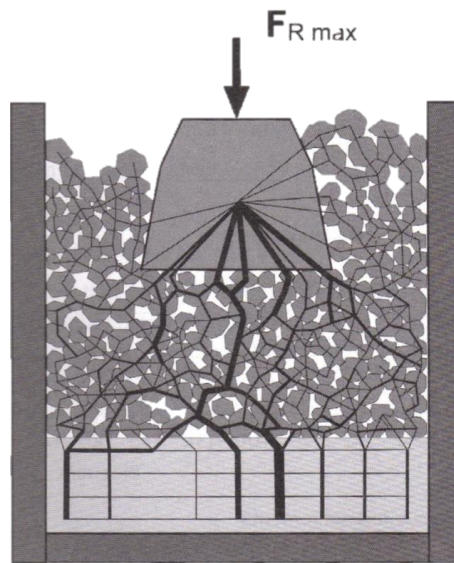
Figure 2.8 Conceptual figure of the contact forces between ballast particles and at the ballast-tie interface (Litchberger, 2011)

It is clear, based on this figure, that the forces acting on the ballast particles could theoretically be reduced by having more particles (hence smaller particles) to carry the load.

Related Research Using Thin Film Pressure Sensors

Previous research has demonstrated the capability of thin film pressure sensing technology in a wide range of related applications. Marshek et al. (1986) used a pressure sensitive film to measure the static pressure distribution under a truck tire. Marsili (2000) used polyvinylidene fluoride (PVDF) film to study the normal pressure distribution between tires and the ground. Christian (2005), and

21

Anderson (2005) used Matrix Based Tactile Surface Sensor (MBTSS) technology to also measure pressures between vehicle tires and pavement. Paikowski and Hajduk (1997) studied the use of MBTSS in granular materials for geotechnical engineering research.

For railway applications, MBTSS technology has been limited to use in the rail seat area of the track, specifically in the study of rail seat deterioration on concrete ties at the University of Illinois (Rapp et al., 2012), and beneath conventional steel tie plates on wood ties (Stith, 2005 and Rose and Stith, 2005) at the University of Kentucky. There has been no previous application of MBTSS technology for study of the ballast-tie interface. The use of MBTSS at the ballast-tie interface represents a novel application of the technology to accomplish the objectives of this research study.

CHAPTER 3. THE MATRIX BASED TACTILE SURFACE SENSOR SYSTEM

Accurate measurement of the true pressure distribution at the ballast-tie interface requires a nonintrusive, durable, and reliable sensing system. As one of the primary objectives of the research was to measure the peak pressure and contact areas at the ballast-tie interface under loading, a sensor was needed with a high enough resolution to observe the small contact areas of individual ballast particles. The sensing technology employed also had to be functional over a wide range of anticipated forces. Matrix Based Tactile Surface Sensor (MBTSS) technology was chosen as it could be adapted to meet these requirements.

MBTSS System Components

The MBTSS system used for this study is manufactured by Tekscan, Inc. Tekscan manufactures pressure sensors and pressure mapping systems for use in a wide range of fields including dentistry, automotive, and healthcare applications (Tekscan, 2013). The Tekscan pressure mapping system consists of pressure sensors, a data acquisition handle, and a PC running Tekscan's *I-Scan* software.

The thin film pressure sensors are composed of conductive silver ink printed onto thin polyester substrate sheets. Two sheets, one printed with conductive rows and the other printed with conductive columns, are sandwiched together in the manufacturing process to create a matrix. A pressure sensitive semi-conductive material is place on the inner surface of the conductive rows and columns. Figure 3.1 shows a schematic of the sensor manufacturing process.
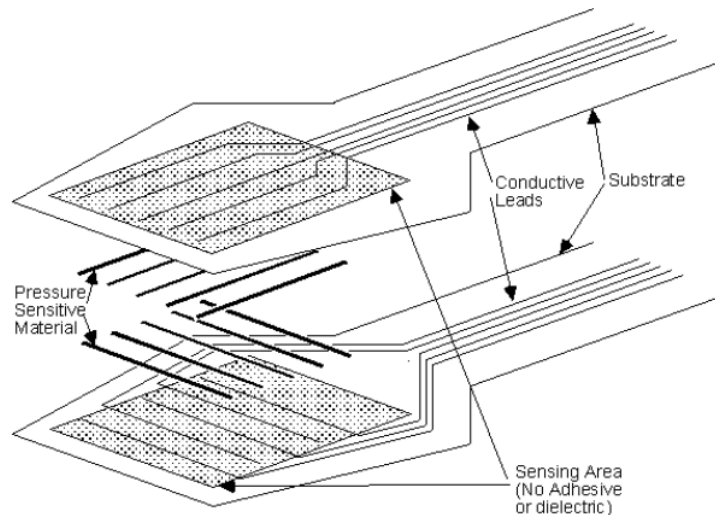
Figure 3.1 Schematic of the manufacturing of a Tekscan pressure sensor (Tekscan, 2012)

The intersection of a row and column creates one point on the matrix called a sensel. Sensels are the locations where pressure is measured. They can be thought of as "pressure pixels." A sensel records the magnitude of force, which is then divided out over the surface area of the sensel to obtain pressure. While collecting data, an individual row and column are excited with a known voltage. This isolates one particular sensel. The change in resistivity is recorded at each sensel as the entire matrix is scanned. As pressure is applied or released at a given sensel, the resistance in that sensel's circuit changes. A data frame consists of the output of every sensel on the sensor at a given time. The Tekscan system is an 8-bit system. As such, force at each sensel is output as a raw unit ranging from 0-255. This arbitrary unit is called *raw sum*. The total *raw sum* for a data frame is equal to the summation of the *raw sum* output of each sensel on the sensor.

A Tekscan handle, shown in Figure 3.2, serves as the data acquisition device. It is clamped onto the electrical leads of the sensor.

<div align="center">(a)   (b)</div>
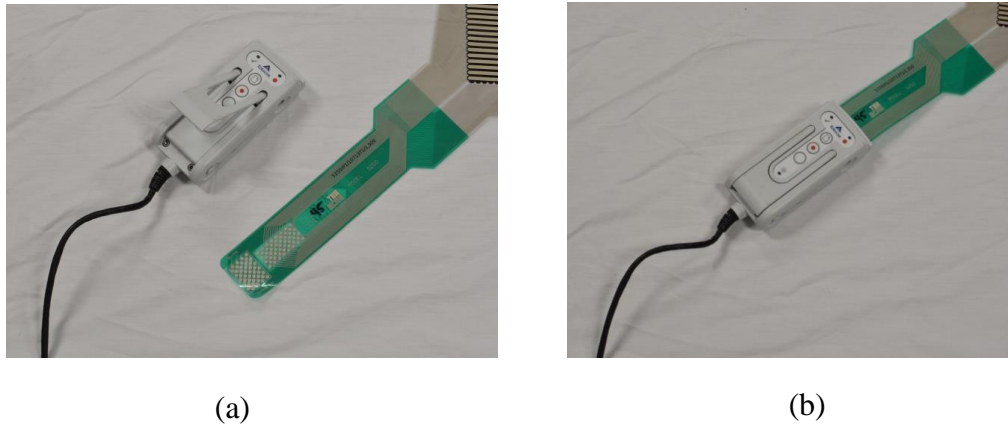
Figure 3.2 (a) A Tekscan *VersaTek* handle and (b) the handle connected to a sensor

The handle is tethered to a computer running Tekscan's proprietary *I-Scan* software. The handle provides the sensor excitation, analog to digital signal conversion, and controls the scanning frequency and sensor sensitivity. The scanning frequency and sensor sensitivity are input through the *I-Scan* software's graphical user interface. The *I-Scan* software allows real time observations of sensor output, data collection (recording), and basic data analysis including: total force and pressure, force and pressure at each sensel, center of force, peak pressure, and contact area. The software also allows single point (linear) and two point (nonlinear) sensor calibration without the need to export the data to an external program. For more advanced, customized analysis, data can be exported from the *I-Scan* program in ASCII format for use in an external spreadsheet application such as Microsoft Excel or a user-executed program. Within the *I-Scan* software, data is viewed as a *movie* (a video of the sensing area over time) showing the magnitude of pressure on a 16 color scale. *Movies* are simply a series of individual frames. When collecting data, the user inputs the number of frames to be collected for a *movie* and at what frequency they are collected. Figure 3.3 is a screenshot of the *I-Scan* program showing a *movie* frame (data frame) and a typical force versus time plot that can be generated in-software. For a more detailed explanation of the *I-Scan* software's capability, the reader is referred to the *Tekscan I-Scan and High Speed I-Scan User Manual* (2012).
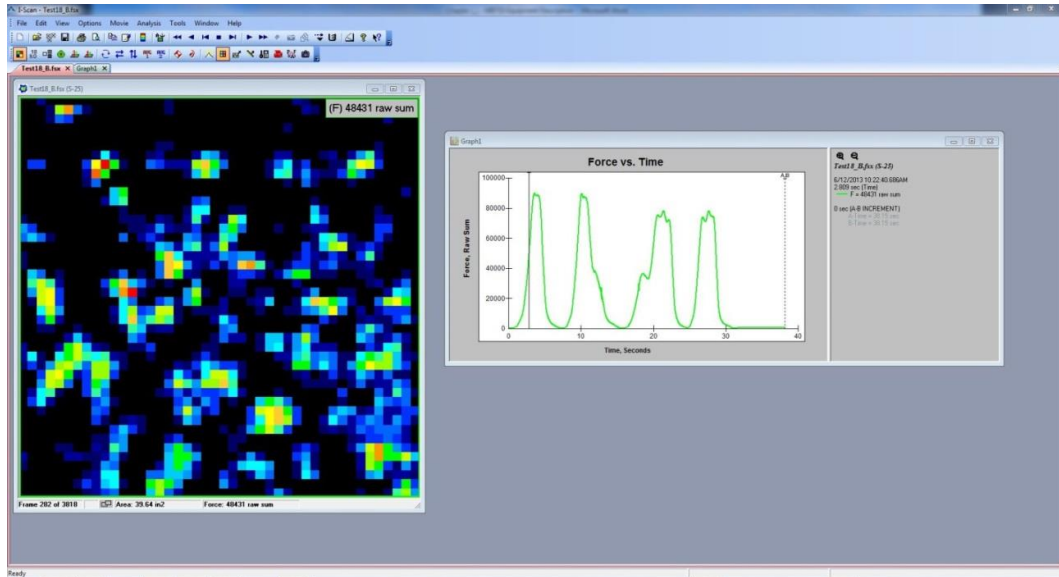
Figure 3.3 Example Screenshot of I-Scan Program showing movie frame on the left and Force versus Time Plot on the right

Sensor Selection

Tekscan manufactures off-the-shelf sensors in a variety of shapes and dimensions. Custom sensors can be designed as well. Tekscan model number 5250 sensors were used for the study. The 5250 sensor's dimensions are shown in Table 3.1. These dimensions correspond to those shown in Figure 3.4. Figure 3.5 shows a photo of a 5250 sensor and Figure 3.6 shows a detail of a sensel on the 5250 sensor.

Table 3.1 Tekscan 5250 Sensor Specifications

Overall Length (in.)	24.51
Overall Width (in.)	14.11
Matrix Height (in.)	9.68
Matrix Width (in.)	9.68
Sensing Area (in^2)	93.7
Row Width (in.)	0.13
Row Spacing (in.)	0.22
Number of Rows	44
Column Width (in.)	0.13
Column Spacing (in.)	0.22
Number of Columns	44
Number of sensels	1936
Sensel Density (resolution) (sensels/in^2)	20.7/in^2
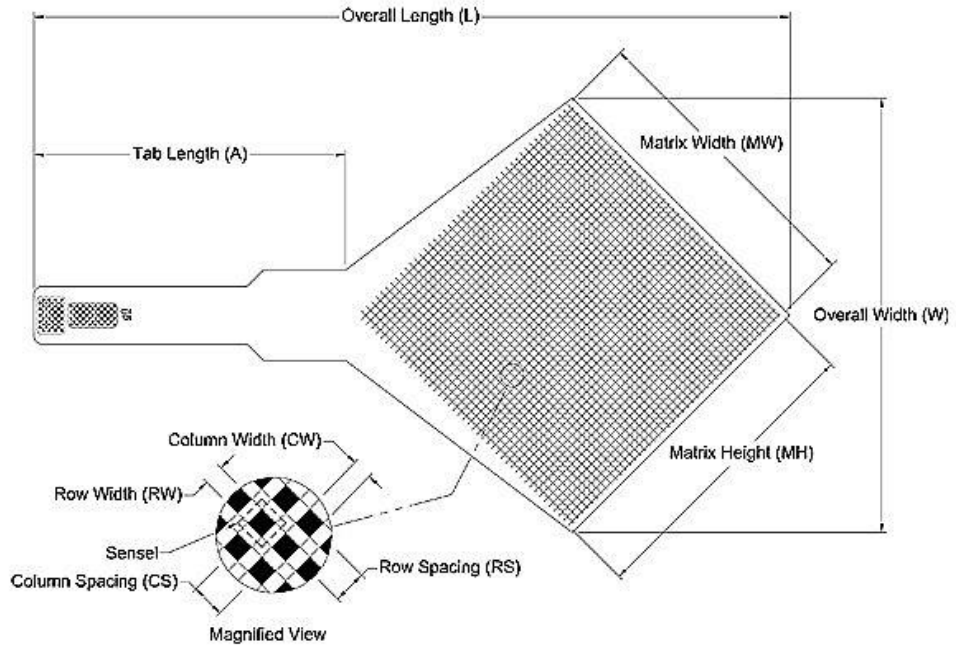
Figure 3.4 Tekscan 5250 Sensor Geometry
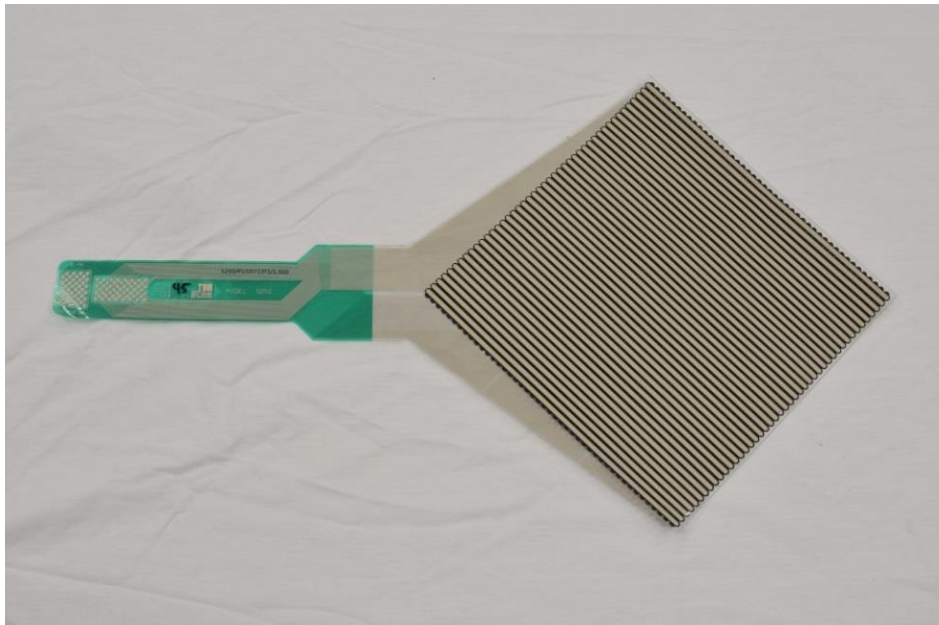
Figure 3.5 Photo of Tekscan 5250 Sensor

One *sensel*
Area = 0.0484 in^2
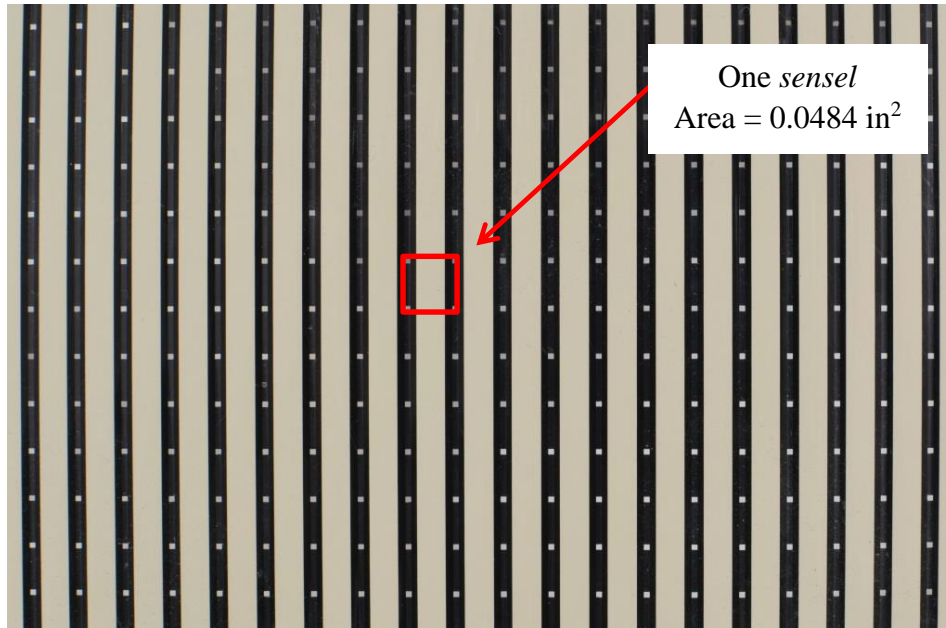
Figure 3.6 Detail photo of a sensel on a 5250 sensor

For a standard, off-the-shelf sensor, the 5250 provides a suitable balance between sensing area and resolution (sensels per area). A single data acquisition handle is capable of reading up to a 44 by 52 matrix of sensels (2,288 sensels) on an individual sensor. Additional handles are required to collect data from a sensor with more than 2,288 sensels. Thus, the 5250 model's 1,936 sensels use about 85% of the capacity of the connected handle. The matrix width of 9.68 inches allows the sensor to cover the entire underside of a conventional timber or composite tie. For a conventional concrete tie with a width of 10.5 inches, the 5250 leaves 0.41 inches on either side of the sensor. This was considered acceptable as customized sensors would have exceeded the project's budget. Using a standard sensor size decreased the cost per sensing elements. As one of the primary concerns of implementing the system at the ballast-tie interface was sensor durability and longevity, more sensors allowed for more data to be collected before sensors were overly damaged.

The location of the handle relative to the sensing area also needed to be considered. It was desirable to locate the handle away from the tie to reduce the potential of damage. For the 5250 model, the location of the sensor's electrical leads on the diagonal of the sensor allows for an attached handle to be placed level in an

excavated crib adjacent to a test tie in the track (see Figure 7.5 and 7.6). This resulted in little bending or twisting of the sensor's electrical leads when connected to the handle and easy connection of the handles in the field. Based on these considerations, the 5250 sensor proved suitable for application at the ballast-tie interface.

Sensor Sensitivity

The Tekscan *I-Scan* software allows for adjustment of the sensors sensitivity to applied force. A range of sensitivities (S-1, S-2, S-3… through S-40) can be applied. Figure 3.7 shows the same load applied to the same sensor set at four different sensitivity levels.

    (a) S-7   (b) S-25   (c) S-35   (d) S-40
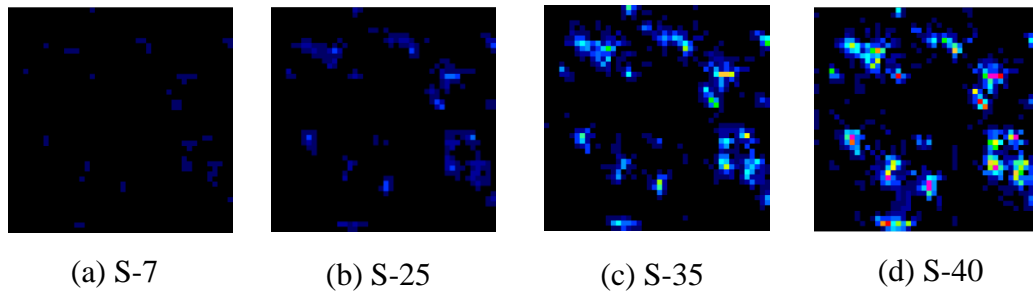
Figure 3.7 Four data frames showing the effect of sensitivity on sensor output

Note that in Figure 3.7 (d), the sensor's output has been saturated (indicated by pink colored sensels), and additional increases in load cannot be observed. A saturated sensel indicates an output of 255 *raw sum*, the capacity of the 8-bit output. The goal in selecting a sensitivity setting for a sensor is to maximize the range of sensel output (0-255 *raw sum*). Thus, in selecting a sensitivity level, it is desirable to know the maximum anticipated load on the sensor. With this maximum anticipated load applied, the sensitivity can be tuned up or down to utilize the most of the 8-bit capacity of each sensel. For example, if the maximum anticipated load were being applied in Figure 3.7, S-35 would be a suitable selection of sensitivity. Two datasets collected from a sensor can only be compared if they were collected at the same sensitivity level. A review of the literature did not find a relationship to convert data at one sensitivity level to another sensitivity level. It is not known whether the

sensitivity settings are a linear scale or if the relationship is more complex. The development of such a relationship, while outside the scope of this research, would be useful.

Sensor Pressure Range

Additionally, Tekscan sensors, including the 5250 model are manufactured in a variety of pressure ranges. The pressure range of a given sensor approximates the pressure at which it becomes saturated at a nominal sensitivity setting. The 5250 model sensors used for this research study were either 1200 psi or 1500 psi sensors. Because the I-Scan software allows on-the-fly adjustment of sensor sensitivity, only a rough estimate of the pressure range to be encountered is necessary. Essentially, the adjustable sensitivity allows a lower pressure range sensor to behave like a sensor with a higher pressure range and vice versa.

Further information on selecting a Tekscan sensor for a particular application can be found in the *Tekscan Industrial Sensor Catalog Introduction*.

Multiple Tekscan Data Acquisition Devices

It should be noted that while Tekscan's pressure sensors all operate on the same principle, there are numerous data acquisition systems that can be connected to a given sensor. These include the *Evolution* handle and the *VersaTek* handle. The *Evolution* system is capable of recording a 5250 sensor at 100 Hz. It is tethered to the PC through a single USB cable. The *VersaTek* system is designed for higher scanning rates, up to 750 Hz with the 5250 sensor. The VersaTek handle is tethered to the PC through a hub as shown in Figure 3.8. The hub does require an external power source in addition to the power required for the PC. Both the *VersaTek* and *Evolution* systems were used in this research. For a given sensor set at a given sensitivity under a given load, the two systems do not output the same raw sum value. It is recommended by the manufacturer to maintain consistency in the type of handle used.
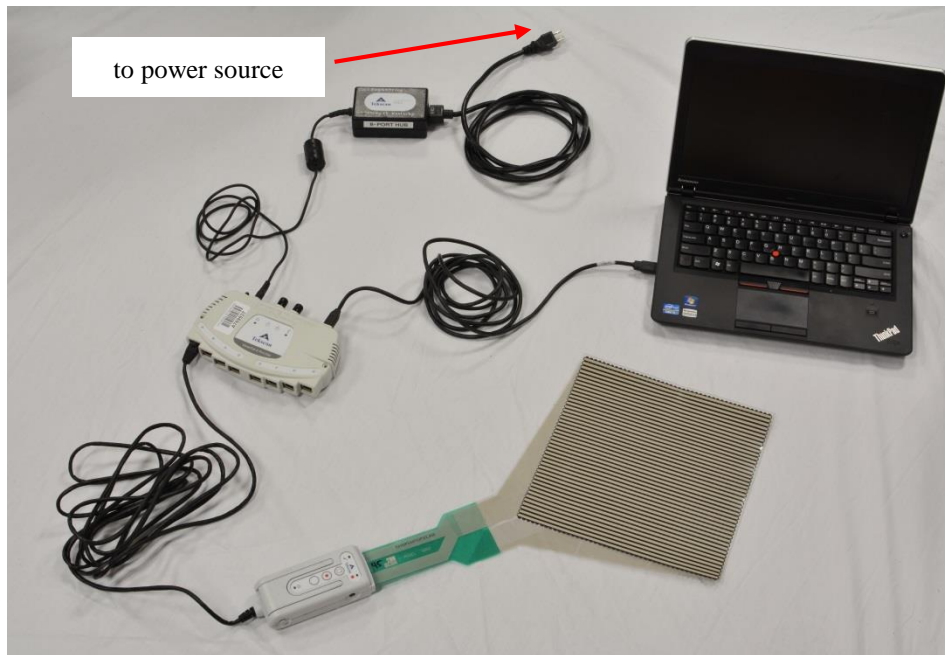
Figure 3.8 – Tekscan *VersaTek* data acquisition system showing sensor, handle, hub, power cord, and USB connection to a laptop PC

Sensor Durability and Protection

No prior use of MBTSS sensors at the ballast-tie interface was found in the review of literature. MBTSS sensors are typically used to measure uniform and/or smooth loading distributions relative to those anticipated for a surface of railroad ballast.

Being a non-uniform, rough contact surface, the ballast-tie interface application of MBTSS requires careful attention to the protection of the sensor component. Given the loading environment, the time limitations for testing, the need to install and remove the sensors on multiple ties throughout a testing regime, and the project's budget, it was determined that the protection layers needed to meet the following criteria:

1) Elastic

2) Consistent for each passing wheel load

3) Sufficiently thick to prevent sensor puncture, abrasion, or creasing

4) Sufficiently thin to allow maximum resolution of ballast particle loads and remain nonintrusive

5) Easily installed and removed in track and laboratory test setups

6) Economical

Sensor Protection versus Resolution

Any protection layer will tend to have the effect of distributing small point type loads over more area of the sensor. The thicker and stiffer the protection layer, the more this effect can be observed. Thus, the design of a protection scheme for the MBTSS sensors is a balance between sensor resolution, and sensor protection as shown in Figure 3.9. Maximum resolution in Figure 3.9 refers to the maximum resolution of an unprotected sensor – in the case of the 5250 model, 1,936 sensels in the sensing area. Minimum resolution implies that the sensor would effectively act as a single, large sensel, much in the way a single pressure cell works. In this case, the thick protection would evenly distribute the rough surface load such that when it reached the sensor, only an average pressure could be recorded.
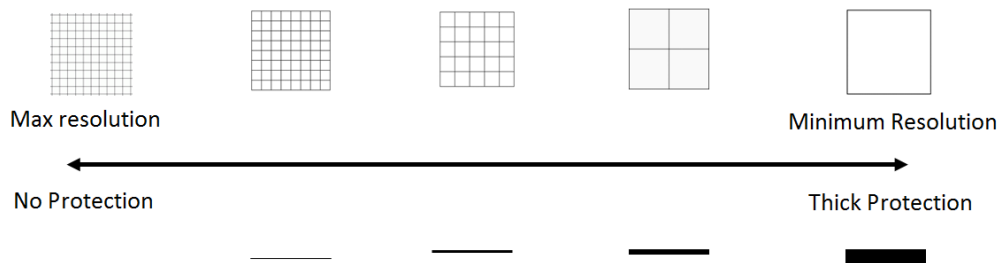
Figure 3.9 Conceptual figure depicting the balance of sensor protection and sensor resolution

Initial Durability and Protection Testing

To implement the system in the harsh loading environment beneath the tie and to best determine a means of protection, it was first necessary to understand the damage that might be caused to the sensors. Four inoperable, but otherwise undamaged, sensors were obtained. These four sensors were installed beneath a conventional concrete tie at the Facility for Accelerated Service Testing (FAST)

loop at the Transportation Technology Center, Inc. (TTCI) – each with a different protection scheme, as shown in Figure 3.10 and Table 3.2. Figure 3.11 shows the location of the sensors in-track after installation. The location of the sensors was chosen randomly, and while lower loads may be expected towards the center of the tie, the author felt as though the loads would be sufficient enough to qualitatively assess protection performance.
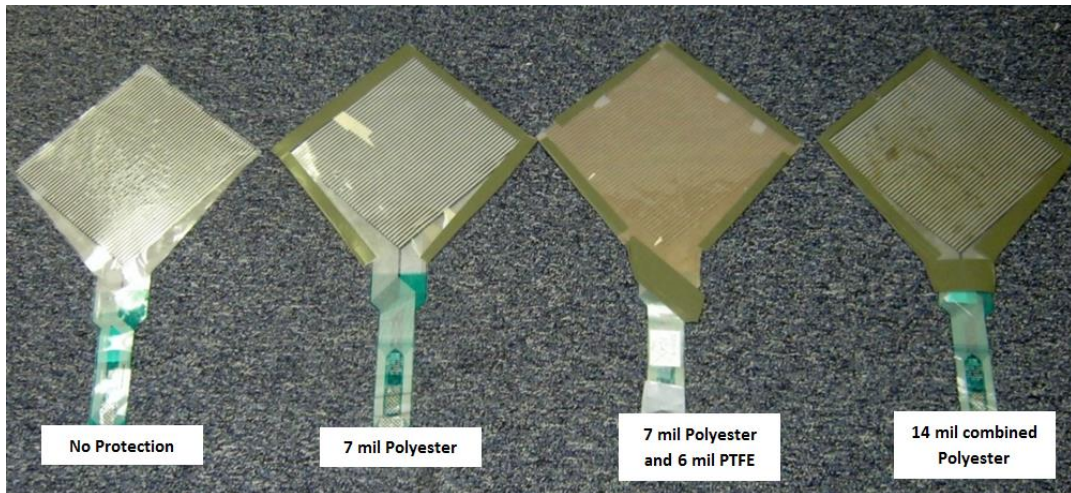
Figure 3.10: Four inoperable MBTSS sensors. From Left to Right: Sensor 0.1, 0.2, 0.3, and 0.4

Table 3.2 Initial Protection schemes tested

Sensor	Protection on Each Side of Sensor
0.1	No protection
0.2	7 mil Polyester
0.3	2 layers of 7 mil Polyester (14 mil total)
0.4	6 mil of PTFE against sensor and 7 mil of Polyester

Figure 3.11 Installation of inoperable MBTSS sensors to qualitatively test various protection schemes

To install the sensors, the crib ballast on either side of the tie was removed and the track jacked up slightly to allow the sensor/protection sandwiches to slide under the tie. The sensors, along with their protection, were taped to the tie to ensure that they would not shift. The initial test protection schemes shown in Table 3.2 were chosen based on previously used MBTSS protection materials in high load environments (Rapp et al., 2012 and Stith, 2005). It was decided to test the application of a polytetrafluoroethylene (commonly known as PTFE or Teflon) sheet on either side of one of the sensors as this had been shown in previous research to reduce shear forces on the sensors (Rapp et al., 2012 and Stith,2005). It was not known how influential shear forces would be on the sensor at the ballast-tie interface.

After installation, ballast was placed back in the cribs. The sensors remained in track for two nights of traffic on the FAST loop, roughly 3.4 million gross tons (MGT) of cumulative loading. This provided a realistic and harsh loading environment to test the MBTSS sensor protection schemes. Following the loading

period, the sensors were removed from the track and examined. Figure 3.12 shows the sensors after removal.

It was observed that neither the 7 mil polyester, nor the combined 14mil polyester, was sufficient to protect the sensor from puncture due to high ballast particle loads. Furthermore, plastic deformation (indentations) or abrasions due to ballast particle contact were observed. The plastic deformation was not desirable in a protection scheme as the protection needed to be reusable over numerous tests, and indentations had been observed to affect the output of the sensor unpredictably. On sensor 0.2, a fold developed in a corner of the sensor. This fold appeared to correspond to an indentation in the concrete tie. It was also observed that the PTFE layer on Sensor 0.4 did not significantly contribute to the protection of the sensor as it too, was punctured. Shear forces at the ballast-tie interface, if any, were not observed to affect the sensors. Further research may be necessary to determine the magnitude of shear stress acting at the ballast-tie interface under loading. Based on the results of this rough, qualitative test, polyester sheets were ruled out as a potential protection material.
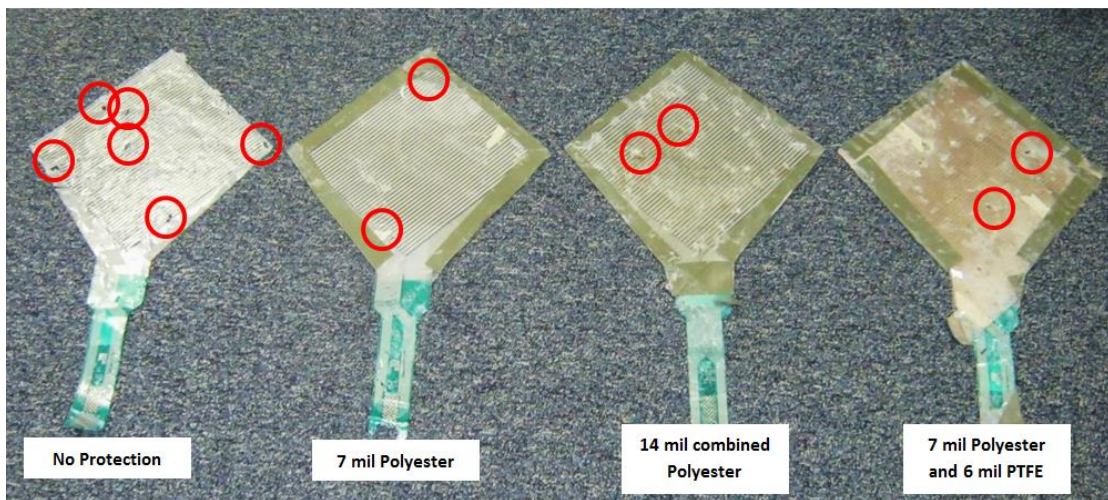
Figure 3.12 Test sensors after 3.4 MGT of traffic beneath a concrete tie on the FAST loop. Punctures and significant damage locations are circled in red.

Protection Recommendations

Through discussions with the manufacturer, it was determined that rubber may be the best protection material for the sensors in this application. To follow up

on this suggestion, a series of laboratory ballast-box tests were carried out to assess the performance of various thicknesses and hardnesses of rubber protection for the sensors. Laboratory testing allowed the applied load and sensor condition to be more closely monitored.

Rubber sheets of 50A and 70A Shore durometer hardness were tested in thicknesses of 1/64 inch, 1/32 inch, 1/16 inch and 1/8 inch respectively. Inoperable sensors were used to test the qualitative performance of the various thicknesses of rubber and hardness. A 25 inch long by 25 inch wide ballast box was filled with a new, conventional granite ballast to a depth of roughly 18 inches. New ballast was used, as the author felt it represented the harshest possible loading conditions that could be expected during data collection. The ballast box was installed in a load frame. A customized fixture that simulated the rail was attached to the load actuator. A section of a conventional concrete tie, 24 inches long, was attached to this fixture using a Pandrol type shoulder and customized fastening system. Directly beneath the rail seat at the ballast-tie interface, a test sensor (with its respective thickness of protection) was placed for each test. Chapter 5 discusses this test setup in more detail. Each test consisted of 200 cycles of a 20 kip load applied at a rate of 1.5 Hz. The performance of a particular thickness of rubber was qualitatively assessed after each test noting punctures, indentations, or other damage on the sensor.

The use of 1/64 inch, 1/32 inch and 1/16 inch rubber sheets on the ballast side of the sensor resulted in sensor damage including punctures and indentations. It was observed that at least 1/8 inch of rubber thickness was required to adequately protect the sensors. The 50A durometer rubber, while more compliant, appeared to be more prone to puncture. At least 60A durometer rubber is recommended if its thickness is 1/8 inch. Less thickness was needed on the tie side of the sensor, as the bottom side of the test tie was not as rough as the ballast surface. It was anticipated that field test ties would be similar. Qualitatively, based on the results of this testing, it was determined that 1/16 inch rubber on the tie side and 3/16 inch rubber on the

ballast side should be used as the standard protection scheme for the research. Figure 3.13 shows a 5250 sensor with this protection scheme.
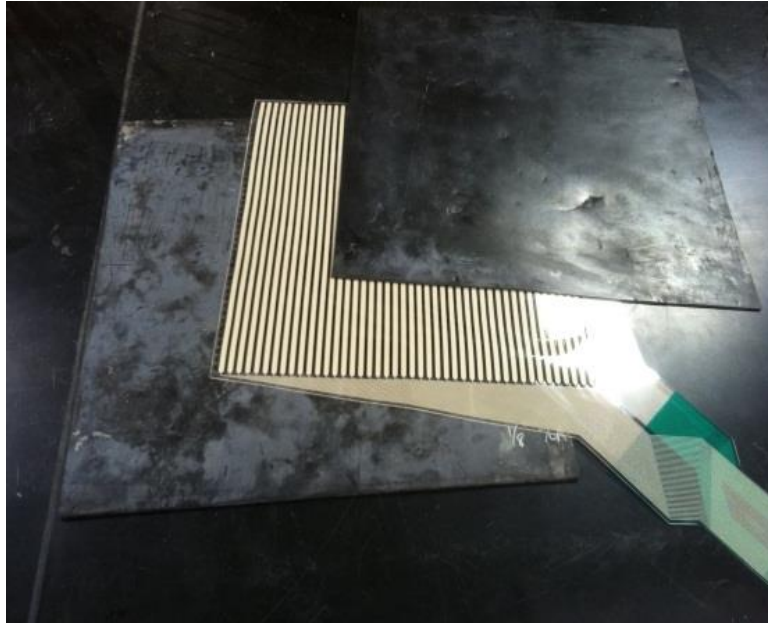
Figure 3.13 5250 sensor with 3/16 inch rubber below, and 1/16 inch rubber above

It is extremely important to note that the thicker rubber protection has the effect of distributing the pressures across more area of the sensor. While the net force being carried through the sensor would be the same, the presence of the 3/16 inch rubber protection on the ballast side of the sensor tends to reduce the magnitude of peak pressures and increase the contact area compared to a thinner rubber protection or no protection at all. The theoretical contact area between the tie and the ballast will always be less than the contact area observed on the MBTSS sensor because of the protection layer. For information from the manufacturer on sensor shim stock and protection, the reader is referred to *Tekscan I-Scan Pressure Measurement System Help File, Appendix: Equilibration & Calibration Practical Suggestions* (2012). Chapter 4 covers the calibration of the MBTSS system for use at the ballast-tie interface.

CHAPTER 4. CALIBRATION AND VALIDATION OF THE MBTSS

Calibration

Calibrations are required to convert force and pressure outputs in arbitrary units (*raw sum)* to outputs in terms of engineering units. Calibration of the sensors requires applying a known load acting through the sensor and developing a relationship between this applied load and the sensors output in *raw sum*. This is typically presented as a calibration curve with *raw* sum on the x-axis and applied force (e.g. in pounds) on the y-axis.

Contact Area Output

It should be noted that the contact area output of the sensor does not need to be calibrated for. As previously stated, contact area is calculated as the sum of all sensel areas, whose sensels are in contact. A sensel is considered in contact if its output is greater than a user specified threshold (e.g. 3 *raw sum*). Varying the threshold essentially controls the sensors sensitivity to low magnitude forces. A sensel whose output is lower than this threshold does not have its sensel area contributed to the total contact area for the sensor. If the output of an individual sensel is below this threshold, it is not counted towards the total *raw sum* of a frame either.

In-Software Calibration

The Tekscan *I-Scan* software is capable of performing either a linear calibration or two-point (nonlinear) calibration for a sensor. These methods require interpolation between points when obtaining the calibration curve. The calibration can be saved and applied to data from that sensor in the future. The in-software calibration of Tekscan sensors is useful if all analysis being performed will also be in-software, or if the anticipated range of applied force is relatively small. More involved calibrations were conducted for this research due to the large anticipated range of forces. These calibrations involved multiple thousands of points.

Considerations for a Calibration for the Ballast-Tie Interface

The anticipated rough contact between the ballast and tie and the large range of load magnitudes expected (especially for sensors under the rail), required the

development of a unique calibration procedure. A single calibration method was sought that could accurately calibrate the MBTSS sensors for a range of loads, ballast conditions, and contact areas. As with the calibration of any instrumentation, it is desirable to replicate, in calibration, the conditions expected during testing. This consideration holds especially true for the Tekscan pressure sensors. The calibration process must replicate the range of load magnitudes, sensor protection, and contact surface encountered during testing. The same protection scheme must be used in calibration and testing, as well. As a general matter, anything that can be replicated in calibration, should.

It was originally considered to calibrate the sensors against a bed of ballast similar to the ballast that would be expected to be encountered in the field. However, a consistent calibration test was needed, and multiple contact surfaces were anticipated to be encountered. In order to consistently control the contact area and roughness of the contact surface, a machined aluminum waffle plate was implemented. The squares machined into the plate are intended to mimic the individual contact points of the ballast surface. Figure 4.1 shows the waffle plate with 0.5 inch squares used for the calibration testing.
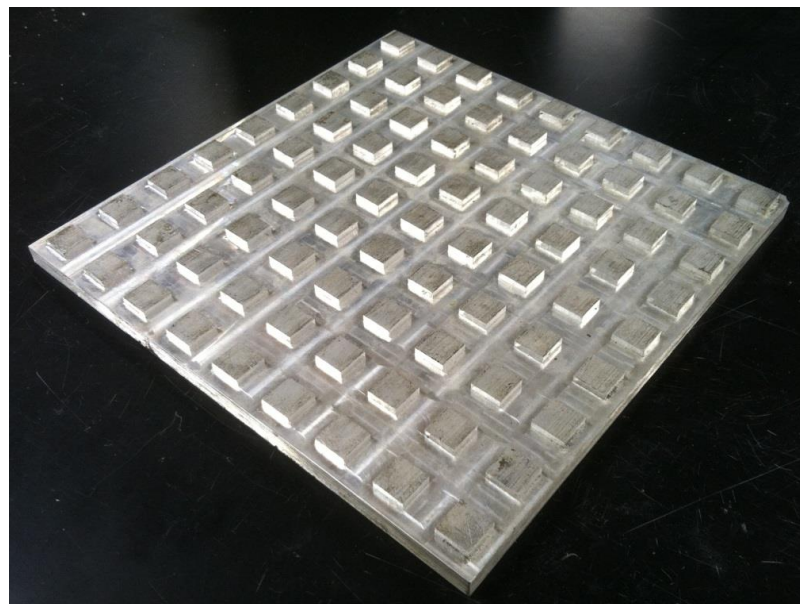
Figure 4.1 The 0.5 inch waffle plate

The 0.5 inch waffle plate was designed such that the applied load would act entirely within the active area of the sensor. The plate measures 9 inches by 9 inches and has 81 raised squares, 0.5 inches by 0.5 inches that are placed 1 inch on center.

Calibration Procedure

Calibration tests were completed using a load frame and an actuator to supply the known load. Figure 4.2 shows the calibration setup in the load frame.
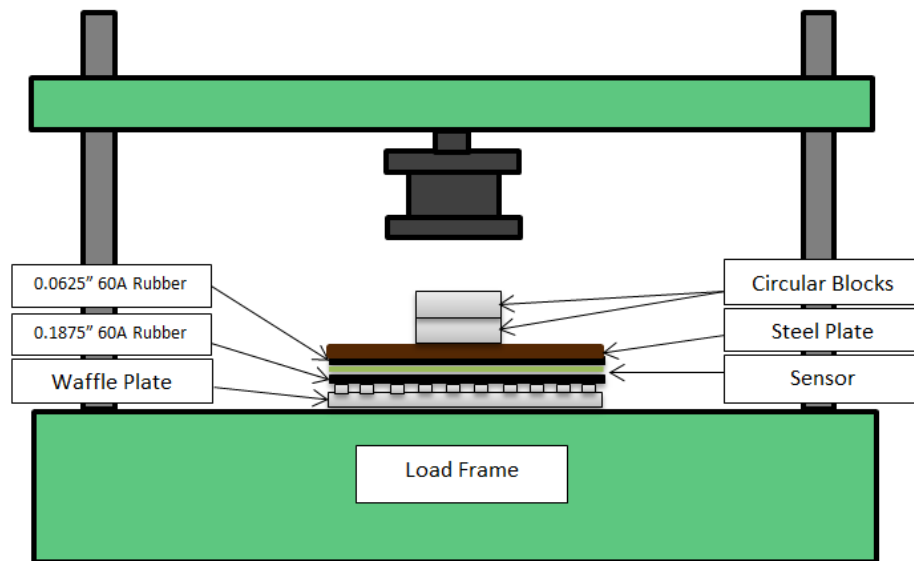
Figure 4.2 Calibration testing setup

To distribute the load from the actuator through the sensor, a series of circular blocks were used. A steel plate was used to evenly distribute the load across the sensor and waffle plate. The protection layers, 1/16 inch 60A rubber on the tie side of the sensor, and 3/16 inch 60A rubber on the ballast side of the sensor, were identical to those to be used for testing.

Calibration tests were performed using the 0.5 inch waffle plate. To perform a calibration test, the waffle plate/sensor/rubber stack was placed on the lower platen of the load frame. The steel load distribution plate and circular blocks were added on top of the stack and centered in the load frame. The sensor was connected to a PC running the I-Scan Software via a handle. Sensor sensitivity was set to a S-25 – a value that had proven suitable in preliminary tests on ballast surfaces. The MBTSS system and the load frame's PC collected *raw sum* and applied force data, respectively, at a sample rate of 100 Hz.

Load was applied by a user controlled dial. The load frame could not be programed to applied load automatically. Efforts were made to ensure that the load application was as consistent as possible for each test. For a given calibration, load was applied over roughly 100 seconds nonlinearly. Peak loads were between 13,000 pounds and 15,000 pounds. These peak loads were chosen based on initial lab and field data collected at the Transportation Technology Center as well as preliminary calculations of maximum load magnitudes at the ballast-tie interface.

The load frame data and MBTSS data needed to be aligned before a calibration curve could be obtained. To synchronize the two data sets, the time at which the peak load was recorded on both systems was used. Data from each system was output as a comma-delimited text file and imported into an external spreadsheet program. The peak load was identified within each dataset and the MBTSS *raw sum* data was shifted to align with the load frame output. Figure 4.3 depicts the alignment of the two datasets for a calibration of Sensor 39.
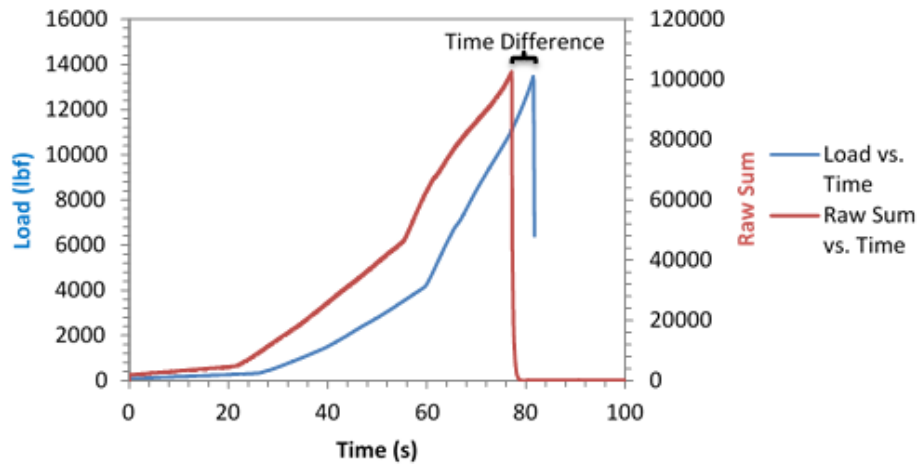
(a)
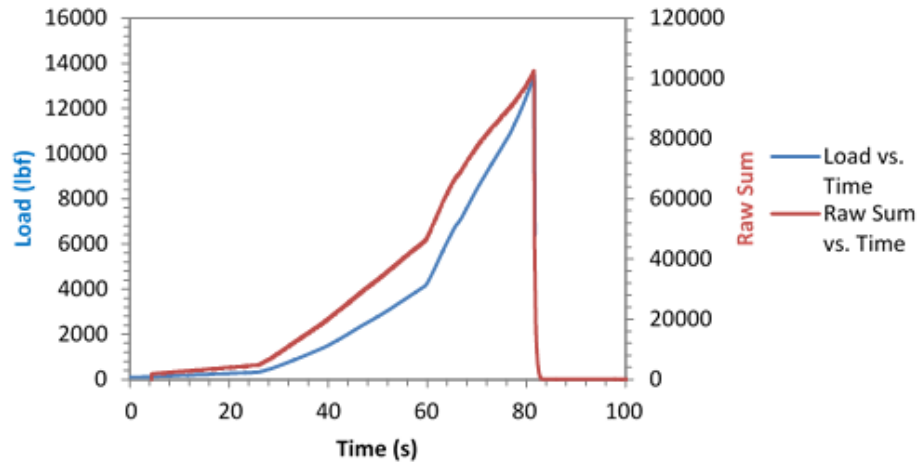
(b)

Figure 4.3 Load versus time and raw sum versus time showing the alignment of MBTSS and load frame data. (a) Data from Sensor 39 Calibration 1 and (b) Synchronized data from Sensor 39 Calibration 1

After aligning the datasets, interpolation was used to generate the relationship between raw sum and applied load. This interpolation was carried out in an external database software package. Given the high sampling frequency, the resulting calibration curve contained noise. The noise observed in the calibration curves was ± 150 lbs. A moving average noise reduction method was applied to the calibration curve to improve the smoothness of the result as shown in Figure 4.4.
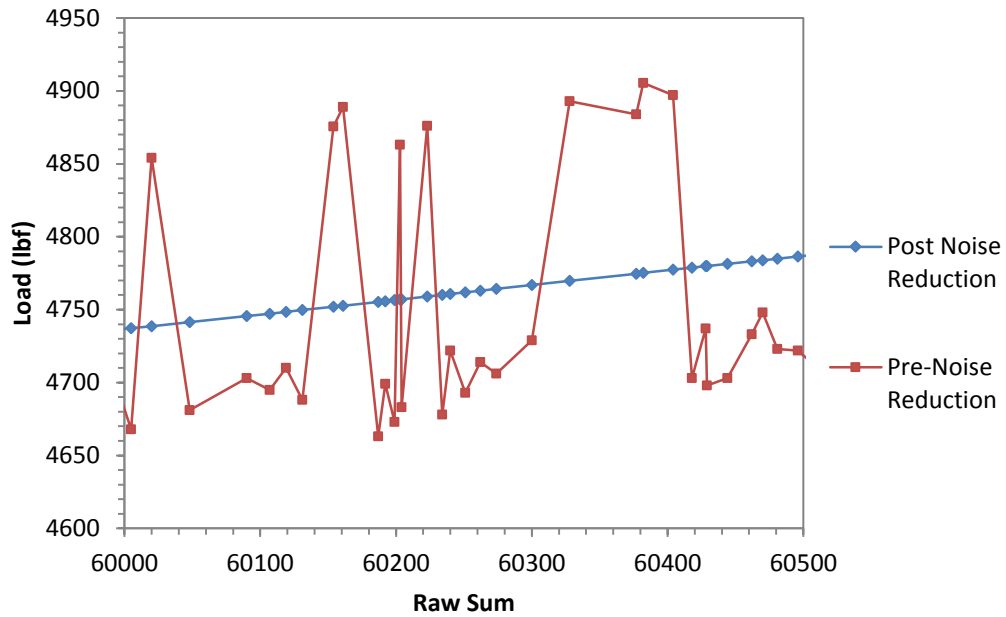
Figure 4.4 Calibration curve noise reduction using a moving average technique

Calibration Results

The calibration curves for two sensors, Sensors 32 and 39, are shown in Figure 4.5. For a given sensor, little variation was observed within the three calibrations performed, demonstrating the repeatability of the calibration methodology. Figure 4.6 shows the calibration curves for 26 MBTSS sensors. It is clear that the calibration curves vary between sensors, especially at higher loads. Figure 4.6 affirms that calibrations are not interchangeable between sensors, as the manufacturing process introduces some variability from one sensor to the next (Tekscan, 2013).
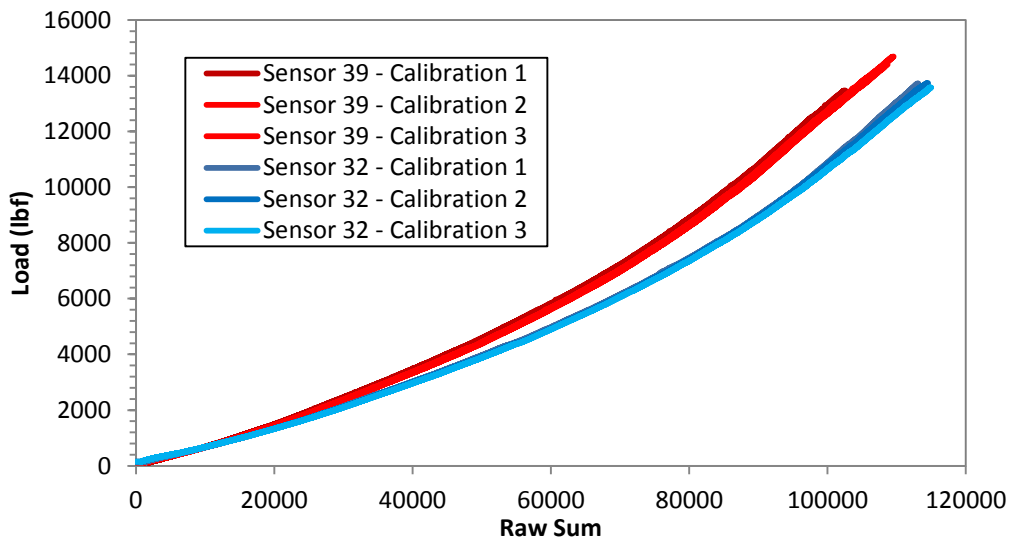
Figure 4.5 Calibration curves for Sensors 32 and 39
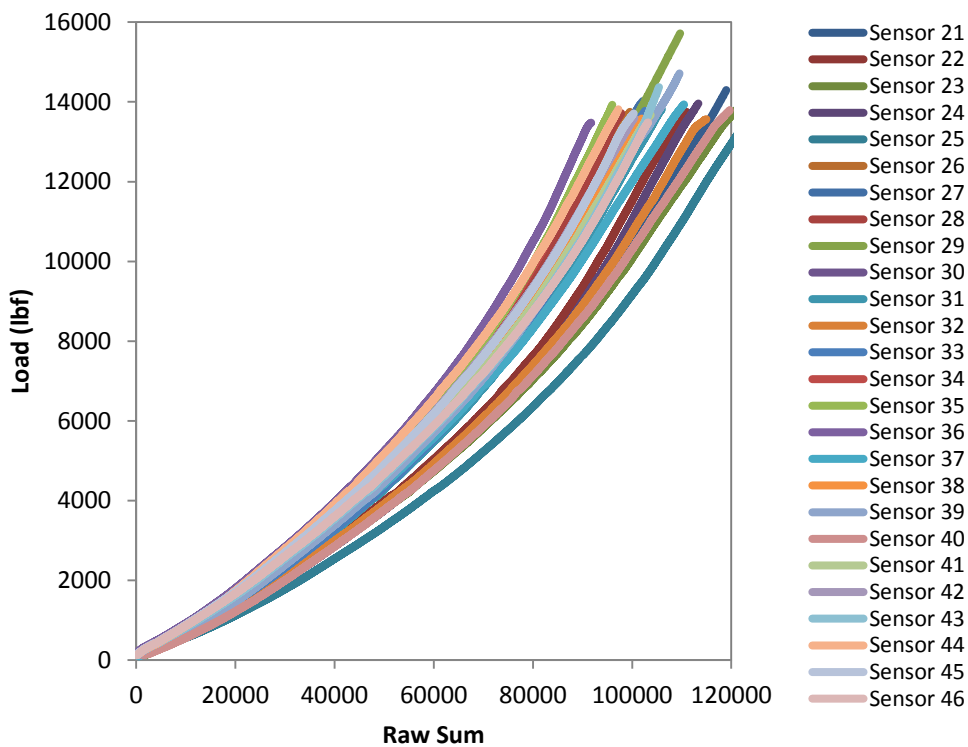
Figure 4.6 – Calibration curves for 26 MBTSS sensors

Because these curves represent actual load versus *raw sum* data, a regression equation to represent the calibration curve is not used. Linear interpolation between the calibration points or over-fitting a high order polynomial to the data is recommended in the application of these calibration curves.

Validation

A validation process was undertaken to assess the applicability of the proposed calibration procedure for use in measuring pressure at the ballast-tie interface. Sensors 32 and 39 were used for the validation testing.

Validation Procedure

Two square 1.5 foot by 1.5 foot wooden ballast boxes were constructed. One ballast box was filled with new AREMA 3A gradation granite ballast. The other ballast box was filled with a heavily fouled ballast of the same rock (particles no greater than 1 inch (25.4 mm) with approximately 20 percent passing the 3/8 inch sieve). The fouled ballast had been rounded in an LA Abrasion machine to simulate aged ballast beneath a tie. These ballasts were selected to reflect the entire range of potential field conditions.

Figure 4.7 shows the validation test setup. Essentially, the waffle plate used the in the calibration tests was replaced with the bed of ballast contained in the ballast box. An additional load distribution plate was used to direct the entire applied load through the sensor and eliminate the potential of the load "bridging" over the sensor.
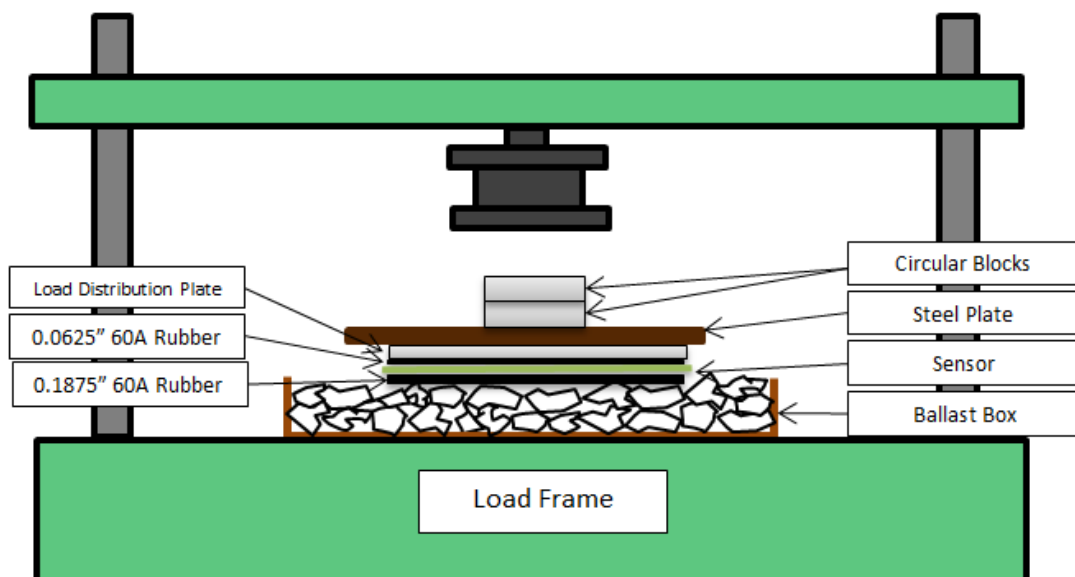
Figure 4.7 Validation testing setup

For each validation test, the loading procedure was carried out the same as during calibration testing. Loads were applied at the same rate and sensor sensitivity

remained at S-25. Prior to each validation test, the ballast was agitated and recompacted under a load of 10,000 lbs. This ensured a consistent, compacted ballast bed prior to each test and reduced permanent deformation of the ballast layer during testing. As during calibration, peak loads ranged from 13,000 lbs. and 15,000 lbs. for the fouled ballast validations. Peak loads were decreased to approximately 7,000 lbs. on the new ballast sample to avoid saturation of the highest senels due to the new, angular ballast. It was observed that the new ballast produced a much rougher pressure distribution than the fouled ballast.

Validation data was processed using the same procedure as the calibration data. The load cell dataset and the MBTSS dataset were aligned such that the peak load and peak *raw sum* value occurred at the same time. A curve of applied load versus *raw sum* was generated for each validation test.

Validation Results

The validation results for the two separate ballast types and the corresponding sensor calibration curve is shown in Figure 4.8. Eleven validation tests were run on the fouled ballast (shown in blue) and twelve validation tests were run on the new ballast (shown in red).
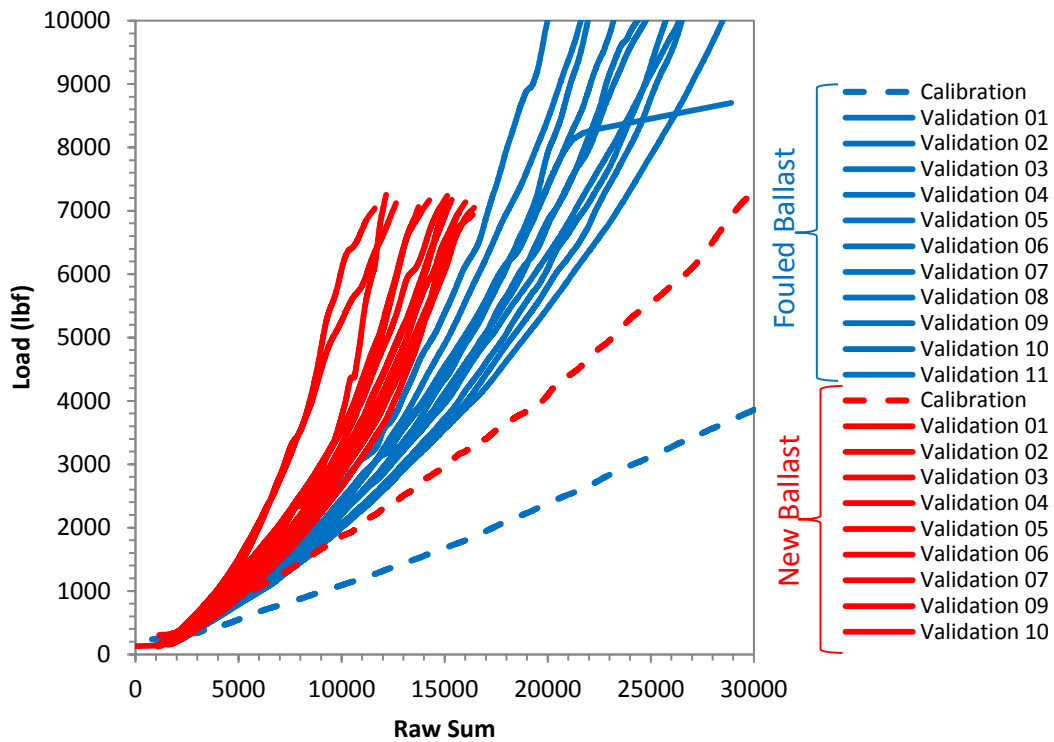
Figure 4.8 - Validation tests compared to calibration for fouled ballast and new ballast.

It can be observed in these results that variability exists between the validation curves, even for the same ballast type. The rearranging of the ballast particles in the ballast box clearly has an influence on the output of the MBTSS sensor. In general, for a given *raw sum*, the applied load during validation was significantly higher than predicted by the calibration curve. This trend is apparent for both ballast gradations. The discrepancy between the calibration and validation curves grows as raw sum increases.

Validation results showed significant differences between actual applied loads and anticipated loads based on the sensor's calibration. The only variable that changed was the surface the sensor was reacting against. It is clear from these results, that the 0.5 inch waffle plate does not replicate the ballast sufficiently for a useful calibration.

Effect of Varying the Waffle Size

The research team wanted to determine the effects of a waffle plate with smaller squares on the sensor's output. It was thought that smaller waffle plate squares may better replicate the ballast surface. A 0.25 inch waffle plate was

machined. The 0.25 inch waffle plate had 100 squares, spaced 1 inch on center; the squares were 0.25 inches by 0.25 inches. Figure 4.7 shows a comparison between the 0.5 inch waffle plate calibration, the 0.25 inch waffle plate calibration, and the validation tests run on fouled ballast.
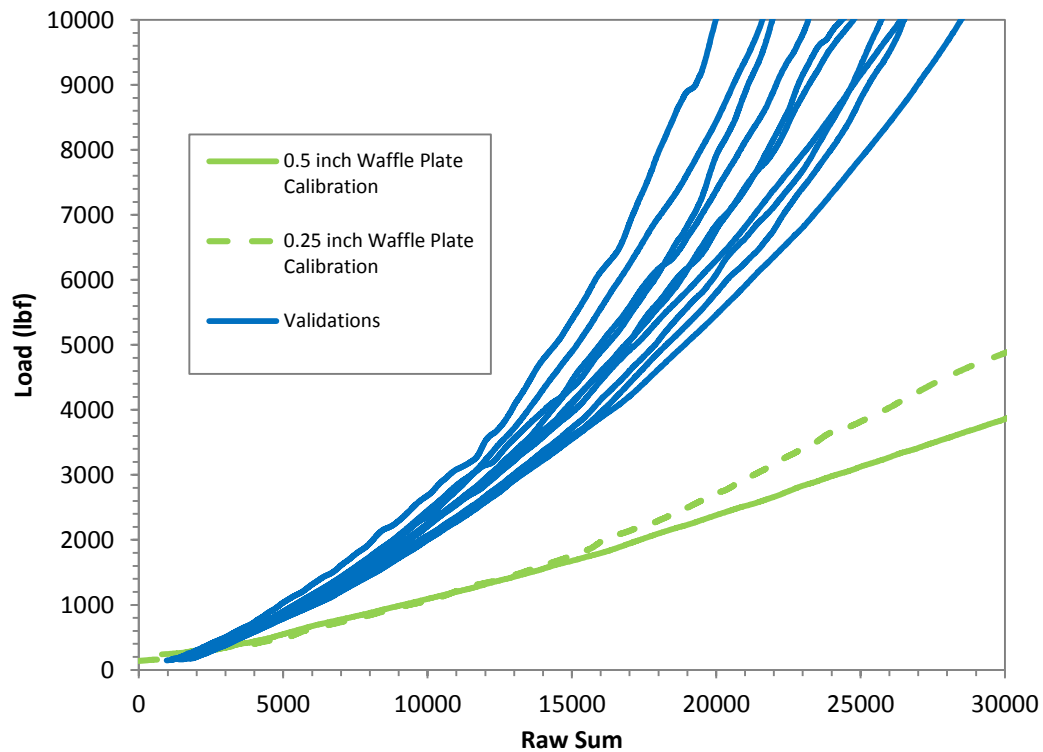
Figure 4.9 The 0.5 inch waffle plate calibration and 0.25 inch waffle plate calibration curves compared to validation curves for fouled ballast

Figure 4.9 shows that the 0.25 inch waffle plate shifted the calibration curve higher (and closer to the validation data). However, the square size of the waffle plate does not appear to affect the calibration curve dramatically.

Thoughts on the Proposed Calibration Procedure

A simple, repeatable, and reliable calibration procedure for use of MBTSS sensors on non-uniform contact surfaces such at the ballast-tie interface of railroad track is desirable. From the calibration and validation results, it is clear that consistent, reliable and repeatable calibrations can be obtained using the proposed methodology. The validation results show significant differences between the actual applied load and the anticipated load from the calibration curve. As all other variables were held constant, the author concludes that the only significant difference between the validation and calibration process was the surface against which the sensors were reacting.

Upon observation, the waffle plates appear to simulate an ideal ballast bed, one where ballast particles are spaced evenly across the surface.

It is likely that the waffle square spacing, size, and shape play a significant role in the output of the sensor. Early exploration into the magnitude of these effects has begun as shown in Figure 4.8. Figure 4.8 compares the shape of the distribution for the same sensor reacting against the 0.5 inch waffle plate, the 0.25 inch waffle plate, and a surface of fouled ballast at the same *raw sum* output.

(a)   (b)   (c)
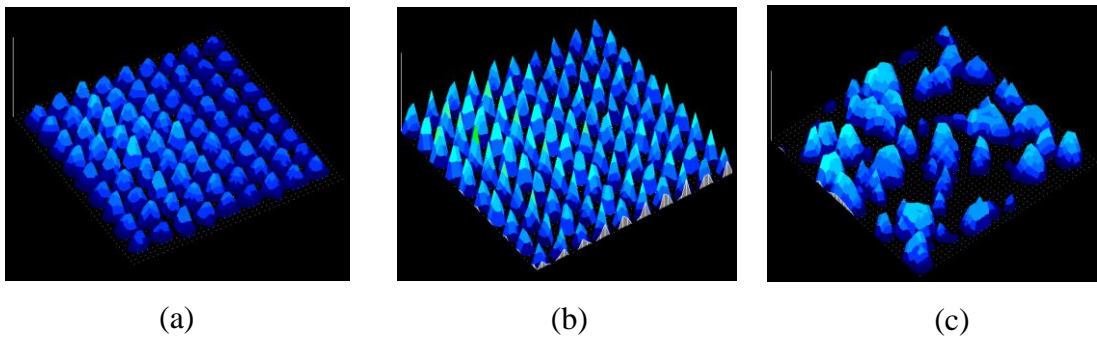
Figure 4.10 Comparing the pressure distribution shapes for the same sensor reacting against (a) 0.5 inch waffle plate, (b) 0.25 inch waffle plate, and (c) surface of fouled ballast at the same *raw sum*

While the proposed calibration method yields repeatable results over multiple calibration tests, the results are not consistent with validation curves developed on actual ballast beds. To improve the calibration setup, the waffle plate component of the calibration stack requires modification to better represent true ballast conditions.

Useful data can still be obtained from the MBTSS system without calibration, however. This includes relative magnitudes of force and contact area. Applications of the calibration method presented above is only recommended for data with a pressure distribution shape similar to that of the 0.5 inch waffle plate.

CHAPTER 5. LABORATORY BALLAST BOX TESTING

Objectives of Ballast Box Testing

Before the MBTSS system could be used in the field, it was desirable to test the system in a more controlled environment. The research team had access to the exact same load frame and ballast box configuration that was used for the FRA Task Order 225 study at the Transportation Technology Center, Inc. (TTCI). The following objectives were developed for the laboratory testing:

1) Prove the concept of the MBTSS system at the ballast-tie interface
2) Determine the effect of five ballast gradations/conditions on:
    a. pressure distribution
    b. contact area
    c. peak pressure
3) Determine the effect, if any of three different tie types – wood, composite, and concrete on the pressure distribution and
4) Assess the longevity of the chosen sensor/protection combination

Ballast Box Test Setup

Laboratory testing was conducted at TTCI over a four day period in July, 2013 and an additional day in November of 2013. Three identical steel boxes, 25 inch long by 25 inch wide by 25 inch tall, were used to contain the ballast material for laboratory testing. Five variations of ballast were tested – new ballast, moderate ballast, heavily fouled ballast, pea gravel, and sand. Representative samples were acquired in five-gallon plastic buckets. All ballast samples were allowed to dry such that any effects of moisture in the ballast were removed from consideration. One ballast box was filled with approximately eight five-gallon buckets of ballast material.

Figure 5.1 shows the gradation curves of the five ballast materials used for the laboratory ballast box testing. The specification limits for AREMA 4a ballast are shown for reference (AREMA, 2012).
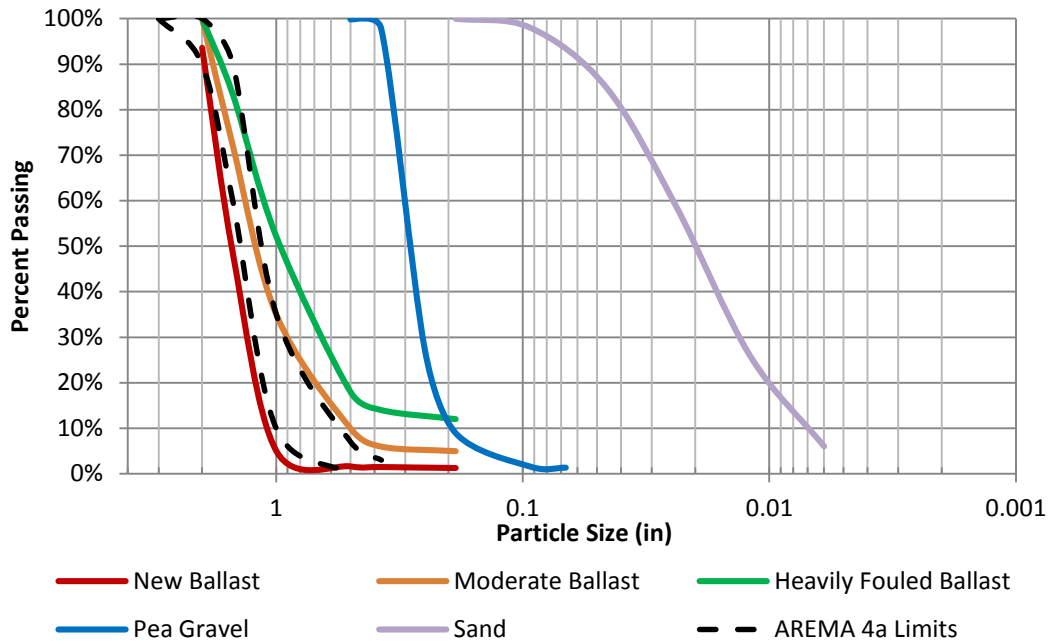
Figure 5.1 Gradations of the five ballasts used in the laboratory ballast box tests

After being filled with ballast, the ballast box was installed in the load frame using a fork lift. Figure 5.2 shows a ballast box and buckets of ballast.

Figure 5.2 Steel ballast box and nine five-gallon buckets of ballast

Three sections of tie, one concrete, one wood, and one composite were chosen for the laboratory testing. Each tie was approximately 24 inches long. A Pandrol type plate had been spiked to the wood tie and the composite tie. The concrete tie section had Pandrol type shoulders already cast into it. Figure 5.3 shows the three ties used.

Figure 5.3 Three sections of tie used for laboratory ballast box testing

Once the ballast box was installed, the section of tie was lifted into place directly under the load actuator. A customized fixture that simulated the rail was bolted to the load actuator and load cell. The tie section was attached to this fixture using customized clips as shown in Figure 5.4. The gage side and field side clips each had two bolts to adjust the toe load on the base of the rail fixture. Prior to each test, these bolts were hand tightened to ensure the fixture remained snug against the rail seat.

Figure 5.4 Fastening system used to connect the custom load fixture to the tie during ballast-box testing. Shown with the concrete tie section.

Once attached, the tie was held up to allow the MBTSS system to be installed. Centered directly beneath the rail at the ballast-tie interface, the MBTSS sensor was placed as shown in Figure 5.5. Each sensor was protected using the recommended scheme discussed in Chapter 3 (3/16 inch 60A rubber on the ballast side, and 1/16 inch 60A rubber on the tie side). Figure 5.6 shows the entire laboratory test setup.

Figure 5.5 Detail of MBTSS sensor/protection location
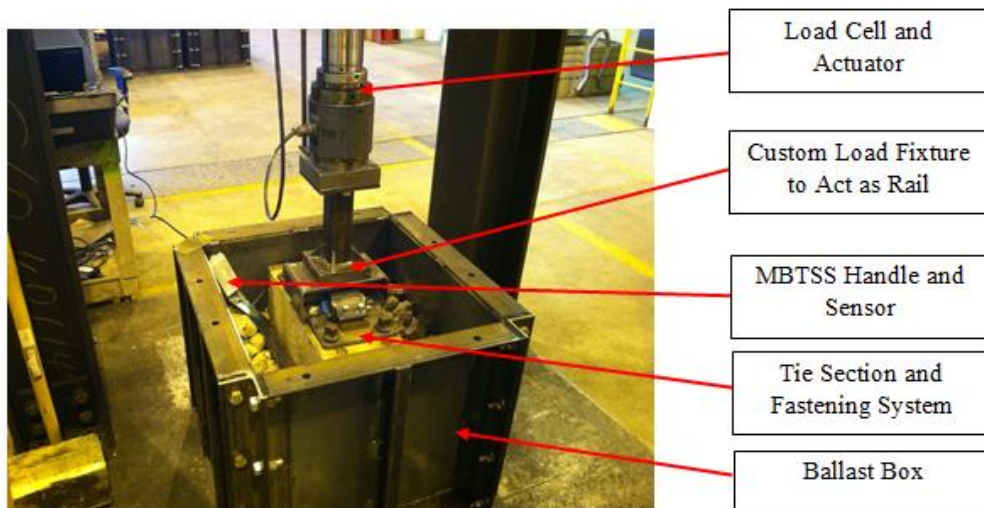
Figure 5.6 Laboratory Ballast Box Testing Configuration

The electrical leads for the sensor and the handle were located in the corner of the ballast box. The handle was gently taped to the ballast box to avoid any creasing of the sensor and to reduce movement of the sensor while installing.

Prior to testing on each ballast material, a compaction phase of 20 kips applied at 1 Hz for 1500 cycles was performed. Compaction allowed any permanent deformation of the ballast layer to occur prior to testing with the MBTSS. Compaction also generated a bedding surface between the tie and ballast similar to in-track conditions. A compacted surface of the moderate ballast is shown in Figure 5.7.

Figure 5.7 - Compacted bed of moderate ballast in a ballast box

After compaction, the MBTSS system was installed beneath the tie as described. The tie section was then lowered onto the ballast surface. Each test consisted of a series of cyclic loading increments. Load was applied for all increments at a rate of 1.5 Hz. Each increment lasted 200 cycles. The first load increment was at 2 kips. The peak load magnitude was increased by 2 kips for each subsequent increment. The last increment was at 20 kips. Thus, 10 load increments in total were applied for a single test ranging from 2 kips to 20 kips. For each cycle in each increment, a released load of 500 lbs was maintained to prevent the sensor or protection from shifting. The sensor was not removed between each increment. Incrementing the load allowed the sensor output to be observed for each magnitude of load. For each increment, MBTSS data was collected for a 10 second recording at a sample rate of 500 Hz. The duration of the recording allowed at least 14 cycles to be recorded for each increment. Although a much slower sample rate could have been used, it was desirable to test the quicker sampling rate of the system for future use in in-track testing.

In total, 39 such tests were performed varying the ballast material and the tie type. This resulted in 390 MBTSS data files (one for each load increment of each

test). Table 5.1shows the test number for each combination of tie type and ballast material.

Table 5.1 Configurations of ballast material and tie type for laboratory testing.

| | | | Tie Type | | |
			Wood	Concrete	Composite
Ballast Material	July, 2012	New	33, 35, 36, 37, 38	20, 21	39, 41, 42, 43
		Moderate		8, 9, 10, 12	
		Heavily Fouled	25, 26, 27, 28	23, 24	29, 30, 31, 32
	Nov., 2012	Pea Gravel	Nov 01, Nov 02, Nov 03	Nov 07, Nov 08, Nov 09, Nov10	Nov 04, Nov 05, Nov 06
		Sand	Nov 13, Nov 14	Nov 11, Nov 12	Nov 15, Nov 16

Considerable time was involved in setting up a new test. The process of exchanging the ballast boxes in the load frame, uninstalling a tie section from the load frame and reinstalling another tie section took approximately one hour. To acquire as much data as possible, multiple tests were run on the same combination of tie and ballast. When multiple tests were performed on the same combination, the pressure sensor was shifted to a different location beneath the tie so as to react against a different surface of the same ballast material.

Laboratory Ballast Box Testing Results

The foremost objective of the laboratory testing was to prove the concept of MBTSS system at the ballast-tie interface. An initial qualitative assessment of the data shows that the MBTSS system can distinguish between the five ballast materials. The pressure distributions obtained for the five different ballast gradations are reasonable. Figure 5.8 shows a representative pressure distribution for each of the five ballasts with an applied load of 10 kips.

(b) New Ballast   (b) Moderate Ballast   (c) Fouled Ballast

(d) Pea Gravel   (e) Sand
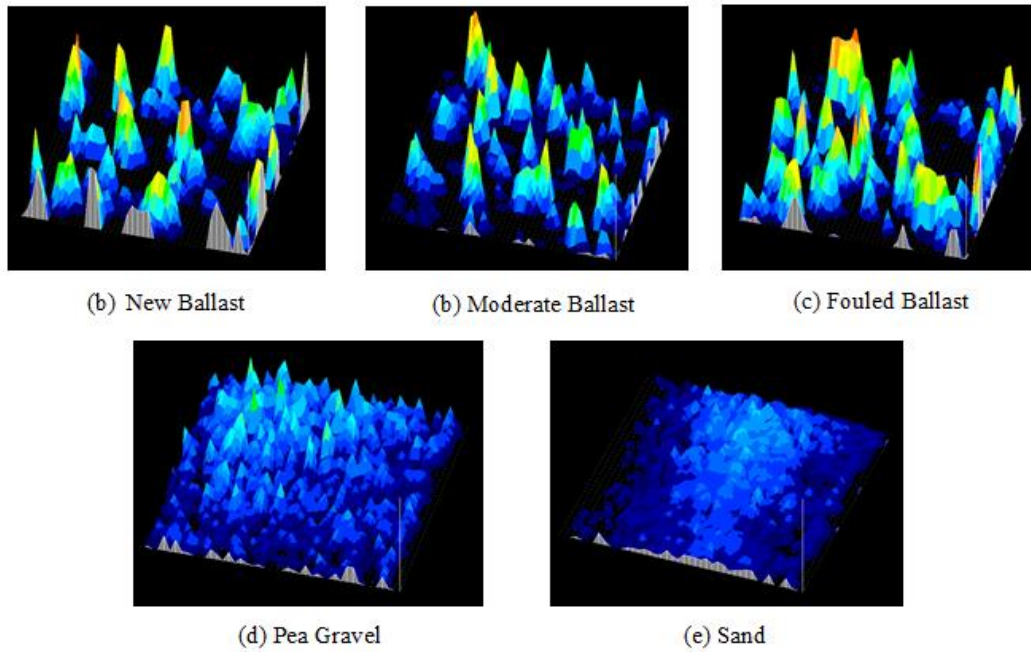
Figure 5.8 A typical pressure distribution for each of the five ballast materials at 10 kips of applied load

New ballast pressure distributions were characterized by sharp peaks, and lower contact areas. Fouled ballast distributions had higher contact areas and slightly duller peaks. The moderate ballast showed some characteristics of the new and fouled ballasts, as might be expected. The pea gravel distributions had many sharp, but low magnitude peaks corresponding to the individual particles of gravel. The sand distributions were relatively uniform and lacked any prominent peaks of pressure.

Because the tie sections (24 inches) were longer than the length of the active sensing area of the 5250 sensor (9.68 inches), a portion of the applied load was "bridged" over the sensor. This was not of particular concern because the objectives of the testing could still be realized without 100% of the applied load moving through the sensor.

Analysis of the laboratory data began by reviewing the recordings in the *I-Scan* software. For some datasets, a missing row or column was observed. These datasets were corrected in-software using an averaging technique that uses the surrounding sensels to estimate the value of the missing row or column. Figure 5.9 depicts this correction process.

| Original | Corrected |
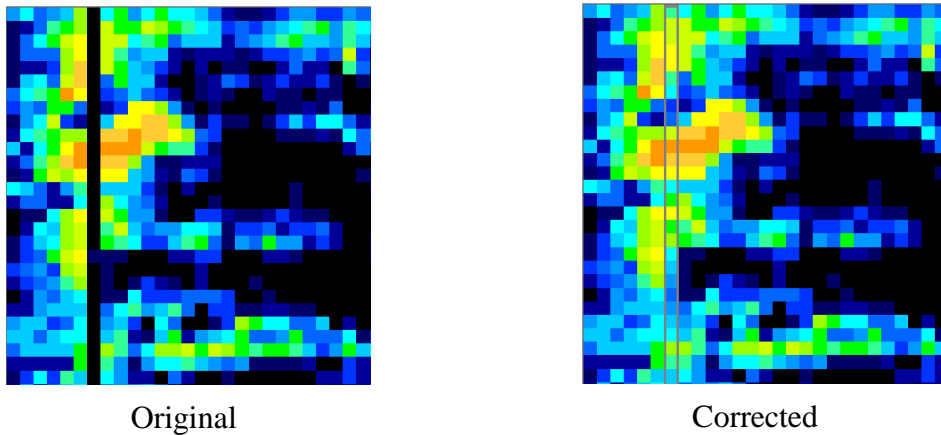
Figure 5.9 Averaging technique to correct for a missing column in a recorded dataset

After all data recordings were reviewed and corrections made, the data was exported as a comma-separated text file. These files were input into an external spreadsheet program. The 14 or 15 (depending on the number of cycles in the recording) frames with the highest raw sum were used as representative frames for that cycle. These peak frames were averaged to provide a single representative frame at that load increment. This process was repeated for each load increment. The peak frames at each load increment were input into a summary spreadsheet for each test. In this spreadsheet, the following parameters were calculated for each peak frame:

1) Contact Area
2) Average Pressure
3) Average Pressure over contact area
4) Peak pressure and
5) Ballast-Tie Contact Index (as described in Chapter 6)

Data was sorted by tie type, ballast material and applied load. Given the complications of obtaining a direct calibration of the sensors (discussed in Chapter 3), the load moving through the sensor was assumed to be one-third of the applied load from the actuator. Given the short length of each tie section, this allows a conservative estimate of peak pressures to be obtained from the data. Assuming one-third of the applied load travels through the sensor, corresponds to an average pressure of 71.15 psi under an applied load of 20 kips – a value that falls between the 65 psi and 85 psi ballast pressure limits found in the AREMA Manual. Thus, the 20 kip increment can be considered a reasonable estimate of a nominal wheel load in-track.

Contact Area

As previously noted, the contact area output of the sensor does not need to be calibrated for as it simply accounts for sensels that are experiencing load. The contact area value is somewhat dependent on the sensitivity setting of the sensor (see Figure 3.7). As all sensors were of the same pressure range and set at the same sensitivity setting, this consideration can be ignored. The effect of the rubber protection distributing pressure, albeit slightly, does increase the contact area output by the sensor; the magnitude of this effect is not known but is likely consistent for the range of ballasts gradations tested.

Figure 5.10 presents a plot of contact area against applied load for the five ballast materials. Figure 5.10 includes data points from all tie types.
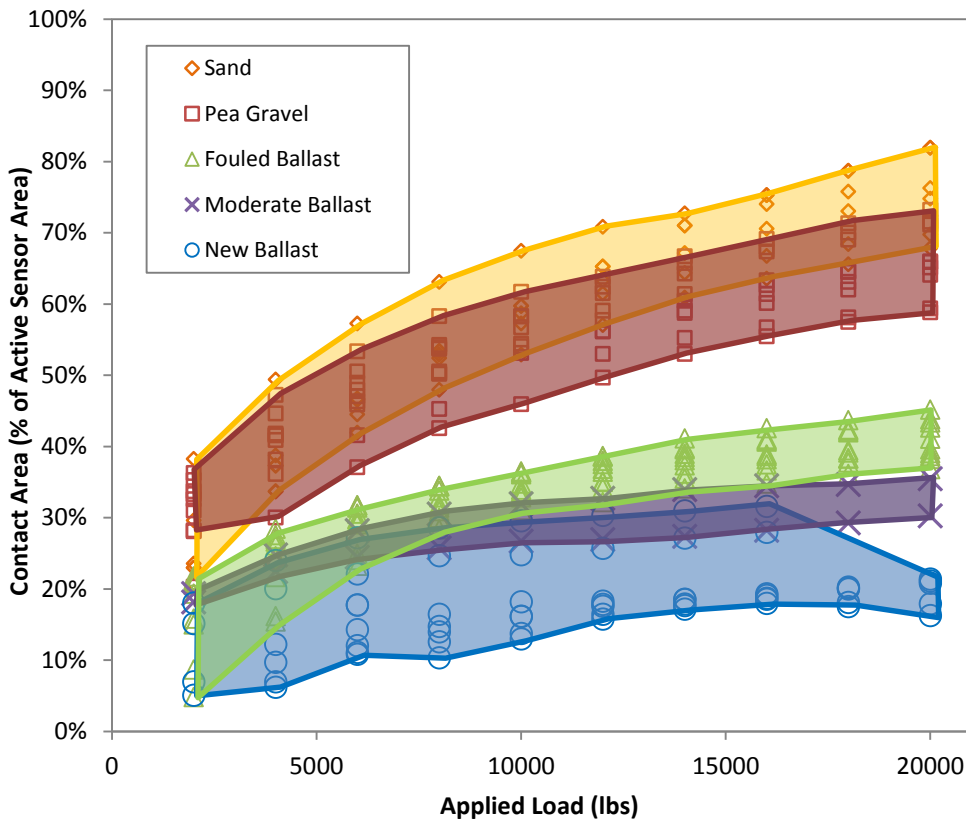
Figure 5.10 Contact area versus applied load for the five ballast materials used in laboratory testing

It can be observed that, as load increases, the contact area also increases for all five ballast materials. The differentiation of contact area for the ballasts is generally clearer as load increases as well. Table 5.2 summarizes the average contact area at an applied load of 20 kips.

Table 5.2 Average contact area for each ballast material – applied load equal to 20 kips

Ballast Material	Average Contact Area at Applied Load of 10 kips (% of Sensor)	Average Contact Area at Applied Load of 20 kips (% of Sensor)
Sand	59.33%	75.5%
Pea Gravel	55.34%	66.2%
Fouled Ballast	34.51%	40.9%
Moderate Ballast	29.38%	32.9%
New Ballast	16.77%	20.4%

The FRA Task Order 225 study concluded that the contact area at the ballast tie interface increased as the number of applied load cycles increased. The magnitudes of contact area presented in Table 5.2 and Figure 5.9 compare favorably with the contact areas between 10 percent and 40 percent reported in the Task Order 225 report. The Task Order 225 study likely gives a better approximation of actual contact areas because no rubber protection was necessary.

The results presented in Table 5.2 and Figure 5.9 also show that contact area increases as load is applied to the tie. Observing the MBTSS data for the tests on the new, moderate, and fouled ballast, it can be seen that the contact area increase is partially due to the rubber protection distributing the ballast contact over more area. It can also partially be attributed to additional ballast particles being engaged as the load is applied. The concept that contact area may be changing at the ballast-tie interface during loading is a significant finding of this research. Previous research, discussed in the introduction, has been unable to dynamically measure changes in contact area − a substantial advancement due to the MBTSS technology.

Peak Pressure

Peak pressure is considered to be the maximum pressure acting at an individual sensel on the sensor. It is equal to the force at the maximum sensel divided by that sensel's area. Peak pressure is an important value to consider for the pressure

distributions, because it is the highest load that an individual ballast particle is experiencing and, consequently, the highest pressure experienced by the tie. At the point of peak pressure, the ballast particle experiencing this dynamic load, must be able to carry it to avoid fracture, degradation, or settlement. Peak pressures were calculated for the laboratory tests by assuming that one-third of the applied load was acting thought the sensor.

Using the peak frame data, the peak pressure at a given load increment is calculated using the Equation 5.1

$$P_{peak}(psi) = \frac{\left[\left(\frac{max\ sensel\ raw\ sum}{total\ raw\ sum}\right)*\frac{L_{applied}}{3}\right]}{0.0484\ in^2}$$

(Eq. 5.1)

where $L_{applied}$ is the applied load from the load actuator in pounds, the *max sensel raw sum* is the output of the maximum sensel on the peak frame, and *total raw sum* is the total *raw sum* of the peak frame.

The top half of the fraction in Equation 5.1 converts the sensel's raw sum to a force in pounds. This force is divided over the sensel of 0.0484 in^2 to obtain the peak pressure for the frame in psi. Peak pressure was calculated for each load increment of each test. Figure 5.11 shows a plot of these peak pressure against applied load for the five different ballasts. The theoretical uniform pressure distribution is also plotted for comparison.
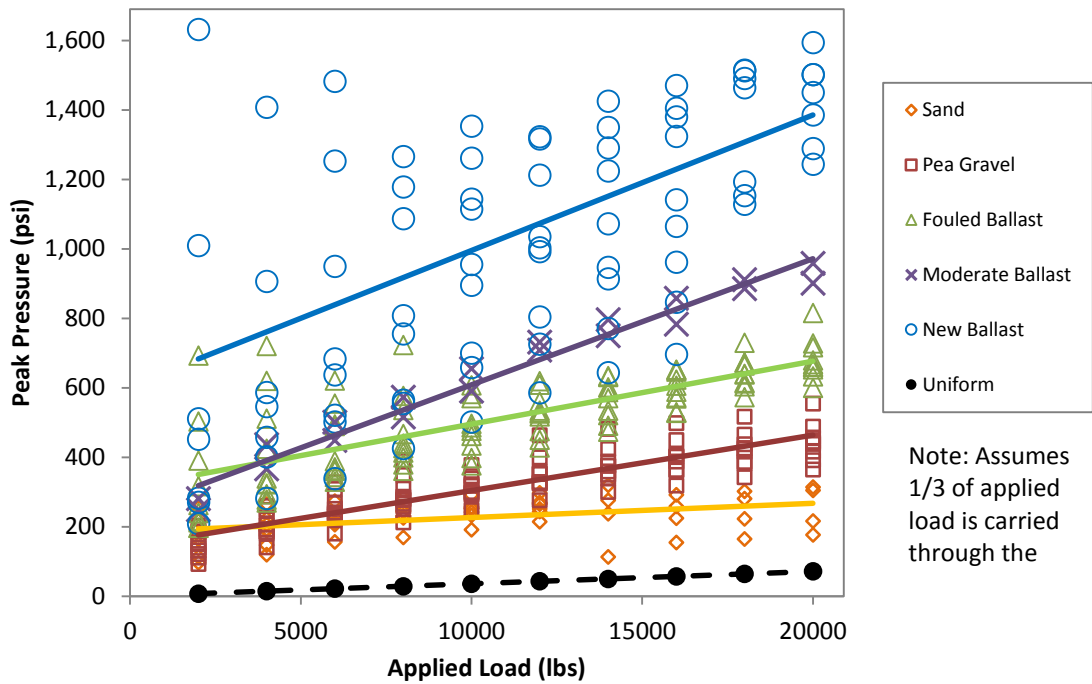
Figure 5.11 Peak pressure against applied load for the five ballast materials. The assumption is made that one-third the applied force acts through the sensor

Table 5.3 shows the average peak pressure for each ballast type (at an applied load of 20 kips). The percent increase over the theoretical uniform pressure is also shown for comparison.

Table 5.3 Average peak pressure for each ballast material – applied load equal to 20 kips

Ballast Material	Average Peak Pressure* (psi)	Percent of the Theoretical Uniform Pressure* (%)
Sand	283.9	399%
Pea Gravel	444.1	624%
Fouled Ballast	681.3	958%
Moderate Ballast	929.7	1307%
New Ballast	1449.9	2036%

Table 5.3 clearly demonstrates the magnitude of the differences between a uniform pressure, and the actual maximum pressures occurring at individual ballast particles.

The author considers these peak pressures to be conservative due to the addition of the rubber protection need for the MBTSS system. It is likely that even higher pressures would be measured under this applied load, if possible, without a rubber protection layer. The high peak pressures measured on new ballast likely account for the more rapid settlement of track after surfacing maintenance noted by Selig and Waters (1994) and Litchberger (2011).

Comparing the Tie Materials

No discernible difference could be made in the pressure transmitted between the three tie types. All three ties had similar pressure distributions for a given ballast material. Given their length of only 24 inches, the various tie materials should not have a significant difference in the pressure carried into the ballast. Differences in the distribution of the pressure can likely be observed over the full length of a tie in-track. As one of the primary differences in the tie materials is their stiffness, the 24 inches of tie length is simply is not enough to affect the flexure of the tie section.

"Ridges" in the pressure distribution can be observed for the concrete tie, especially in the pea gravel and sand materials. These ridges in the pressure distribution correspond to actual ridges on the underside of the concrete tie, a result of the screeding that takes place when a concrete tie in manufactured. Figure 5.12 shows a pressure distribution from a concrete tie reacting against sand at a load of 14 kips.
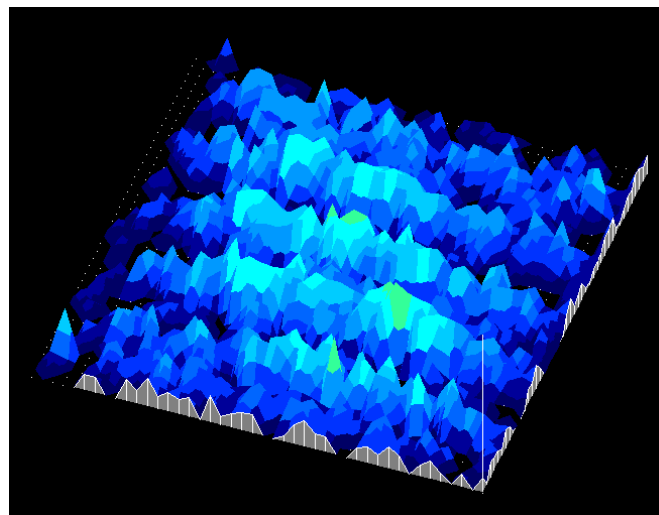
Figure 5.12 Ridge apparent on the pressure distribution of a concrete tie loaded against sand

Longevity of the Sensors

It was desirable for future testing and material purchase to better understand the longevity of the MBTSS system in application at the ballast-tie interface. The sensors, with the implemented protection scheme, became a disposable component of the overall system. Five sensors were used for the laboratory portion of the study. These five sensors were rotated through roughly 40 tests, each with 10 increments of 200 cycles at applied loads ranging from 2 kips to 20 kips. At the end of the laboratory testing, these five sensors had reached the end of their serviceable life. On average, the sensors had a life of about 8 tests or about 16,000 cycles at an average load of 16,000 lbs. With the rubber protection used, sensors can be expected to last much shorter than this if testing on new ballast and significantly longer if testing on sand or pea gravel. Minor punctures and abrasions were noticeable on the sensors as they wore out, especially after testing on the new ballast surface. Punctures and abrasions outside the active sensor area have the potential to break the circuit for a certain row or column. Once enough rows and columns are not operational for a particular sensor, it was replaced with an undamaged sensor.

It is possible that with a thicker rubber protection layer, the sensors could last much longer when testing on a ballast surface. Thicker protection however, would reduce the resolution of the sensor and diminish the advantage of using a sensor with 1936 sensing elements.

Characterizing the Pressure Distribution

While contact area and peak pressure contribute to the understanding of the pressure distribution, they do not provide a comprehensive means to describe it. The ability to assess the "roughness" of the pressure distribution is also important in understanding how force is being carried through the tie and into the ballast. Chapter 6 presents the development of an index to measure the "roughness" of a pressure distribution, called the Ballast-Tie Contact Index (BTCI). Analysis of the laboratory data using BTCI is also presented.

CHAPTER 6. THE BALLAST-TIE CONTACT INDEX

The Need for a Quantitative Index to Assess Pressure "Roughness"

Pressure distribution at the ballast-tie interface, as discussed in Chapter 1, can be thought of in three dimensions. These include the two-dimensional areal distribution on the ballast-tie plane, and the time dimension, or how the pressure distribution changes over time. Characteristics of such a pressure distribution include contact area and pressure magnitude. However, these characteristics do not provide a comprehensive description of a pressure distribution. An additional characteristic, the variability of the pressures in the pressure distribution, in combination with contact area and pressure magnitudes can provide this comprehensive description. The variability of the pressure values on a pressure distribution can be thought of as the "roughness" of the distribution. Figure 6.1 shows a conceptual scale of pressure distribution "roughness".

More Uniform   More "Rough"
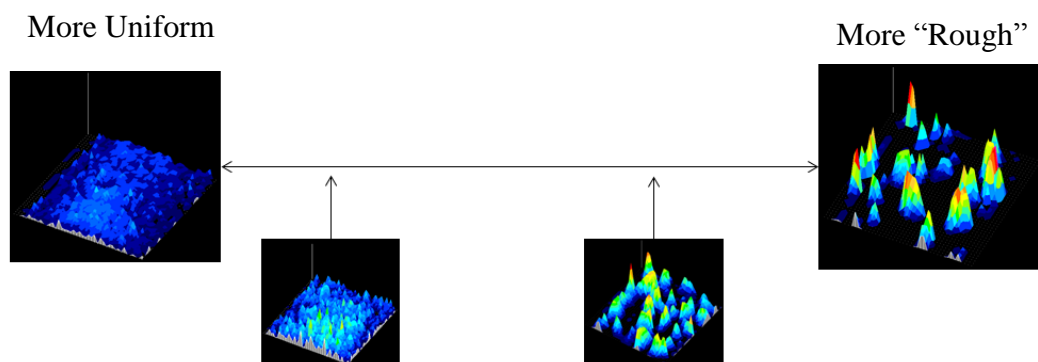
Figure 6.1 A conceptual scale of pressure distribution "roughness"

It is desirable to have means to quantify this "roughness" so as to compare various ballast gradations and quantify changes in the distribution that may occur over time. The research team has developed a quantitative index to characterize the "roughness" of the pressure distribution at the ballast-tie interface. This index is referred to as the Ballast-Tie Contact Index, or BTCI.

An Analogy in the Field of Geography

In the field of geography, terrain roughness is a parameter, defined in numerous ways, to characterize the roughness of a particular area of land. This is used for various purposes in civil engineering including identification of landslide potential, and hydrological channel flow models (Grohmann et al., 2010). The

roughness of terrain is analogous to the roughness of a pressure distribution. In this sense, a ballast-tie pressure data frame can be thought of as topography map of pressure.

A simple technique involving the standard deviation from an "ideal" surface was borrowed from the field of geography (as discussed by Grohmann et al., 2010) to define the Ballast-Tie Contact Index.

Calculation of the Ballast-Tie Contact Index (BTCI)

A typical ballast-tie pressure distribution can be represented as a matrix of *raw sum* at each sensel as shown in Figure 6.2. The matrix is color coded for clarity.
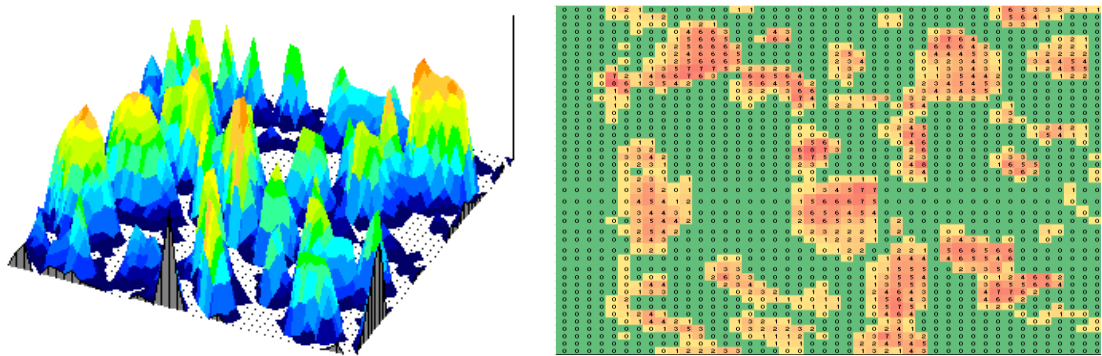
Figure 6.2 – An example ballast-tie pressure distribution and equivalent matrix

A sample 6x5 pressure distribution, represented as a matrix, is shown in Figure 6.3 and will be used as an example to demonstrate the calculation of BTCI for a data frame. This sample matrix is analogous to the 44x44 matrix of a data frame from a 5250 sensor. BTCI is calculated exactly the same for any size matrix. A smaller matrix is shown only for simplicity.

Total *raw sum* = 870
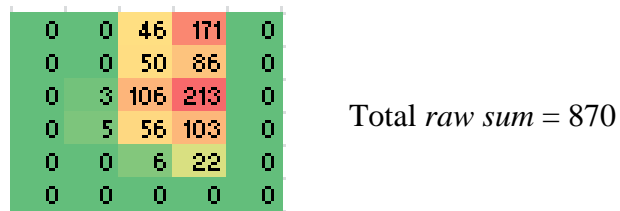
Figure 6.3 – A sample 6x5 pressure distribution with forces shown in *raw sum*

To calculate BTCI, first, an ideal surface must be developed to calculate standard deviations from. This ideal surface can be thought of as a uniform pressure distribution. To calculate the height of the uniform pressure distribution (H_{UD}), the total raw sum for the data frame is divided by the number of sensels on the sensor as shown in Equation 6.1.

66

$$H_{UD} = \frac{\sum sensel\ values}{\#\ of\ sensels} = \frac{total\ raw\ sum}{\#\ of\ sensels} \qquad \text{(Eq. 6.1)}$$

For the sample matrix, H_{UD} is calculated below:

$$H_{UD} = \frac{total\ raw\ sum}{\#\ of\ sensels} = \frac{870}{30} = 29$$

For the sample matrix, this results in a uniform pressure distribution represented by matrix shown in Figure 6.4.

Figure 6.4 The resulting ideal uniform pressure distribution for the calculation of BTCI

The analogous H_{UD} for a full size 44x44 data frame is shown in Figure 6.5.
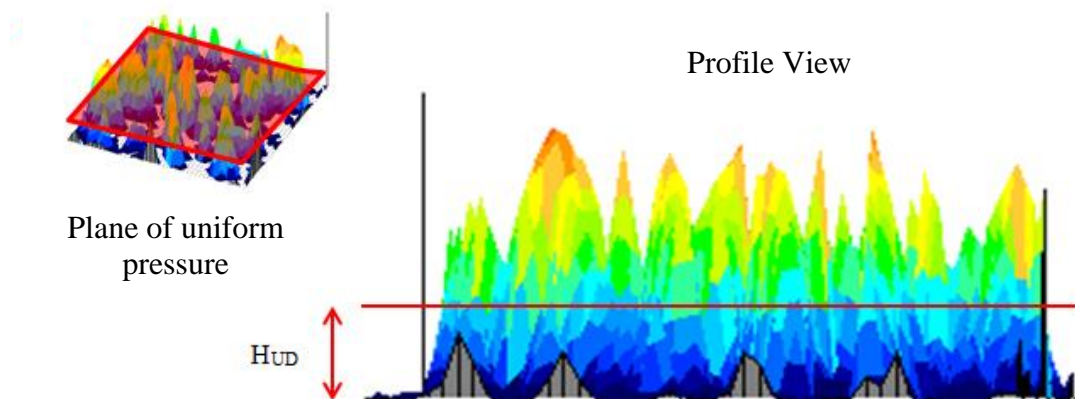
Figure 6.5 Side view of a pressure distribution with red line indicating the height (magnitude) of the theoretically uniform pressure distribution (H_{UD})

After the calculation of the equivalent uniform distribution, a matrix of ratios is computed that normalize the raw sum value at each sensel to the height of the uniform distribution, H_{UD}. This is referred to as the normalized ratio, R_N. The

generalized calculation of the normalized ratio for a sensel, *i,j*, is shown in Equation 6.2.

$$R_{N\ i,j} = \frac{raw\ sum\ of\ sensel_{i,j}}{H_{UD}} \qquad \text{(Eq. 6.2)}$$

The calculation of R_N for sensel 3,3 in the sample matrix is calculated below:

$$R_{N\ i,j} = \frac{raw\ sum\ of\ sensel_{3,3}}{H_{UD}} = \frac{106}{29} = 3.7$$

R_N is calculated similarly for the remaining sensels. A value of R_N less than one means that sensel has a value less than the uniform distribution, a value of R_N greater than one means that sensel's value is greater than the uniform distribution, and a value of R_N equal to one implies the sensel's value lies directly on the uniform distribution. After calculating the normalized ratios for each sensel, a matrix of normalized ratios is generated as shown in Figure 6.6.

Figure 6.6 Matrix of normalized ratios

BTCI is calculated as the standard deviation of the normalized ratios that are greater than zero as shown in Equation 6.3.

$$BTCI = \sigma(Normalized\ Ratios > 0) \qquad \text{(Eq. 6.3)}$$

This method only uses R_N values greater than zero so as to factor contact area out of the calculation. It computes the "roughness" only in the loaded area of the sensor so that pressure distributions with varying contact areas can be compared. The BTCI for the sample matrix is calculated as follows.

$$BTCI = \sigma(1.6, 5.9, 1.7, 3, 0.1, 3.7, 7.3, 0.2, 1.9, 3.6, 0.2, 0.8) = 1.86$$

BTCI can similarly be calculated for any MBTSS data frame. Figure 6.7 shows the BTCI values for four different ballast materials under the same load.
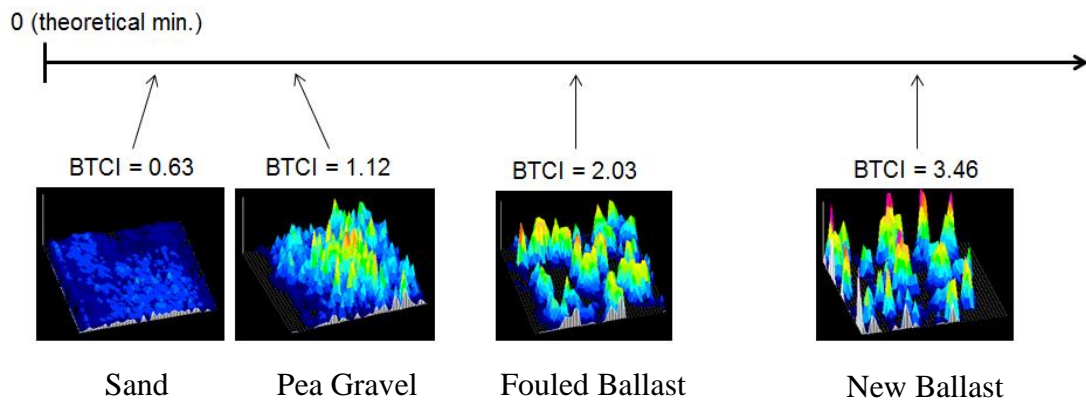
Figure 6.7 BTCI scale showing the BTCI values of pressure distributions from four ballast gradations

Observing the BTCI calculations, it can be seen that BTCI increases as the "roughness" of the pressure distribution increases. A uniform pressure distribution would have a BTCI equal to zero as all normalized ratios would be the same, namely, a value of one. Relationships between BTCI and independent variables in the test can now be generated.

BTCI Relationships

BTCI for Varying Ballast Gradations

Intuitively, new ballast, with larger and more angular particles, should produce a pressure distribution that is relatively rougher. Fouled ballast, with more rounded particles, should produce less sharp loads and have a slightly smoother pressure distribution.

Ballast gradation is characterized by a curve as shown in Figure 5.1. By their nature, curves are difficult to characterize with one parameter. In geotechnical engineering, gradation curves can be characterized by various parameters that describe the shape of the curve such as effective size, uniformity coefficient, or the coefficient of gradation. Gradations performed by TTCI on the ballast samples were conducted through six sieves – a 2 inch sieve, a 1.5 inch sieve, a 1 inch sieve, a 0.5 inch sieve, a 0.375 inch sieve, and a No. 4 (0.187 inch) sieve. Thus, linear

interpolation was used to determine various gradation parameters and percent passing values for certain grain sizes. Table 6.1 shows an example of some of the parameters calculated for the five laboratory ballasts.

Table 6.1 – Various Gradation Parameters of the five ballasts used in laboratory testing

	Sand	Pea Gravel	Fouled Ballast	Mod. Ballast	New Ballast
Effective Size (D_{10}) (inches)	0.01	0.53	0.17	0.49	1.04
Uniformity Coef. (D_{60}/D_{10})	3.45	2.28	6.47	2.68	1.54
Coef. of Gradation ($D_{30}^2/(D_{60}*D_{10})$)	1.01	1.56	2.33	1.21	0.96
% Passing 1.45 inches	1.00	0.98	0.83	0.71	0.47
% Passing 1.65 inches	1.00	0.98	0.89	0.82	0.65

The Effective Size parameter did not correlate well with the pressure distributions observed. The pea gravel actually had a larger effective size than the fouled ballast and moderate ballast. Effective size is typically used for correlation with hydraulic conductivity (drainage), so correlation with pressure distributions was not expected. The uniformity coefficient and coefficient of curvature describe the shape of the gradation curve and are not sufficient as a representative value for a wide range of material sizes. Of the ballast gradation parameters calculated, it was found that BTCI was most closely related to the percent of ballast material passing 1.65 inches. As can be seen in Table 6.1, the percent passing 1.65 inches parameter discriminates sufficiently between the five ballast gradations and corresponds linearly with the range of BTCI values. New ballast of consists largely of particles greater than 1.65 inches. As the ballast becomes more fouled, these larger particles become fractured and degraded imparting a more uniform (less rough) pressure distribution at the ballast-tie interface. Figure 6.8 presents the relationship between BTCI and percent of ballast passing 1.65 inches. Error bars representing one standard deviation are shown to provide a sense of the distribution of the BTCI values for a given ballast gradation.
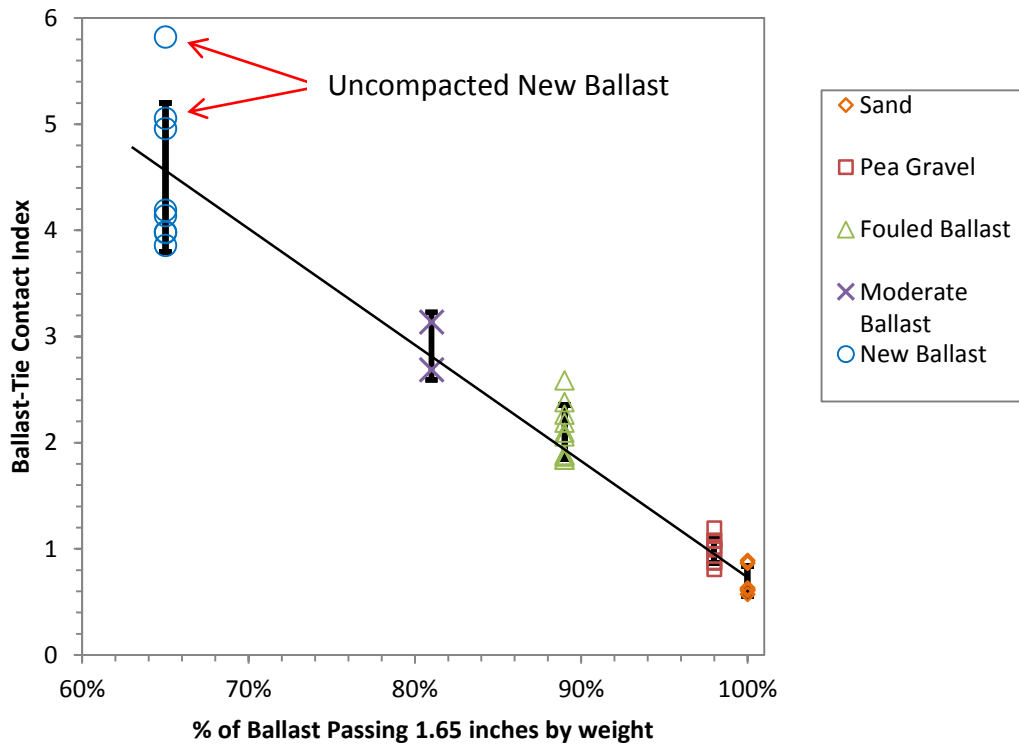
Figure 6.8 BTCI versus Percent of ballast material passing 1.65 inches for the ballast box laboratory testing at an applied load of 20 kip.

Applying a line of best fit to the data points in Figure 6.8 yields the relationship shown in Equation 6.4.

$$BTCI = -11.31\left(\frac{\%\ Passing\ 1.65\ inches}{100}\right) + 12.03 \qquad \text{(Eq. 6.4)}$$

Figure 6.8 also shows two BTCI values for tests ran on uncompacted new ballast. It can be seen that these BTCI values represent the two roughest pressure distributions recorded during laboratory testing. The two uncompacted ballast tests can be considered an example of a pressure distribution that might be typical of a newly surfaced tie.

BTCI versus load magnitude

The BTCI, inherently, is normalized to the magnitude of the load being applied. As a measure of roughness, the BTCI can show how the uniformity of the pressure distribution changes as load is applied. During testing, it was observed that pressure distributions at low loads (2 kips and 4 kips for example) were much

"rougher" than pressure distributions at higher load increments. Figure 6.9 shows a plot of BTCI versus applied load for the new, moderate and fouled ballasts. Table 6.2 presents the equations for the logarithmic and linear curves plotted in Figure 6.9
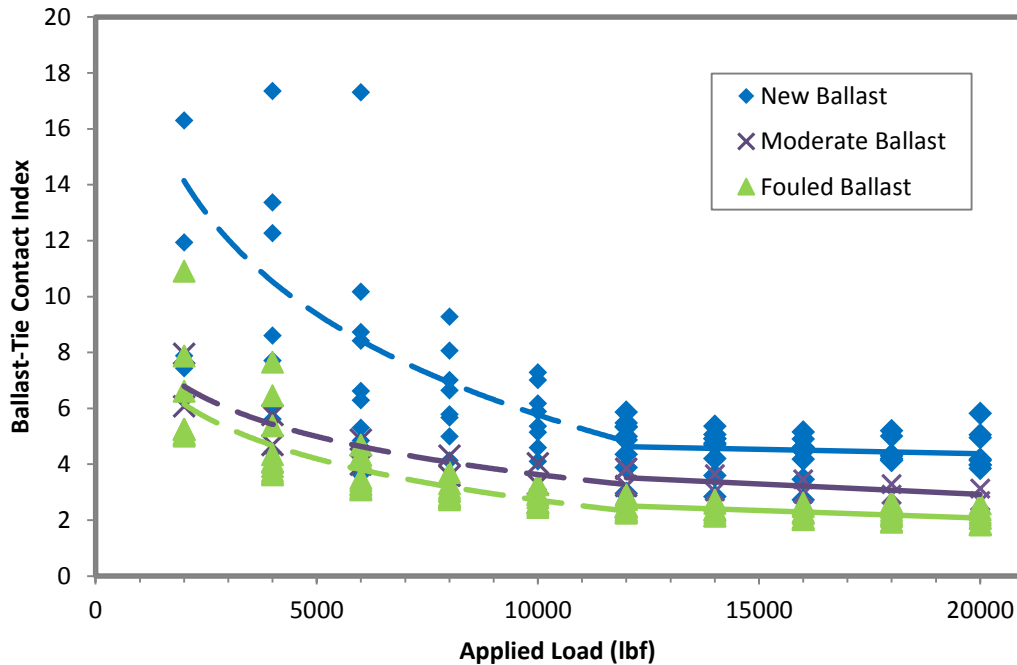
Figure 6.9 BTCI versus applied load for new ballast, moderate ballast, and fouled ballast and

Table 6.2 – Equations for trend lines plotted in Figure 6.9

	Logarithmic Equation (0-12 kips) − − − − − −	Linear Equation (12-20 kips) ————
New Ballast	BTCI = -5.206ln(x) + 53.716	BTCI = -3E-05(x) + 5.00
Moderate Ballast	BTCI = -1.964ln(x) + 21.719	BTCI = -7E-05(x) + 4.41
Fouled Ballast	BTCI = -2.135ln(x) + 22.378	BTCI = -5E-05(x) + 3.16

* x is the applied load in lbf

It can be observed that as load is applied, BTCI tends to decrease for all three ballasts. The values of BTCI for the new ballast appear to be much more variable at lower applied loads. As the BTCI decreases, it appears to plateau at a fairly constant value after about 12 kips of applied load. Logarithmic trend lines are applied to the data points below 12 kips of applied load and linear trend lines are applied to the data points above 12 kips of applied load. The equations of these trend lines are shown in Table 6.2.

Of note in Table 6.2 is the small values of slope in the linear trend lines. This demonstrates that the BTCI nearly plateaus in excess of 12 kips of applied load. It is likely that the plateauing of the BTCI data represents the pressure distribution reaching some type of equilibrium. At the point the BTCI begins to plateau, all ballast particles in contact the tie are fully supporting the load being transmitted. The presentation of these equations is not intended as a mathematical model, but instead, a means of demonstrating the tendency of the BTCI data to plateau after it has reached a point of equilibrium.

Application of BTCI as a Performance Indicator

The MBTSS system has the ability to measure the contact area and pressure magnitudes at the ballast-tie interface. With the use of the BTCI, in addition to these variables, the relative "roughness" of the pressure distribution can also be acquired. The measurement of these three dependent variables in concert with one another, over the life cycle of the track, may lead to a better understanding of how ballast degradation occurs and how it affects the pressure distribution at the ballast-tie interface. Calculation of BTCI does not require sensor calibration as the calculation is normalized to the total, uncalibrated raw sum of the data frame. It is thus, an additional dependent variable (along with contact area) that can be obtained from uncalibrated MBTSS sensors

As ballast degrades beneath a tie, the contact area would likely increase, peak pressure may go down, and the BTCI would decrease indicating a slightly less rough distribution. It is therefore possible to consider the BTCI as a variable that could be tied to performance. Measuring the rate of deterioration of BTCI, for example, would give an indication of performance for various techniques to reduce ballast pressures. These techniques, as discussed in Chapter 2 include larger footprint ties (frame and half-frame ties) or under-tie elastic pads. Faster rates of decrease in BTCI would indicate degradation of ballast and poorer performance. In this sense, the ability of a track improvement technique to maintain a level of BTCI over time would be desirable.

CHAPTER 7. IN-TRACK TESTING

Objectives of In-Track Testing

After the completion of laboratory testing, the MBTSS system proved feasible under realistic load magnitudes at the ballast-tie interface and over a range of ballast gradations. It was desirable to test the feasibility of the system in the field, and collect data at the ballast-tie interface in-track. Testing in the field allows nearly all limitations of the ballast box testing to be avoided including the shortened tie section, and the need for confinement of the ballast material. In-track testing allows realistic loads to be applied by an actual consist with varying axle loads. The following objectives for the in-track testing were identified

1) Prove the concept of the MBTSS system in-track
2) Use MBTSS to measure the pressure distribution along the length of multiple ties and compare results to previous research
3) Determine the effect of five different ballast gradations/conditions on:
   a. pressure distribution
   b. contact area
   c. peak pressure

Test Procedure

In-track testing was conducted at the Transportation Technology Center's (TTCI) Facility for Accelerated Service Testing (FAST) loop. Section 33 of the loop was selected and scheduled for testing in June, 2013. Section 33 is a tangent section of track with conventional concrete ties throughout. Ties used for the testing were 102 inches in length and 10.5 inches wide at their base. Figure 7.1 shows the location of Section 33 on the FAST loop.
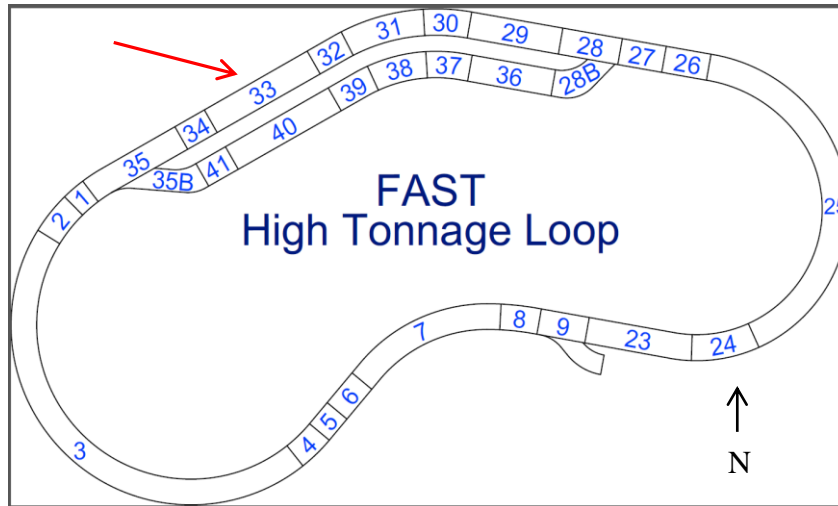
Figure 7.1 Section 33 on the FAST loop at TTCI

From the laboratory testing results, it was determined that ballast gradation had a significant effect on the distribution of pressure at the ballast-tie interface. To determine the effects of ballast gradation on pressure distribution in the field, five ballast materials, similar to those used in the laboratory testing, were implemented.

Preparation of the Test Zones

Five zones, consisting of three ties each, were designated. Each zone was assigned a ballast material to be installed beneath the zone's three ties. TTCI personnel prepared the section for testing. The existing crib ballast around each test tie was excavated as shown in Figure 7.2. The clips for 7-8 ties adjacent to the zone were removed and the track was jacked up, lifting the three test ties in the zone slightly. With the test ties lifted, a 2-3 inch layer of the existing ballast was carefully removed and replaced with the ballast material assigned to that zone. The installation of the ballast material did not disturb the existing ballast bed. The existing ballast, similar in condition to the "moderate" ballast in the laboratory testing, was left in place in Zone 1. New, angular ballast was placed in Zone 2, fouled ballast in Zone 3, pea gravel in Zone 4, and Sand in Zone 5. Table 7.1, reproduced from the test plan, shows the zone numbers, ballast material installed, and tie numbers. After installation of the test ballast beneath the ties, the track accumulated 1.5 million gross tons of traffic prior to testing.
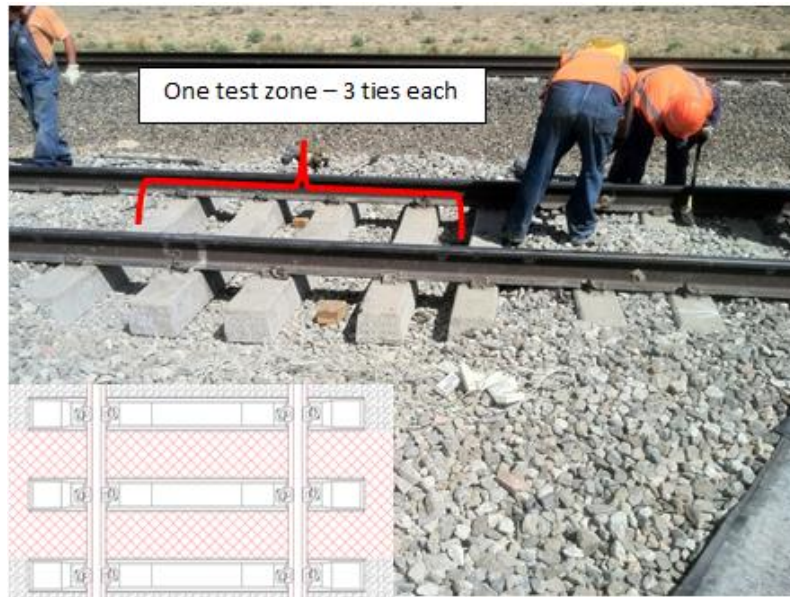
Figure 7.2 Schematic of ballast excavation from the cribs of each test zone

Table 7.1 – Test Zones in Section 33 of the FAST loop used for in-track testing

Zone Number	Tie Numbers	Ballast Material
1	2, 3 and 4	Existing, moderate ballast
2	38, 39, and 40	New ballast
3	58, 59, and 60	Fouled ballast
4	78, 79, and 80	Pea gravel
5	98, 99, and 100	Sand

Figure 7.3 shows gradation curves obtained from samples taken from directly below the bottom of the ties in each zone.
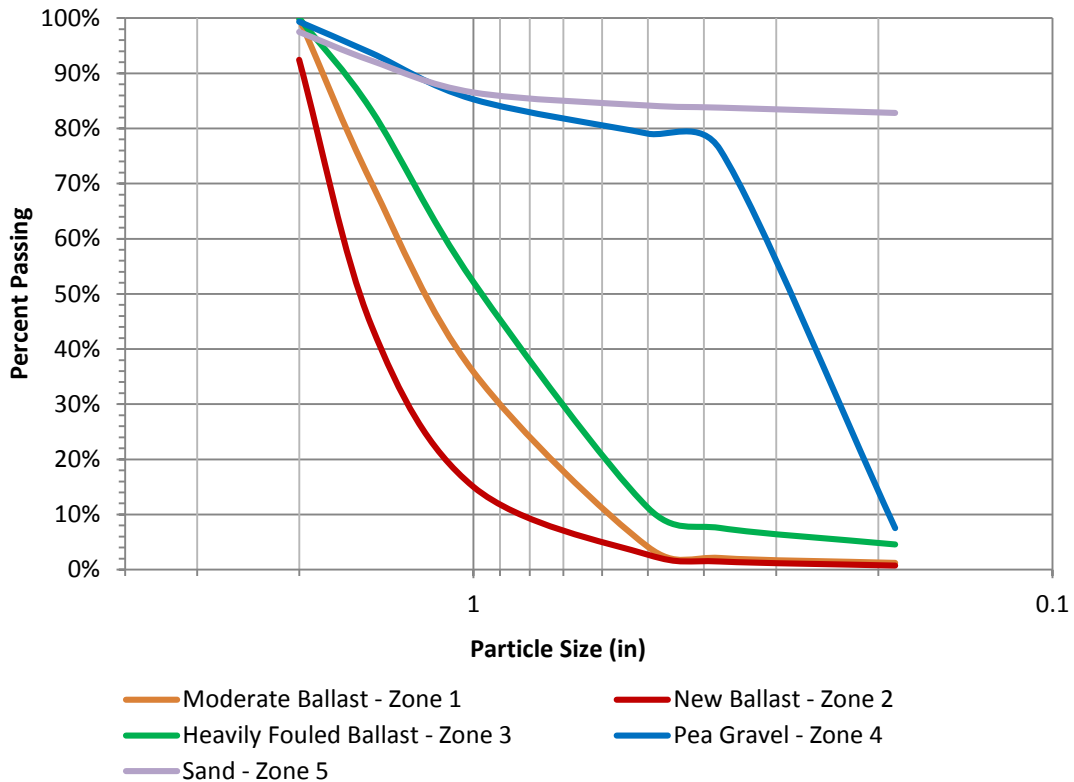
Figure 7.3 Ballast gradations of the samples taken from beneath the ties in each test zone

A thin layer of ballast material was added beneath the test ties to assess the effects of various ballast gradations without impacting the existing stiffness of the ballast bed. Thus, the resulting average pressure distributions along the length of the tie could be related to the existing ballast bed stiffness, while small scale pressure distributions acting on the sensors would be representative of each ballast material. The cribs between the test ties remained empty for later installation of the pressure sensors during testing.

Load Application and Data Collection Procedure

Loading was applied to the test ties by a three vehicle consist consisting of a six axle locomotive, a four axle empty hopper car, and a four axle loaded hopper car, in that order counterclockwise on the loop. Figure 7.4 shows the order of the consist.
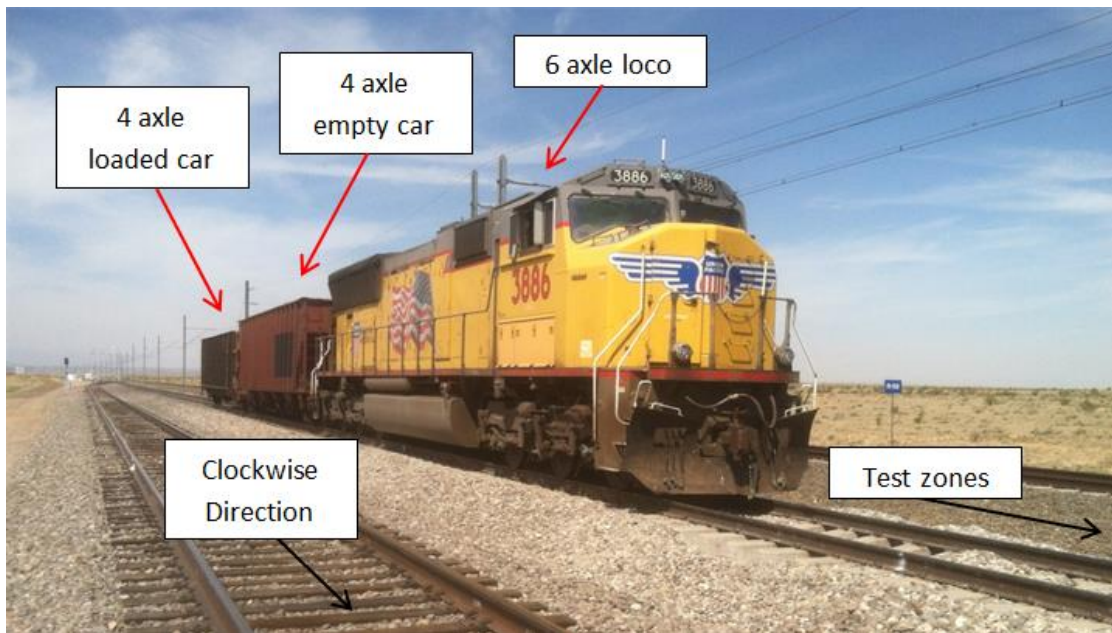
Figure 7.4 Consist used for load application for in-track testing

Prior to testing, the three vehicles in the consist were weighed. Table 7.2 presents the axle loads for each vehicle used in calculations.

Table 7.2 Axle Loads for the three vehicles used in the in-track test consist

Vehicle	Axle Load (lbs)
Locomotive	71825
Heavy Car	79425
Empty Car	16688

To install the MBTSS system, the test tie was jacked up slightly and the pressure sensors and rubber protection sheets (of the same thickness and hardness as used in laboratory testing) were slid beneath the tie as shown in Figure 7.5.

Figure 7.5 Pressure sensors being installed under raised track

Eight sensors were used for each test in conjunction with eight Tekscan *Evolution* handles. The first seven sensors were lined up adjacent to each other starting at the south end of the tie, while the eighth was placed directly under the north rail as shown in Figure 7.6.
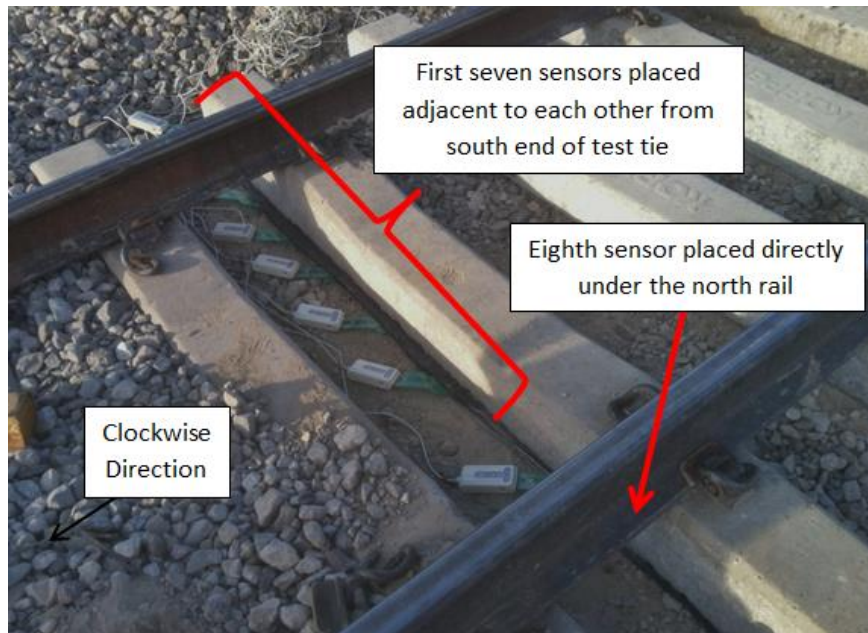
Figure 7.6 Location of pressure sensors on each test tie during in-track testing

Each test consisted of one pass of the consist over a test tie. At least two tests were run on each tie – one clockwise pass and one counterclockwise pass. The train speed varied between 5 and 10 miles per hour. This reduced the effects of any

dynamic forces on the track. MBTSS data was collected at a sample rate of 100 Hz. (the maximum allowed by the *Evolution* handles and 5250 sensors). Two laptop PC's were used, each collected data from four handles. Data files for each sensor were saved after each test. In total 46 tests were performed. With eight sensors for each test, there were 368 MBTSS recordings and over 2.5 million data frames collected. Figure 7.7 shows a truck of the empty car passing over the test tie.
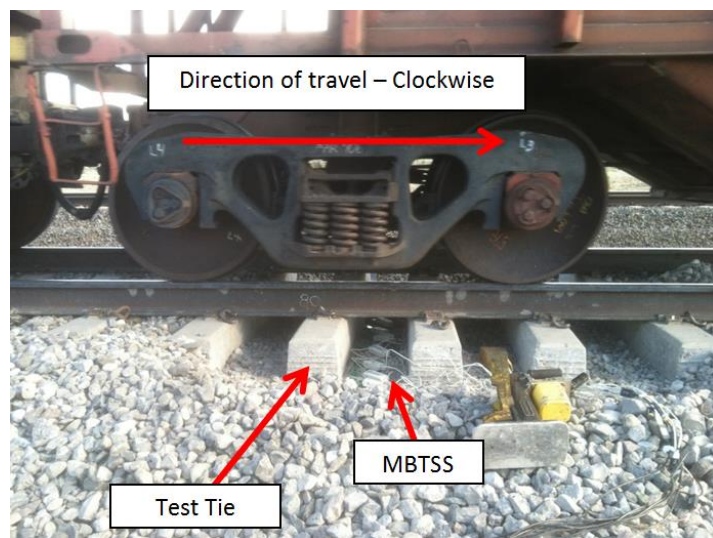
Figure 7.7 Empty car truck applying load to a test tie

Some sensors were damaged during testing. They were immediately replaced prior to the next test.

In-Track Testing Results

The in-track testing data was processed and corrected similar to the laboratory data described in Chapter 5. The only additional variable associated with each dataset was its location along the length of the tie, measured in inches to the center of the sensor from the south end of the tie. The data frames associated with each axle load were located as local maximums in the plot of force versus time. Figure 7.8 shows a typical force versus time plot for a single in-track test (one pass).
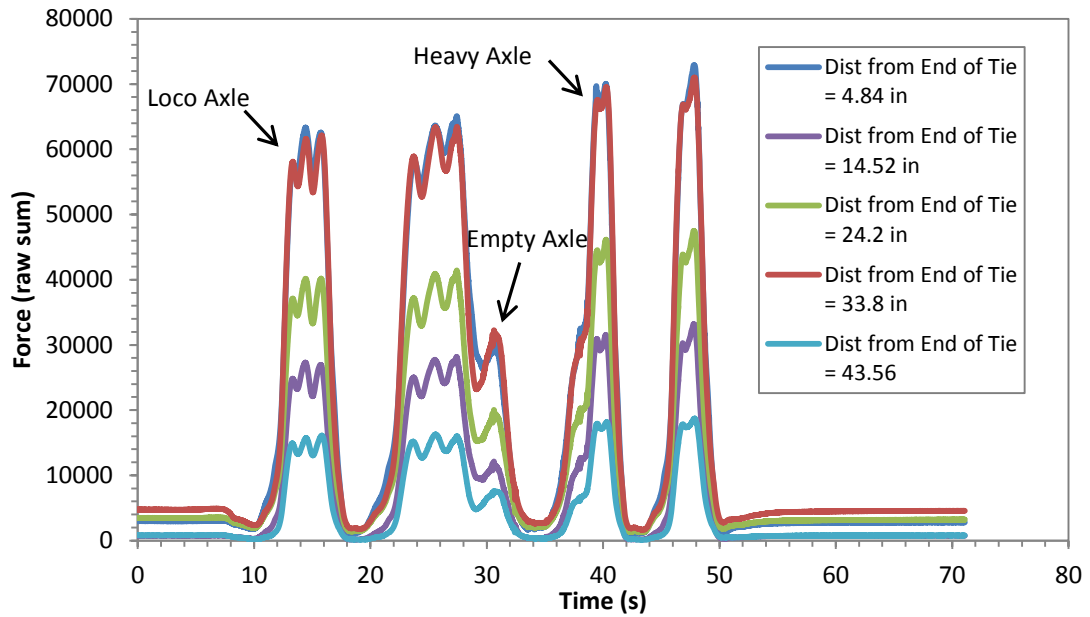
Figure 7.8 – A force versus time plot for Test 31

The axle loads of the locomotive and heavy car were easily identified as the peaks shown in Figure 7.8. The axle loads of the empty car appeared to be affected by the heavier trucks on either side. This washed out definition in the empty car axle loads. At least one empty car axle load could be located for each test and was identified by the peak in Figure 7.8.

Due to the complications in calibrating the sensors for variable contact surfaces, it was decided to calibrate the sensors by assuming the load being carried by each tie. Given the tie spacing (24 inches) and concrete tie track, AREMA (2012) suggests 50 percent of the applied axle load will be carried by each test tie. This assumption was made for the in-track data analysis. The author feels as though the objectives of the testing can still be accomplished through this assumption and that general conclusions can still be drawn. A better method of sensor calibration is needed to accurate measure the pressures

Pressure Distribution along the Length of the Tie

To plot the pressure distribution along the length of each test tie, the average pressure at each sensor was calculated assuming 50 percent of the axle load carried by each test tie. Figures 7.9 through 7.18 show the pressure distribution obtained along the length of ten test ties.
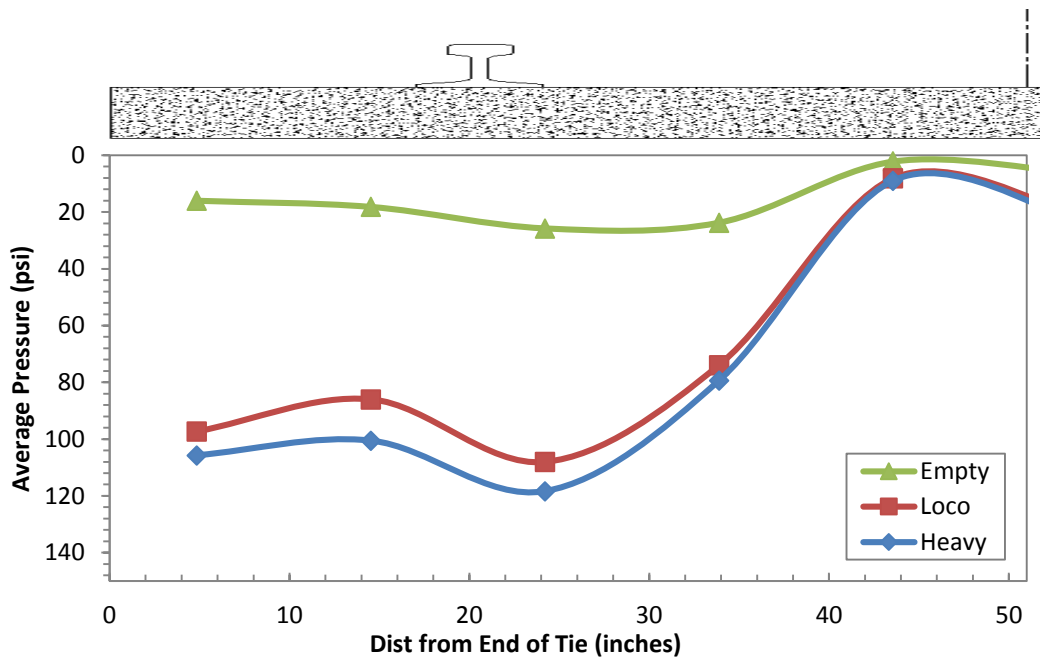
Figure 7.9 Average pressure distributions along Tie 2 for the three applied axle loads
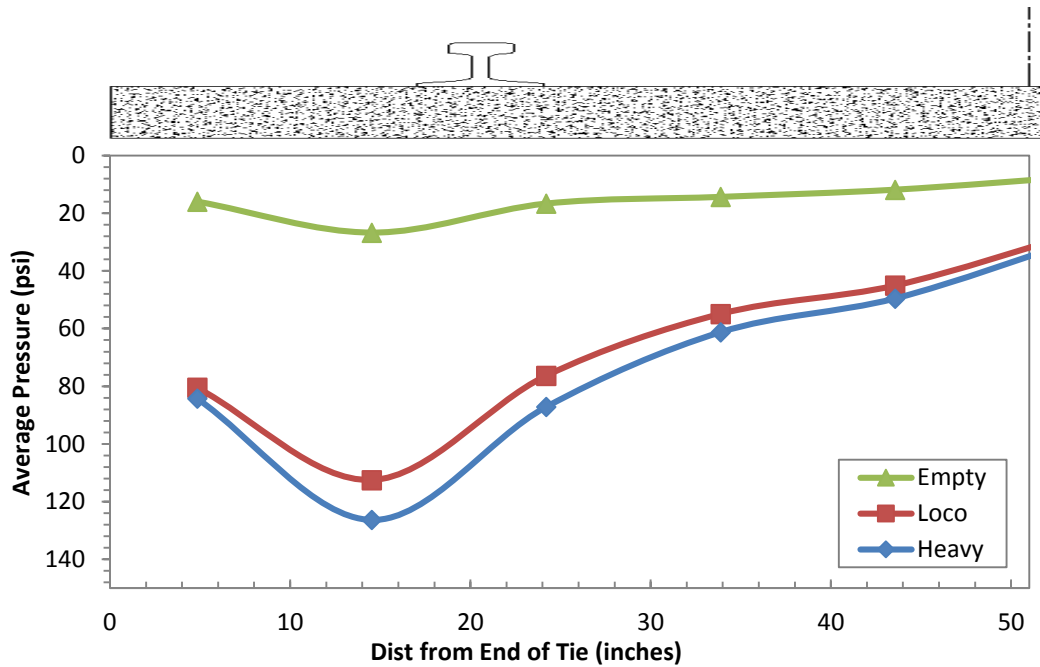
Figure 7.10 Average pressure distributions along Tie 3 for the three applied axle loads
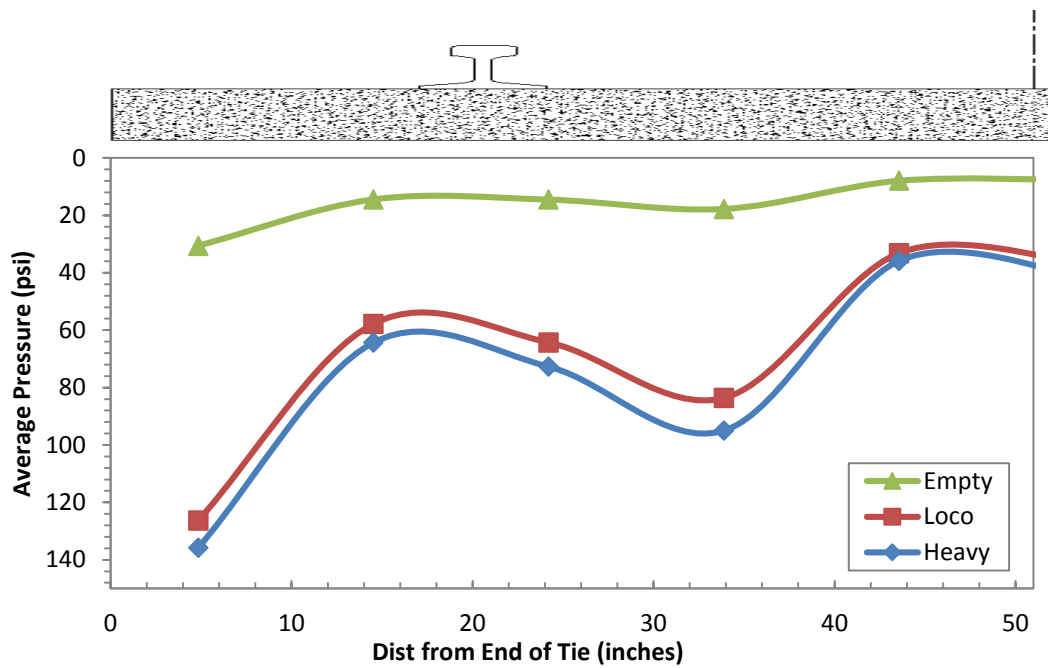
Figure 7.11 Average pressure distributions along Tie 38 for the three applied axle loads
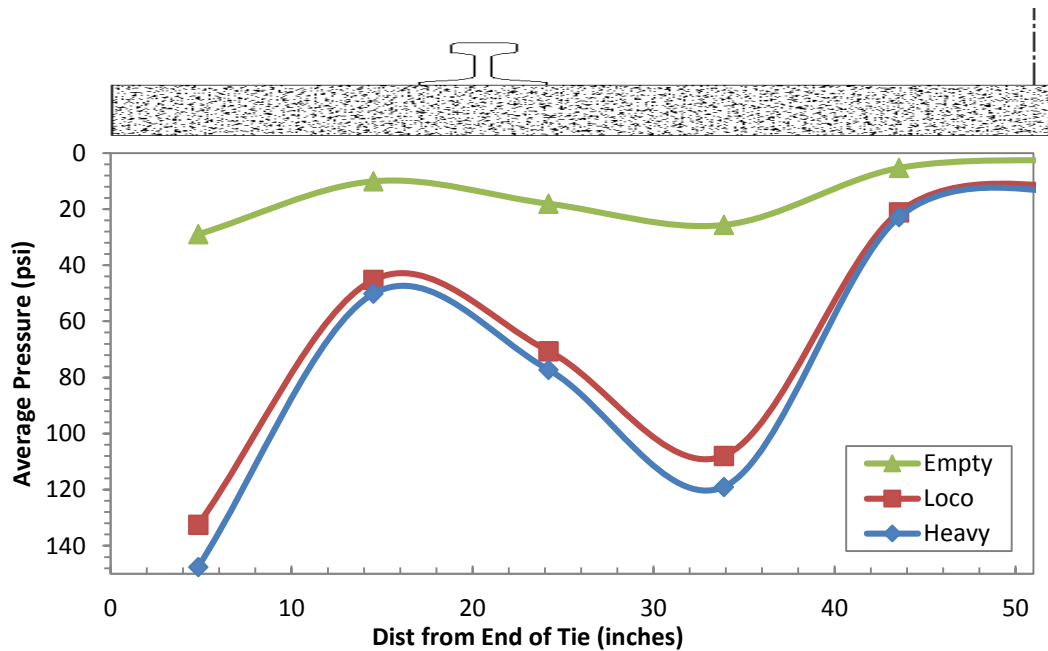
Figure 7.12 Average pressure distributions along Tie 39 for the three applied axle loads
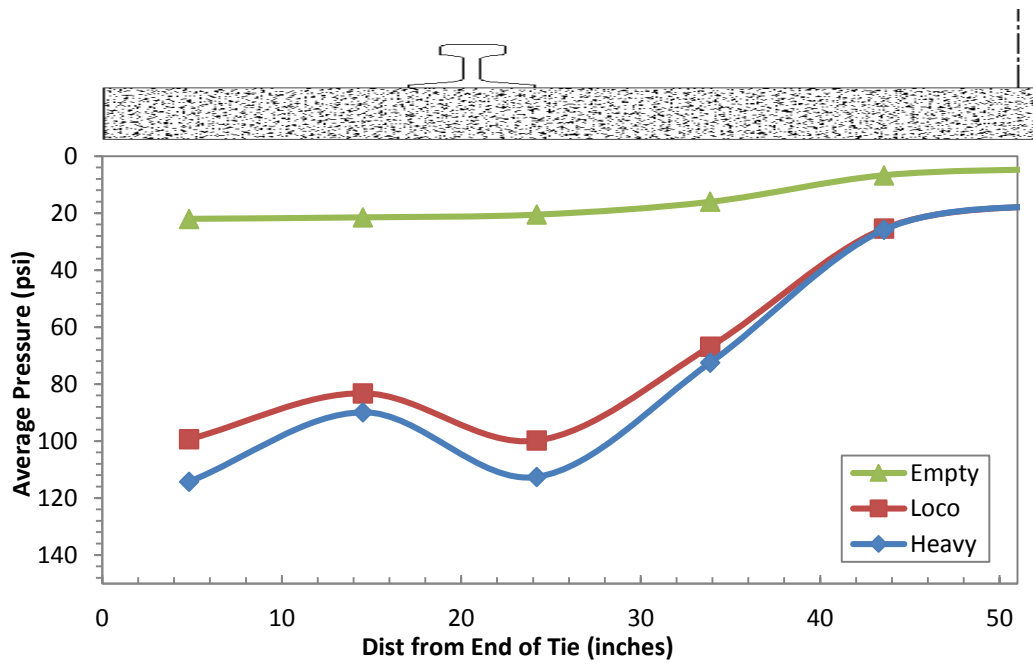
Figure 7.13 Average pressure distributions along Tie 59 for the three applied axle loads
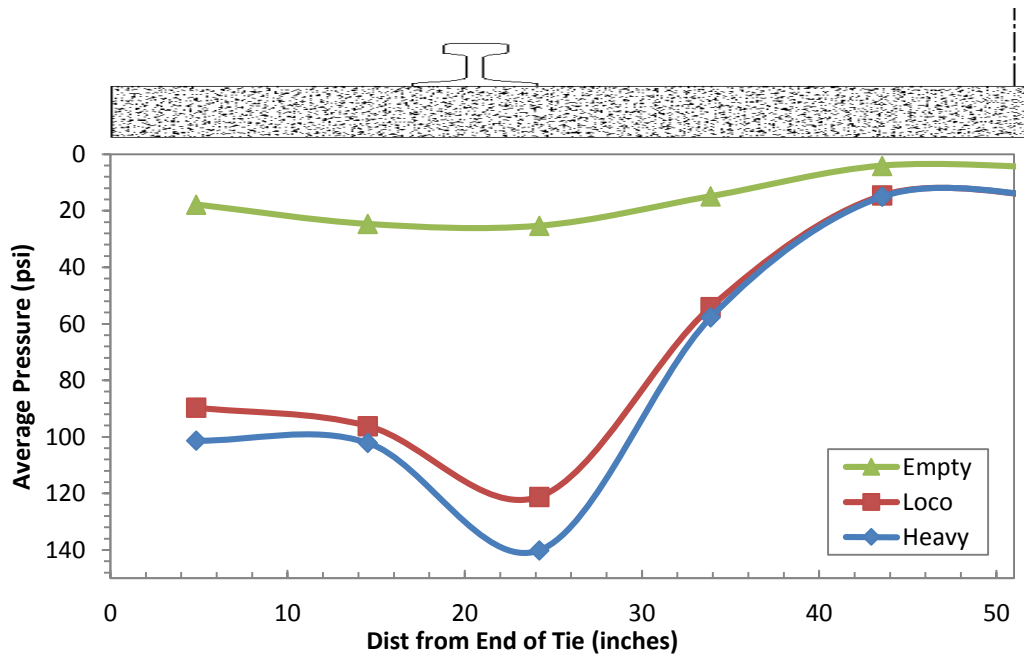
Figure 7.14 Average pressure distributions along Tie 60 for the three applied axle loads
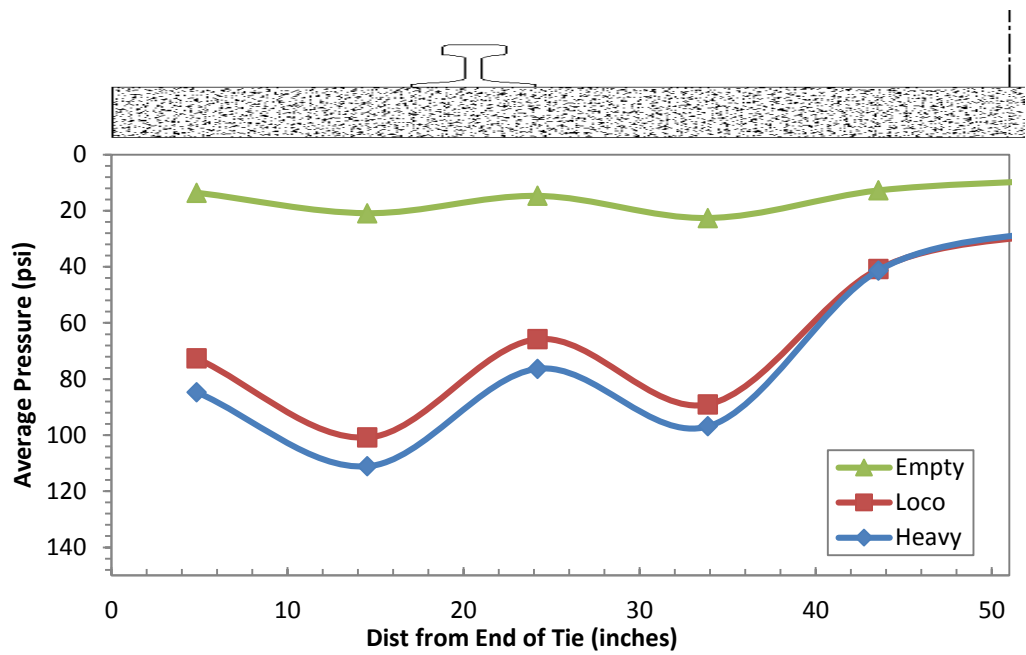
Figure 7.15 Average pressure distributions along Tie 78 for the three applied axle loads
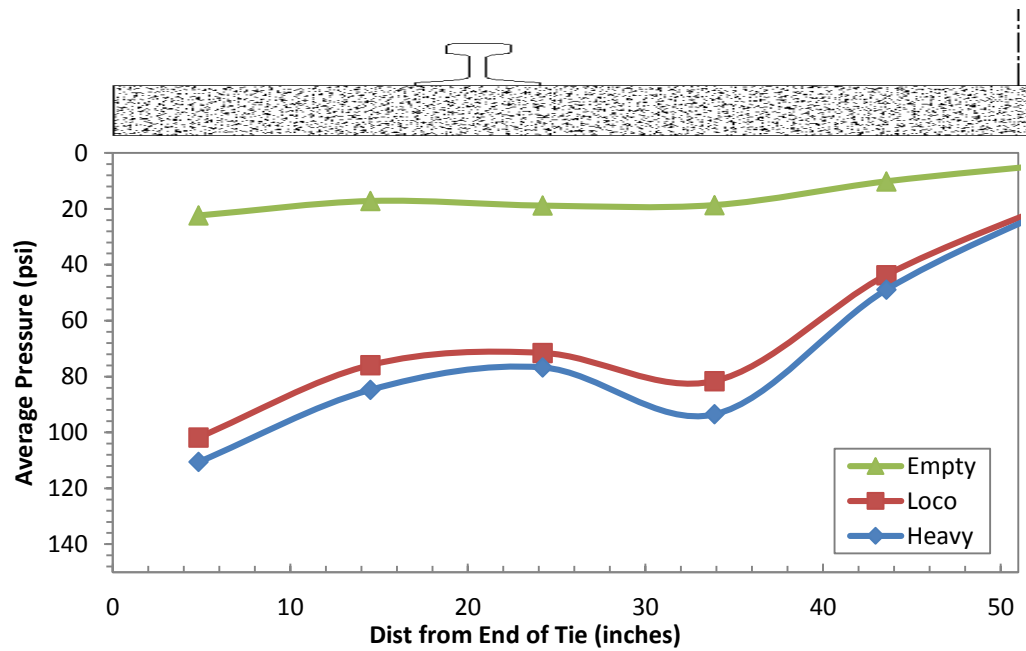
Figure 7.16 Average pressure distributions along Tie 80 for the three applied axle loads
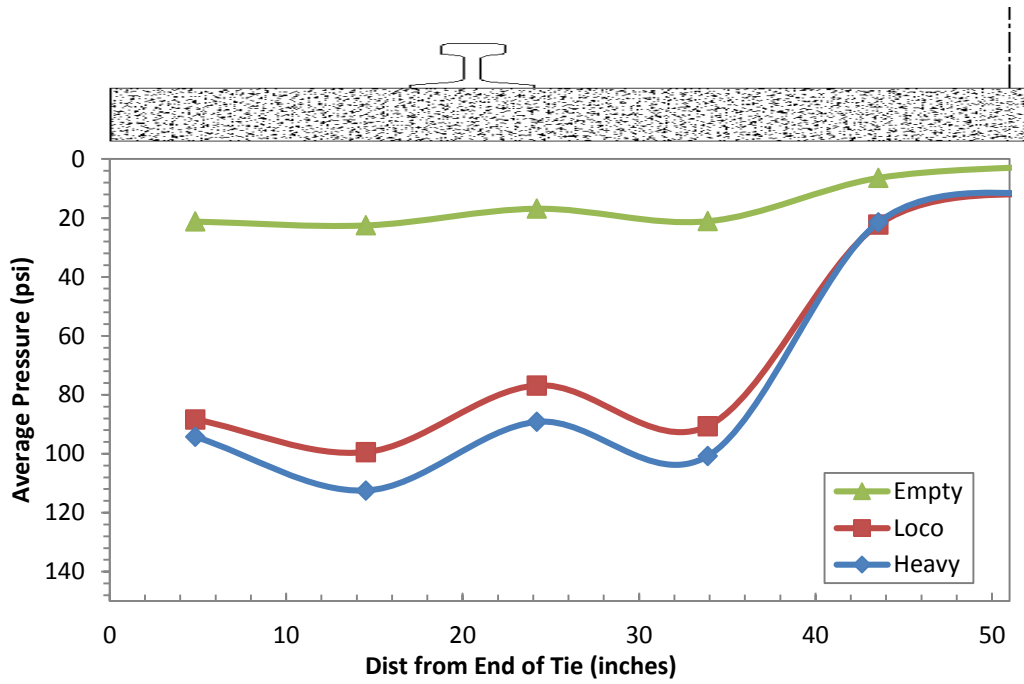
Figure 7.17 Average pressure distributions along Tie 99 for the three applied axle loads
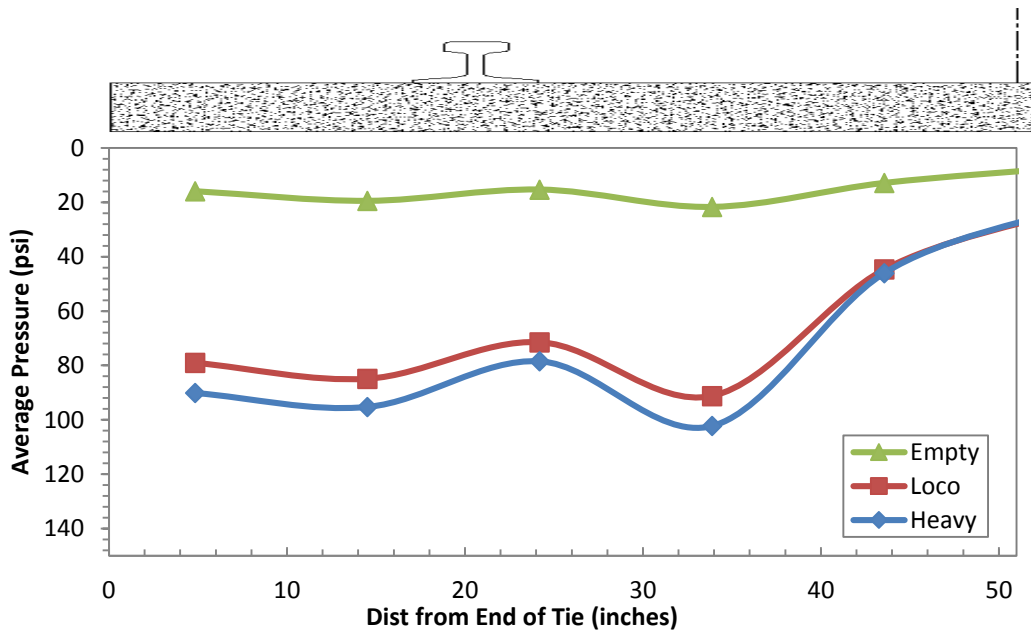
Figure 7.18 Average pressure distributions along Tie 100 for the three applied axle loads

The pressure distributions along the length of the ten test ties demonstrate the variability that can be seen even within the same type of track and adjacent ties. Six of the ten ties clearly show higher average pressures in the areas adjacent to the rail (Ties 38, 39, 78, 80, 99, and 100). The areas of high pressure appear to coincide with the areas conventionally tamped during surfacing maintenance. Tie 39 represents the most dramatic case of higher pressures in the tamped areas.

All ten test ties showed maximum average pressures greater than 100 psi. If compared with the limits recommended by AREMA (2010), namely 65 psi and 85 psi depending on the Chapter referenced, the in-track average pressures that were measured can be twice as large. As with the other calculations made for the in-track data, these values assume 50 percent of the axle load is carried by the test tie. No dynamic forces (impact factors) were used.

The in-track study was limited by the number of handles that could be acquired. The limited number of handles allowed only half of the tie's interface pressures to be measured. Symmetry may be assumed as testing was conducted on tangent track, and speeds were less than 10 miles per hour.

Contact Area for Each Ballast Zone

Contact Area along the length of the tie was plotted for all test ties. Figures 7.19 through 7.23 show the contact area measured for five test ties, one from each zone of ballast.
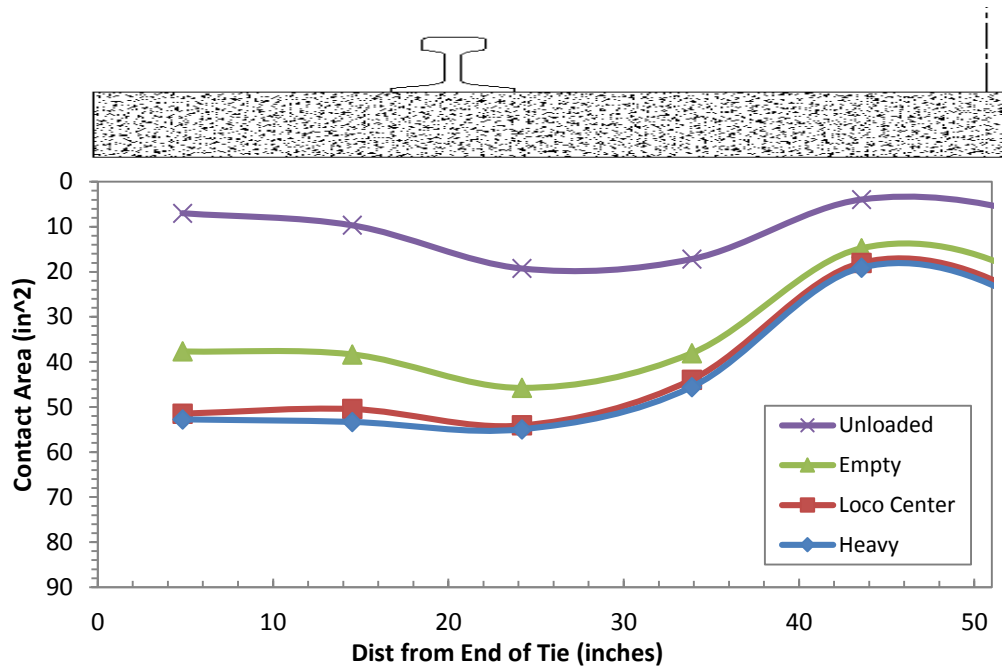
Figure 7.19 Contact areas along the length of Tie 2 for four different loads
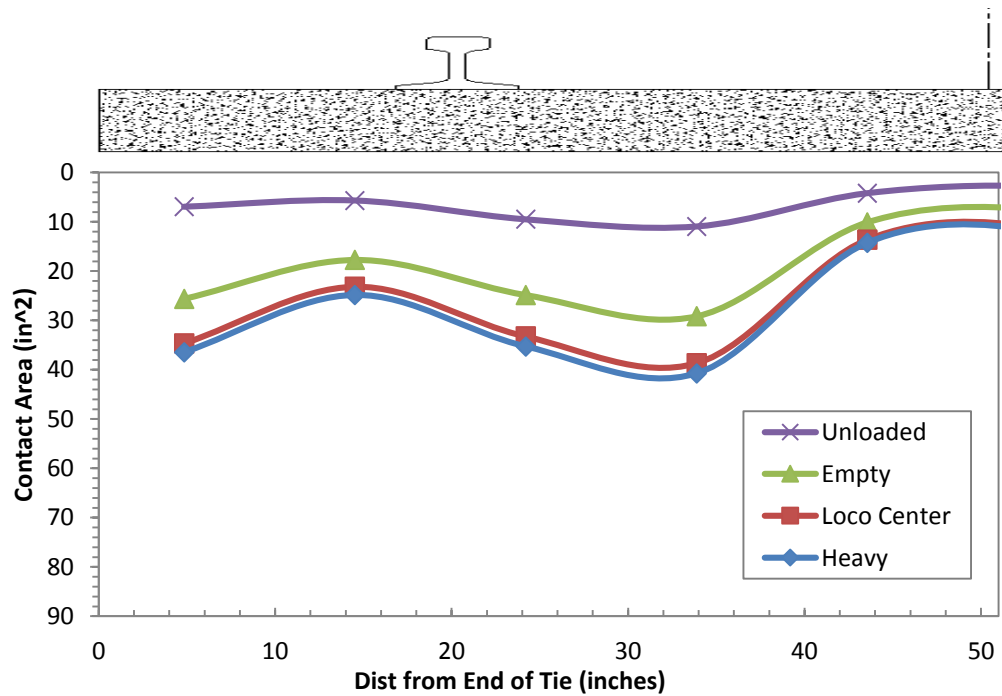
Figure 7.20 Contact areas along the length of Tie 40 for four different loads
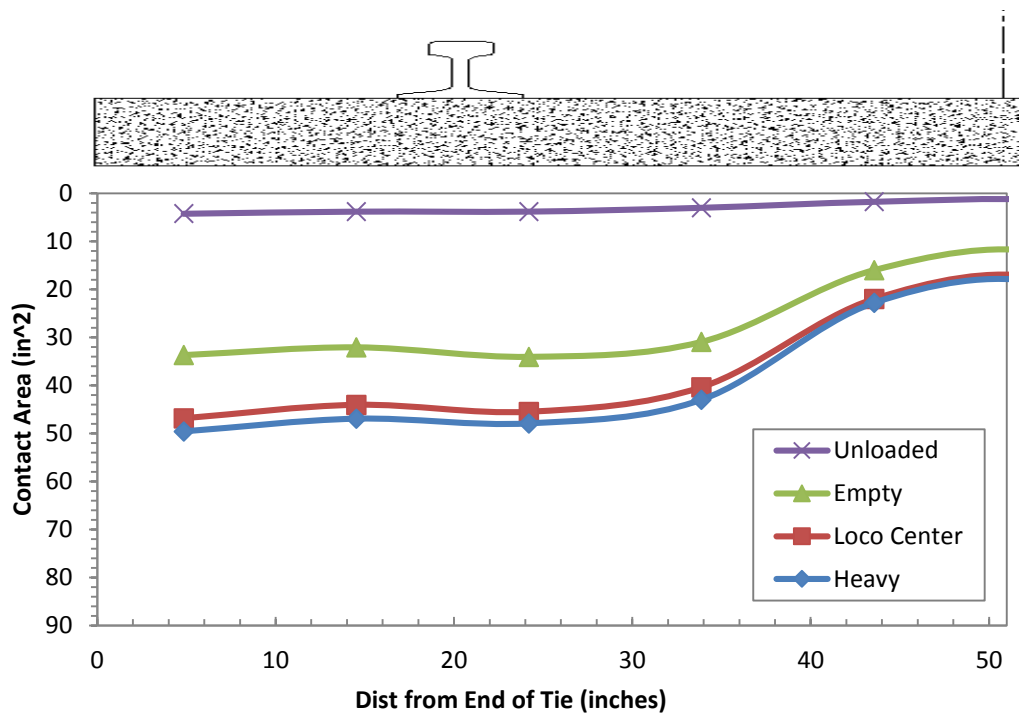
Figure 7.21 Contact areas along the length of Tie 59 for four different loads
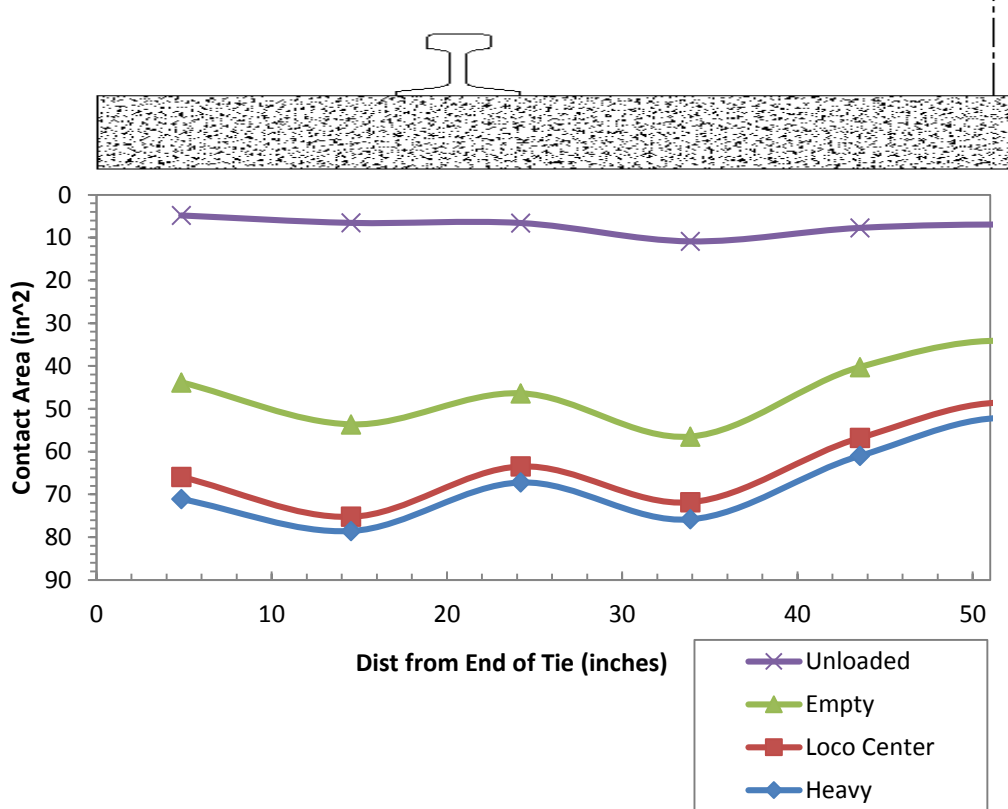
Figure 7.22 Contact areas along the length of Tie 78 for four different loads
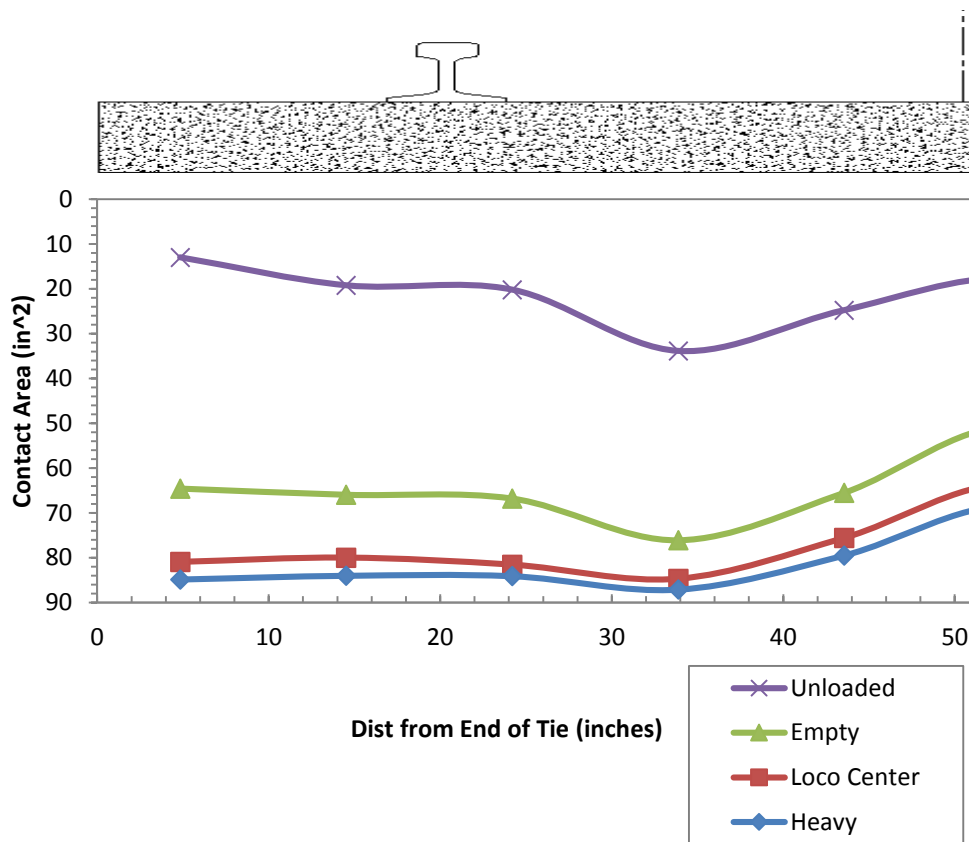
Figure 7.23 Contact areas along the length of Tie 100 for four different loads

Figures 7.19 through 7.23 do show that contact area increases as load is applied. A similar shape to the distribution of contact area is apparent for each tie. The Sand test zone (Zone 5) had the highest contact areas followed by the Pea Gravel in Zone 4, Fouled Ballast in Zone 3, moderate ballast in Zone 1 and new ballast in Zone 2. The contact area curves were integrated to obtain the total contact area beneath the tie. Symmetry was assumed. Table 7.3 summarizes the total average contact area (as a percentage of the tie footprint area) along the entire tie for the five test zones.

Table 7.3 Total average contact area (as a percentage of tie footprint area) for each zone under each axle load

Zone	Axle Load			
	Unloaded	Empty	Loco	Heavy
1 – Mod. Ballast	13.3%	35.7%	42.0%	43.0%
2 – New Ballast	7.4%	21.9%	29.6%	31.2%
3 – Fouled Ballast	2.5%	28.4%	37.7%	39.7%
4 – Pea Gravel	8.2%	47.6%	66.5%	71.0%
5 – Sand	13.1%	59.7%	73.3%	77.4%

Most conservative recommendation from AREMA = 66% for all loads

It is interesting to note that for new ballast, less than one-third of the tie is contacting the ballasts, the new ballast, fouled ballast, and moderate ballast all showed contact areas less than 50 percent of the tie footprint. The contact areas for an unloaded tie were lower than 15% for all test zones. The calculated contact areas, even for the new ballast, are not quite as low as those reported by Henn (1978). They appear, however, to compare favorably with the results presented in the FRA Task Order 225 report.

The contact areas under unloaded ties were significantly lower than loaded ties. The contact areas for unloaded track have implications in lateral track stability, for example, in the track's resistance to buckling in warmer temperatures. Results for these tests suggest that unloaded contact areas are at least one-third less than contact areas when the tie is loaded by an empty car. Lower contact areas contribute to reduced friction and ultimately reduced lateral track stability.

CHAPTER 8. DISCUSSION, CONCLUSION AND FUTURE RESEARCH

Current technology, Matrix Based Tactile Surface Sensors (MBTSS), allows for the complete areal and temporal pressure distribution at the ballast-tie interface to be realized. The technology has been proven viable on the rough contact surface characteristic of the interface, however an accurate calibration method for ballast-tie interface application is still required. Results are discussed and conclusions are presented below. Where appropriate, recommendations for future research are also made.

Calibration Results and Discussion

The calibration method proposed has yielded consist, repeatable calibration curves for the pressure sensors. However, the calibration curves obtained using the 0.5 inch waffle plate fail to sufficiently replicate the ballast surface. The calibration curves obtained using the 0.5 inch waffle plate significantly underpredict the actual applied force shown in validation testing. The following justifications are proposed to account for this discrepancy.

Varying Stiffness between waffle plate and actual ballast

Validation tests were performed on a thin layer (roughly 6 inches) of ballast contained by a ballast box. While a single compaction phase was run to reduce plastic deformation of the ballast layer, it is possible that accumulation of plastic strain occurred throughout the validation tests. The difference in stiffness between the thin aluminum waffle plate, and the thicker layer of ballast may contribute to the discrepancy in sensor output when reacted on these two surfaces.

Differing Contact Areas between Waffle Plate and Ballast

The 0.5 inch waffle plate was originally designed to simulate a fully bedded contact surface of ballast. It was initially considered that the rough surface of the waffle plate would sufficiently mimic the contact surface of a range of ballasts within some tolerable level of error. As shown in Chapter 4, reducing the contact area of waffle plate by 75 percent (by using a 0.25 inch waffle pattern), did shift the calibration curve closer to the validation curves, but differences between the two were

still significant (See Figure 4.7). If such a dramatic change in contact area could not produce a drastically different calibration curve, there is likely at least one other factor that has a more influential role in sensor output.

Differences in Roughness between the Waffle Plate and Ballast

The roughness of the waffle plate was not initially considered since the roughness parameter was developed after calibration testing. Because reducing the contact area of the waffle plate by 75 percent had minimal effect of the position of the calibration curve, there is clearly another factor that needs to be considered. The author believes that, not only the contact area, but also the "roughness" (i.e. the variability) of the pressure distribution induced by the waffle plate needs to be taken into account to obtain a more accurate calibration procedure.

The results of the calibration and validation testing suggest that the pressure sensors are very sensitive to changes in contact surface – whether these changes are in contact area, stiffness, material characteristics, or roughness. The influence of each of these variables should be explored in further research.

Assumptions Made to Obtain Force and Pressure Output

Given the complications in obtaining an accurate calibration curve for all the contact surfaces encountered, the calibration curves obtained for the pressure sensors were not applied to the data for the laboratory ballast box tests and the in-track tests. To convert raw sum output into engineering units the following assumptions were made:

1) For the laboratory ballast box tests, a portion of the applied load was "bridged" over the sensor because the sensor did not cover the entire bottom of the tie. For these tests, it was assumed that one-third the applied load was carried through the sensor. A calibration of the data was made based on this assumed load

2) For the in-track testing, it was assumed that every test tie carried 50 percent of the axle load and that the remaining 50 percent of the axle load was carried by adjacent ties; this is in line with AREMA recommendations for the track used for testing.

These assumptions are dangerous to make, especially in the case of the in-track testing. Variability in support conditions between adjacent ties has documented,

most notably by Talbot (1919). The assumptions made render the pressure data presented in this thesis *relative*, that is, the data should only be compared with other data obtained from these tests. Absolute pressure data would require an improved calibration process.

The assumptions made, however, are considered by the author to be conservative. The assumption of one-third of the applied force acting through the sensor during the laboratory testing is conservative because the force acting through the sensor (when placed directly under the rail) is likely higher than a uniform distribution would suggest. Also, the active length of the sensing area (9.68 inches) is greater than one-third the length of each tie section (equal to 24 inches divided by 3, or 8 inches).

The assumption that 50 percent of the axle load is carried by each test tie for the in-track testing, is based on AREMA recommendations for the actual track materials (concrete ties) and tie spacing (24 inches) as shown in Figure 2.4. Also, no dynamic impact factors are included which would increase the effective load experienced by each tie.

The justification of these assumptions as conservative only suggests that the pressure data reported (peak pressure and pressure distribution along the tie) may be considered as conservative estimates of the actual values.

A Proposed Technique to Avoid Traditional Calibration

To avoid the need to conventionally calibrate the MBTSS an alternative method could be employed using pressure cells. Pressure cells, if placed in series with the MBTSS system could measure absolute force at the ballast-tie interface. The force output from the pressure cell (conceivably placed on top of the MBTSS) would be used to calibrate the *raw sum* matrix output from the MBTSS. This technique would obviously require more instrumentation (one pressure cell for each MBTSS). Also, if placed above the MBTSS, the pressure cells would prevent the MBTSS from reacting directly against the tie. A distribution medium of some sort would be needed between the pressure cell and the MBTSS.

Similarly, if the force being carried by an individual tie could be obtained (e.g. through the use of strain gages or string potentiometers), the MBTSS output could be calibrated much in the same way it was for the data presented herein. The only difference being instead of assuming the force being carried by the tie, the actual

force could be obtained and aligned with the MBTSS data. The technique of measuring force acting through the sensor during the actual MBTSS data collection is discussed in the *Tekscan I-Scan and High Speed I-Scan User Manual* and is referred to as "frame calibration."

Contact Area Results

Contact area output does not need to be calibrated for as it simply accounts for sensels that are experiencing load. Contact area output is dependent on sensor protection thickness and material characteristics, the sensel *raw sum* threshold set for the sensor, and the overall sensitivity of the sensor.

Contact Area Increase as Load is Applied

MBTSS data from both the laboratory ballast box testing and in-track testing both show that contact area is dependent on load. The contact area at the ballast-tie interface tends to increase as increased load is applied. This is a significant conclusion as it supports a more dynamic view of the ballast-tie interface and adds to the previous "static" concept of the contact area explored by Henn (1978) and the FRA Task Order 225 study (2009).

Contact Area for Varied Ballast Gradations

Results indicate that contact area increases with an increased level of ballast deterioration. New ballast showed the lowest contact areas in both the laboratory and in-track tests. As greater load was applied in the laboratory tests, the differences in contact area between the five ballast gradations became clearer. Total contact areas (as a percentage of tie footprint area) under the heavy car axle load ranged from 31 percent to 43 percent for new ballast and fouled ballast respectively. These results compare favorably with those reported in the FRA Task Order 225 study.

Ballast-Tie Contact Index Results

An index has been developed to characterize the "roughness" of the pressure distribution observed at the ballast-tie interface. Using a standard deviation based method that compares the actual pressure distribution to an ideal, uniform pressure distribution, the variability of the distribution can be quantitatively assessed. This variability/roughness is important, because, when coupled with contact area, and peak

pressure data, gives a comprehensive view of the MBTSS pressure data. It is likely that roughness plays an important role when calibrating the pressure sensors.

The BTCI, and hence the "roughness" of the pressure distribution has been shown to decrease under increased applied load. The results suggest that BTCI reaches a plateau during the load increase. The plateau represents an equilibrium state in which all ballast particles with the potential to be engaged, have been engaged, and the relative roughness of the pressure distribution does not change as more load is applied. The load at which the BTCI begins to plateau is indicative of full contact between the ballast and the tie.

Peak Pressure Results

The 20 kip applied load (in the ballast box test setup) results in average ballast pressures between a 65 psi and 85 psi – the recommended maximum pressures provided by AREMA. Thus, the 20 kip applied load can be considered representative of a typical wheel load. Peak pressures for the laboratory ballast box testing are reported in Figure 5.10 and Table 5.3. The peak pressures observed on new ballast for an applied load of 20 kips averaged 1449.9 psi. Fouled ballast had an average peak pressure of 681.3 psi at the same applied load. These values of peak pressure are relative to the assumption that one-third of the applied load is carried through the sensor. If this is considered a conservative assumption, the estimates for peak ballast pressures are ten to twenty times higher than the uniform pressure. Peak pressure is important to consider, because it is the maximum stress that is placed on the ballast and oppositely, on the tie. It is necessary to consider the maximum actual stresses be placed on these track components to reduce the potential of ballast or tie degradation.

Pressure Distribution along the Length of the Tie

In-track measurement of the pressure distribution along the length of the tie (Figures 7.9 through 7.18) showed much variability between test ties. The pressure distributions obtained represent a small sample size (only ten ties), so only general conclusions can be drawn. Results showed 60 percent of ties to have higher pressures adjacent to the rail as opposed to directly underneath the rail. This may provide support for the idea of denser ballast in the areas conventionally tamped during track surfacing. This condition, if excessive enough, could contribute to rail seat positive flexural cracking in concrete ties. In general, the results compare favorably with

distributions proposed by Talbot (1919) and Giannokos (2011) and support the conclusion that distribution of pressure along the tie varies greatly from one tie to another.

Effects of Tie Materials

Laboratory ballast box testing showed little difference between the distributions for the three tie materials used. This is likely a result of having only one pressure sensor installed beneath the tie. With only one sensor, there is no way to observe pressure in the areas outside the active area of the sensor, thus a distribution of pressure along the length of the short tie sections could not be obtained. Also, the tie sections used were only 24 inches long, likely not enough length to observe any significant changes in pressure distribution along the length of the tie due to the material stiffness.

While the in-track data presented was for concrete ties, the system could just as easily be implemented on wood or composite ties. Due to the flexible nature of the sensors, they could also be used on steel ties, which typically do not have a flat bottom surface. It is recommended that future research explore the differences in pressure distributions along the length of ties of varying material properties.

Through discussions with practicing railway engineers and researchers, the author found a common belief that ballast particles tend to embed themselves into wood ties (and perhaps some composite ties). The FRA Task Order 225 study makes mention of this idea. Because a sensor (and its rubber protection) must be installed between the ballast and the tie, there is no realistic way to measure any pressure reduction due to the slightly greater contact area caused by ballast embedding into the tie. However, with the use of the Ballast-Tie Contact Index, the "roughness" of the distribution over time between concrete ties and wood ties could be explored. If peak pressure reductions are indeed occurring in wood ties, it is possible that BTCI would decrease at a slower rate over the life-cycle of the tie implying that ballast would not undergo as significant of degradation. The use of BTCI in such a manner is discussed in a later section of this chapter

The Need for New Recommended Practices in AREMA

Based on the results presented, it is clear that the recommended practices in the AREMA Manual for Railway Engineering require updating. The actual contact

areas observed during testing are in stark contrast to the uniform and average pressure distributions assumed in the AREMA recommended practices for calculating ballast pressures. Depending on the chapter referenced, the AREMA Manual recommends limiting average ballast pressures to 65 psi or 85 psi. Maximum average pressures recorded during the in-track testing (based on the assumption of the load being carried by the tie), were above 100 psi for all test ties. The maximum average pressure recorded using this method was 145 psi.

Further research in this area will be required to obtain better understanding of the stresses being applied to individual ballast particles so that better recommendations can be implemented into American practice.

Commercial interest has been shown in producing elastic under-tie pads for the North American rail industry. Further research to measure the pressures at the ballast tie interface (particularly for various ballast conditions and tie materials) can likely contribute to better under-tie pad designs.

Limitations of MBTSS System

The MBTSS technology implemented for this research study proved sufficient for observing the fine-scale pressure distribution at the ballast-tie interface. The deficiencies in the calibration of these sensors for rough contact surfaces has already been presented. There are, however, additional limitations of the proposed system for application at the ballast-tie interface. The following limitations of the MBTSS system used in this study are identified and described below.

Limited resolution

An applied point load from a ballast particle occurs over a very small area. The larger a sensel area is, the greater the risk of such point loads falling outside the sensel. Discussions with Tekscan have led the author to conclude that when a point load does not occur precisely over the intersection of a row and column, that sensel output would decrease (to what extent isn't known). The rubber protection layer can solve this problem, in some degree, by distributing the smaller point loads over a larger area. While 5250 sensors with a resolution of 20.7 sensels/in^2, were applied, a higher resolution sensor may be desirable for more accurate measurement of contact area and peak pressures. Higher resolution would require substantial financial

investment to manufacturer custom sensors and purchase additional data acquisition handles, however.

Sensor Durability

The thin polyester sheets that the sensors are printed on allow the sensors to be nonintrusive in many applications. The brittleness of this material, however, contributed significantly to puncture and abrasion damage to the sensor throughout testing. Printing the sensor electronics on a more resilient and more durable material would greatly enhance their usability at rough contact surfaces like the ballast-tie interface. Much like increasing sensor resolution, modifying the material the sensors are printed on would require substantial funding.

Handle to Sensor Connection Reliability

It was observed that the sensors were often challenging to connect to the handles, especially during in-track tests. On multiple occasions, handles had to be reconnected to sensors after failing to collect data after a train pass. These challenges were exacerbated by the dusty environment typical ballast (especially after it has been excavated to allow installation of the sensors). The nature of any on-track research requires efficiency to optimize the amount of data that can be collected and to minimize the time required to setup the instrumentation for each test. A more reliable connection between the sensor and MBTSS data acquisition device would allow for increased testing efficiency, requiring less time to check the hardware connections.

Future Implications of MBTSS Ballast-Tie Data

Ballast-Tie Life Cycle Analysis - BTCI as a Performance Indicator

The BTCI results from the laboratory data also show a relationship between pressure distribution roughness and ballast surface gradation. As might be expected, the new, angular ballast showed high BTCI (roughness) values. The two tests run on uncompacted new ballast showed the highest BTCI values of any of the tests. While uncompacted ballast is only a condition encountered for the first few trains to pass over newly surfaced track, the high pressures that result from such a condition need to be considered because they are potentially high enough to cause ballast degradation (even after such few loading cycles).

It is possible that BTCI could be used to give an indication of ballast gradation (hence a level of fouling) over the life-cycle of the ballast-tie interface. The

measurement of BTCI, along with contact area and peak pressure, could be used collective to assess the performance of the ballast-tie interface. The rate of change in the BTCI could be recorded throughout the service life between surfacing maintenance to give insight as to how long new ballast remains so. An application of the MBTSS system, in this sense, could be the performance assessment of various ballast pressure reduction techniques, such as elastic under-tie pads, or frame and half-frame ties. The BTCI measurements could likely be tied with other performance measures such as track settlement or reduction in track geometry.

It should be noted that rate of change of the BTCI throughout the life-cycle of the track is likely more important than its particular value at any given time. If the BTCI can remain relatively unchanged between surfacing operations, there is likely less fracture, rounding, or settling of the ballast (BTCI would change if ballast gradation were changing) and thus relatively less settlement of the superstructure.

Incorporation into Ballast and Tie Modeling Efforts

The MBTSS results from the ballast-tie interface could easily be incorporated into efforts to model the degradation of the ballast layer. Incorporating results into ballast degradation models such as the Discrete Element Model (DEM) for railroad ballast presented by Tutumluer et al. (2011) and Huang (2010) would provide valuable validation of input loads at the model's interface with the tie. Underlying support conditions would provide the input load where the ballast layer interacts with the subgrade. The ballast-tie data would provide the necessary link to couple ballast degradation models (like the DEM model), with tie models, ultimately contributing to a more detailed, comprehensive track model (that would include rails, fastening system, ties, ballast and subgrade).

Figure 8.1 presents a conceptual model that could be used as an approach to incorporate the true ballast-tie interface into tie structural models. The concept treats the ballast-tie interface as a series of variable stiffness springs (indicated by thickness). These springs could act over contact areas consistent with true contact areas observed for various ballast conditions and track types
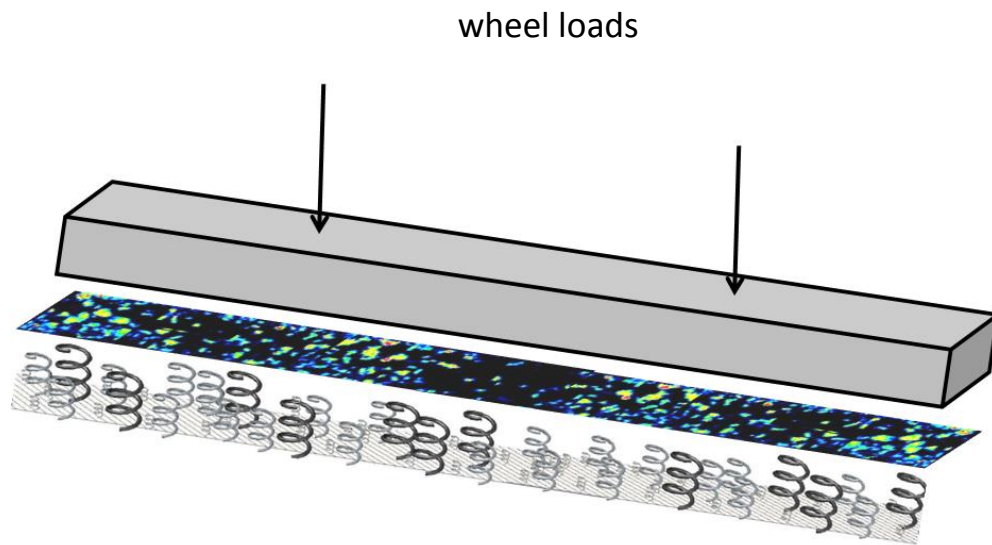
wheel loads

Figure 8.1 Conceptual model treating ballast-tie interface as a series of variable stiffness springs acting over finite contact areas.

A New Way of Viewing the Ballast-Tie Interface

Primarily, the conclusions reached through this research provide a new way of viewing the ballast-tie interface. Early research attempted to measure the average pressures acting along the length of the tie. More recent work has considered the actual contact area between the ballast and tie, and has estimated peak pressures based on these contact areas. However, this research was limited because contact area could only be measured at a single point in time. The research presented herein describes a measure of contact area and peak pressure that can be recorded throughout a loading cycle. These results show the realization of the areal *and* temporal pressure distribution between the ballast and tie, and thus provide a new way to treat the forces on these track components. It is with this new approach that the ballast-tie interface, and hence the loads imparted on the ballast and on the tie, should be considered in future research.

REFERENCES

Akhtar, M., Otter, D., Doe, B. (2006). "Stress State Reduction in Concrete Bridges Using Under Tie Rubber Pads and Wood Ties." Technology Digest, TD-06-016, Association of American Railroads Transportation Technology Center, Pueblo, CO.

Akhtar, M., Davis, D., and LoPresti, J. (2012). "Increasing strength and reducing life-cycle cost of concrete tie track." Railway Track and Structures. June, 2012, pp. 16-19.

American Railway Engineering and Maintenance-of-Way Association (AREMA). (2010). *2010 Manual for Railway Engineering*.

American Railway Engineering and Maintenance-of-Way Association (AREMA). (2012). *2012 Manual for Railway Engineering*.

Brimacombe, J.M., Anglin, C., Hodgson, A., and Wilson, D. (2005). "Validation of Calibration Techniques for Tekscan Pressure Sensors." International Society of Biomechanics Congress XX. Cleveland, OH.

CDM. (2013). "Under Tie Pads." Promotional Brochure. <http://cdm-novitec.com/onewebmedia/Brochures/CDMUTP%20Brochure%20-%20020713.pdf> (Nov. 17, 2013).

Das, B.M. (2010). *Principles of Geotechnical Engineering*. Seventh Edition. Cengage Learning, Stamford, CT.

Douglas, S.C. (2013). "Ballast Quality and Breakdown during Tamping." Proceedings of the 2013 American Railway Engineering and Maintenance-of-Way Association Conference. Indianapolis, IN.

Federal Railroad Administration. (2009). "Evaluation of Tie Bottom Contact with Ballast. Task Order 225." Unpublished. Used with permission.

Getzner. (2013). "Sleeper Pads for Ballasted Track." Promotional Brochure. <http://www.getzner.com/uploads/media/02_Sleeper_Pads_for_ballasted_tracks.pdf> (Nov. 17, 2013).

Giannakos, K., Loizos, A., and Christina, P. (2013). "Hardness, Fouling, Life Cycle, and Ballast Requirements for High Speed and Heavy Haul Railways." Paper 13-1523. Proceedings of the 2013 Transportation Research Board Annual Meeting. Washington, D.C.

Giannakos, K. (2010). Loads on Track, Ballast Fouling, and Life Cycle under Dynamic Loading in Railways. Journal of Transportation Engineering, American Society of Civil Engineering, Vol. 136, No. 12, pp. 1075-1084.

Grohnmann, C.H., Smith, M.J. and Ricconmini, C. (2011). "Multiscale Analysis of Topographic Surface Roughness in the Midland Valley, Scotland." IEEE Transactions on Geoscience and Remote Sensing, Vol. 49, No. 4, pp. 1200-1213.

Hay, W.W. (1982). *Railroad Engineering.* John Wiley & Sons, New York, NY

Henn, W. (1978). "Auswirkung von Oberbauform und Betriebsbelastung auf die Veränderung der Gleishöhenlage." Archiv für Eisenbahntechnik (33), p. 51-64.

Huang, H. (2010). "Discrete Element Modeling of Railroad Ballast Using Imaging Based Aggregate Morphology Characterization," dissertation presented to University of Illinois at Urbana-Champagne, Urbana, IL, in partial fulfillment of the requirements for the degree of Doctor of Philosophy.

Kerr, A.D. (2003). *Fundamentals of Railway Track Engineering.* Simmons-Boardman Books, Inc., Omaha, NE.

Lutch, R. H. (2009). "Capacity Optimization of a Prestressed Concrete Railroad Tie," thesis, presented to Michigan Technological University at Houghton, MI, in partial fulfillment of the requirement for the degree of Master of Science.

Marsili, R. (2000). "Measurement of the Dynamic Normal Pressure Between Tire and Ground Using PVDF Piezoelectric Films." IEEE Transactions on Instrumentation and Measurement, Vol. 49, NO. 4.

Rapp, C., Dersch, M., Edwards, J. R., Barkan, C. P. L., Wilson, B., and Mediavilla, J. (2012). "Measuring Concrete Crosstie Rail Seat Pressure Distribution with Matrix Based Tactile Surface Sensors." Proceedings of the 2012 American Railway Engineering and Maintenance-of-Way Association Conference. September 16-19, Chicago, IL.

Rose, J. and Stith, J. (2005). "Pressure Measurement in Railraod Trackbeds at the Rail/Tie Interface Using Tekscan Sensors." University of Kentucky, Lexington, KY.

Rose, J. and Lees, H. M. (2008). "Long-Term Assessment of Asphalt Trackbed Component Materials' Properties and Performance." Proceedings of the 2008 American Railway Engineering and Maintenance-of-Way Association Conference, Salt Lake City, UT.

Rose, J., Li, D., and Walker, L. (2002). "Tests and Evaluations of In-Service Asphalt Trackbeds." Proceedings of the 2002 American Railway Engineering and Maintenance-of-Way Association Conference, Washington, D.C.

Salem, M. T. and Hay, W. W. (1966). "Vertical Pressure Distribution in the Ballast Section and on the Subgrade beneath Statically Loaded Ties." Civil Engineering Studies, Transportation Series No. 1, University of Illinois, Urbana, IL.

Sato, Y. (1997). "Optimum Track Structure Considering Track Deterioration in Ballast Track." Sixth International Heavy Haul Railway Conference, Conference Papers, Cape Town, South Africa.

Stith, J. (2005). "Railroad Track Pressure Measurement at the Rail/Tie Interface Using Tekscan Sensors," thesis, presented to University of Kentucky at Lexington, KY, in partial fulfillment of the requirement for the degree of Master of Science.

Talbot, A.N. (1919) *Stresses in Railroad Track.* The Second Progress Report of the ASCE-AREA Special Committee on Stresses in Railroad Track, Reprinted, 1980. Published by the American Railway Engineering Association (AREA).

Tekscan, Inc. I-Scan System – Tactile Pressure and Force Measurement. <http://www.tekscan.com/products/industrial/pressure-distribution-measurement-system> (Dec. 1, 2013).

Tekscan, Inc. (2013). "Sensor Model/Map: 5250. Sensor Specifications." <http://www.tekscan.com/5250-pressure-sensor> (Dec. 1, 2013).

Tekscan, Inc. (2012). "Tekscan I-Scan Pressure Measurement System Help File, Appendix: Equilibration & Calibration Practical Suggestions." (accessed through I-Scan software)

Tekscan, Inc. (2013). "Industrial Sensor Catalog Introduction." <http://www.tekscan.com/pdf/Sensor-Catalog-Introduction.pdf> (Dec. 1, 2013).

Tutumluer, E. Qian, Y., Hashash, Y., Ghaboussi, J.Garcia, and Davis, D. (2011). "Field Validated Discrete Element Model for Railroad Ballast." Proceedings of the 2011 American Railway Engineering and Maintenance-of-Way Association Conference. Minneapolis, MN.

Zeman, J. C. (2010). Hydraulic Mechanisms of Concrete-Tie Rail Seat Deterioration," thesis, presented to University of Illinois at Urbana-Champagne at Urbana, IL, in partial fulfillment of the requirement for the degree of Master of Science.

VITA

Michael McHenry completed his Bachelor of Science in Civil Engineering at the University of Kentucky in December, 2011. Michael has worked as an undergraduate and graduate research assistant under Dr. Jerry Rose as well as an intern at the Transportation Technology Center, Inc. in Pueblo, Colorado. Michael has been awarded an Eisenhower Transportation Fellowship and a University of Kentucky Graduate School Wethington Fellowship for his graduate studies.